ABSTRACT

Title: **CHARACTERIZATION OF TATA BOX BINDING PROTEIN INTERACTION WITH MINICIRCLE DNA**

Jung Shin Byun, Ph.D., 2005

Directed By: **Associate Professor Jason D. Kahn, Department of Chemistry and Biochemistry**

Protein-induced bending of DNA plays an important role in regulating its transcription, replication, recombination, and packaging into nucleosomes. In particular, many general and gene-specific transcription factors bend DNA. The TATA box-binding protein (TBP) is essential to promoter recognition, and it provides an especially interesting example of dramatic DNA bending.

Previous work in our laboratory has shown that TBP bound to strained DNA can induce negative supercoiling, proposed to be the result of untwisting without the compensating writhe provided by the Phe stirrups. The structural proposal makes the clear predictions that TBP lacking the Phe stirrups will induce negative supercoiling under all conditions, and that the mutant may require negative supercoiling in order to bind at all.

To test this prediction, we have made the F99A-F116A and F99A-F116A-F190A-F207A site-directed TBP mutants that lack the N and C-terminal stirrups. We have characterized the binding of wild type and mutant TBP to linear DNA and to negatively supercoiled minicircles using quantitative hydroxyl radical footprinting, which is the first application for circular DNA, and electrophoretic mobility shift assays (EMSA).

The results of the quantitative hydroxyl radical footprinting and EMSA suggest that mutant TBP binds better to the negatively supercoiled minicircle than to the linear DNA. We also observed quite different footprinting patterns for circular versus linear DNA at the TATA box. This indicates that the structure of TBP bound to minicircles may be different than the linear DNA. The equilibrium dissociation constants (Kd) of wild type TBP derived from hydroxyl radical footprinting titrations for the linear DNA and the -1 topoisomers of 203 bp are 11 nM and 3 nM respectively. This suggests that pre-bending of the TATA box enhanced DNA binding. From these observations, we propose that TBP binding to promoters upon gene activation may be enhanced by the topological strain induced in the DNA upon chromatin remodeling.

CHARACTERIZATION OF TATA BOX BINDING PROTEIN

INTERACTION WITH MINICIRCLE DNA

By

Jung Shin Byun

Dissertation submitted to the Faculty of the Graduate School of the
University of Maryland, College Park, in partial fulfillment
of the requirements for the degree of
Doctor of Philosophy
2005

Advisory Committee:
Associate Professor Jason D. Kahn, Chair
Professor Janice E. Reutt-Robey
Professor Emeritus Raj K. Khanna
Professor John D. Weeks
Associate Professor Jonathan D. Dinman

DEDICATION

For my Daddy

ACKNOWLEDGEMENTS

First of all, I would like to thank my Heavenly Father for allowing me to overcome the language barriers and all kinds of hardship while studying abroad, and to retain a positive attitude even under difficult situations.

I would like to thank my advisor Professor Jason D. Kahn for his guidance and continuous support during my Ph.D. residency. Without which I would not be able to achieve my research by myself.

I am very grateful to my family, my Dad (Byun, Kyu-Eung) and Mom (Park, Young-Soon), Brother (Byun, Sang-Sub), and Sister (Professor Byun, Jung-Min) who have been extremely patient, supportive, loving and caring since I have left Seoul for my studies.

Special Thanks to Professor Raj K. Khanna for continuous encouragement and thoughtful advice during graduate school years, and to all of my committee members for valuable suggestions on my thesis.

I am very thankful for having wonderful my family friends, and all members of the Korean Presbyterian Church, who have been enormously helpful and supportive during my Ph.D. residency. Thank you all. I will not forget your friendships.

I would also like to give thanks to Thomas H. Charpentier for helping me to engineer plasmids, sharing difficult time during protein purification, and his friendship.

Finally, I would like to devote my achievement and honor to my Daddy, who is constantly cheering me on in Heaven.

TABLE OF CONTENTS

LIST OF TABLES

LIST OF FIGURES

List of Terminology

1. Prokaryote: A unicellular organism with a single chromosome, no nuclear envelope, and no membrane bounded organelles.

2. Eukaryote: A unicellular or multicellular organism with cells having a membrane bounded nucleus, multiple chromosomes, and internal organelles.

3. Transcription: The enzymatic process whereby the genetic information contained in one strand of DNA is used to specify a complementary sequence of bases in an mRNA chain.

4. TBP (Acronym for TATA Box Binding Protein): 43 kDa (human), 27 kDa (yeast). The first component as a subunit of TFIID to bind in the assembly of a preinitiation complex at the TATA box of a typical RNA polymerase II promoter.

5. TATA box: An element with the consensus sequence TATAAAA that begins about 30 base pairs upstream of the start of transcription in most eukaryotic promoters recognized by RNA polymerase II. The Adenovirus Major Late promoter has a TATAAAAG sequence in its TATA box.

6. RNA polymerase: An enzyme that catalyzes the formation of RNA from ribonucleoside 5'-triphosphates, using a strand of DNA or RNA as a template.

7. Promoter: A DNA sequence to which RNA polymerase binds prior to initiation of transcription. Usually found just upstream of the transcription start site of a gene.

8. General Transcription Factor: Eukaryotic factors that participate, along with one of the RNA polymerases, in forming a preinitiation complex.

9. TBP-associated factors (TAFIIs): At least 13 polypeptides in TFIID. They interact with core promoter elements and gene specific transcription factors.

10. Major groove: In a helix, refers to the larger of the unequal grooves that form as a result of the double-helical structure of DNA.

11. Minor groove: In a helix, refers to the smaller of the unequal grooves that are formed as a result of the double-helical structure of DNA.

12. Kinks: A sharp bend in a double stranded DNA made possible by base unstacking.

13. Minicircle DNA: Circular DNA, less than 1000 bp.

14. Supercoil: A form of circular double-stranded DNA in which the double helix coils around itself like a twisted rubber tube.

15. Nucleosome: A repeating structural element in eukaryotic chromosomes, composed of core of eight histone molecules with about 146 base pairs of DNA wrapped around the outside.

16. Chromatin: The material of chromosomes, composed of DNA and chromosomal proteins.

17. DNase I (Deoxyribonuclease I): An enzyme that degrades DNA.

18. Footprinting: A method of detecting the binding site for a protein on DNA by observing the DNA region. DNase footprinting: the protein protects from degradation by DNase.

19. Template: A polynucleotide (RNA or DNA) that serves as the guide for making a complementary polynucleotide. DNA strand serves as the template for ordinary transcription.

20. Primer: A small fragment of single stranded DNA

List of Abbreviations

AdMLP : Adenovirus major late promoter

Ala (A): alanine

ATP: adenosine triphosphate

bp: base pair

DNA: Deoxyribonucleic acid

dNTP: deoxynucleoside 5'-triphosphate

DTT: Dithiothreitol

EDTA: ethylenediamine tetraacetate

EGTA: Ethylene glycol-bis[β-aminoethylether]-N,N,N',N'-tetraacetic acid

Hepes: 4-(2-hydroxyethyl)-1-piperazine ethane sulfonic acid

hTBP: human TATA box binding protein

IPTG: isopropylthiogalactoside

ΔLk: linking number difference

MG (A+G): Maxam Gilbert sequencing for adenine and guanine

PCR: polymerase chain reaction

Phe (F): phenylalanine

PMSF: Phenylmethylsulfonylfluoride

poly(dI-dC): polynucleotide deoxyinosine-cytosine

RNA: Ribonucleic acid

TBE: Tris-borate EDTA buffer

Tris: tris-(hydroxymethyl)aminomethane

tRNA: transfer RNA

yTBP: yeast TATA box binding protein

1. INTRODUCTION

1.1 Uniqueness of TBP

Erwin Schrödinger, the Austrian-born father of wave mechanics, introduced the concept that life could be thought of in terms of storing and passing on biological information (Schrödinger, 1944). At the time of Schrödinger, most biologists supported the idea that proteins would eventually be identified as the primary bearer of genetic instruction. Later, DNA (deoxyribonucleic acid) was found to be essential to our existence because it is the molecule of genetic inheritance in all life forms (Watson, 2003). DNA plays two important roles; it guides its own replication during cell division and serves as a template for transcription of complementary RNA (Nelson and Cox, 2000).

Transcription is the synthesis of RNA (ribonucleic acid) from DNA, and thus it is fundamental to gene expression. In eucaryotic cells, the initiation of transcription of messenger RNA from protein coding genes requires several general transcription factors (Carey, *et al*., 2000). The assembly process starts with the binding of TATA box binding protein (TBP), a component of general transcription factor TFIID, to the TATA sequence (Figure 1) (Alberts, *et al*., 1998). Once TBP is bound to this DNA site, then the other factors are assembled, along with RNA polymerase II, to form a complete transcription complex and finally transcription begins.

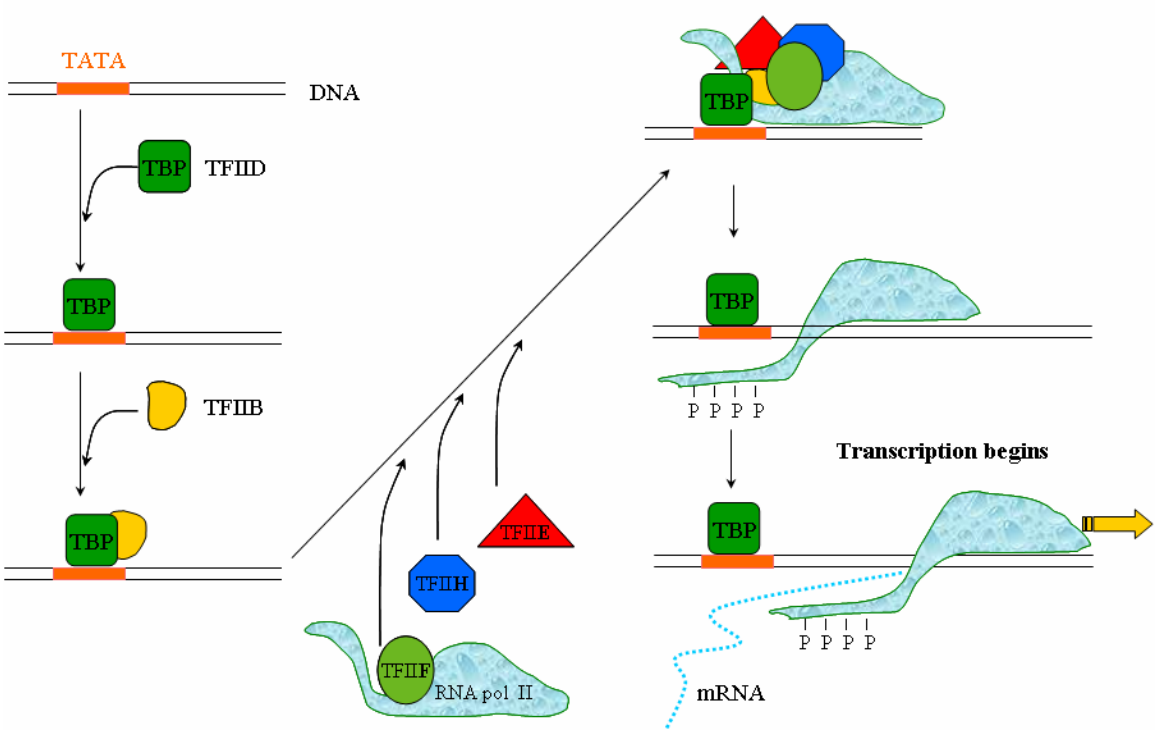

Figure 1. Transcription in Eukaryotes.

The TATA box binding protein (TBP) is a major component in the control of eukaryotic transcription. It acts by binding to the promoter of a gene. The binding site within the promoter typically contains a nucleotide sequence of T-A-T-A, and is thus called the "TATA box" (Siebenlist, *et al*., 1980; Hahn, *et al*., 1989). Although the recognition site of TBP is generally conserved among many organisms, the entire sequence of the TATA box is naturally variable (Smale, 1994). The promoter utilized in this study is the adenovirus Major Late promoter (AdMLP). The crystal structure of the TBP-promoter complex formed on the AdMLP defines the TATA box as an 8 base pair element (TATAAAAG). In the physiological system, TBP is commonly found as

an integral part of a larger protein complex called transcription factor II D (TFIID). This transcription factor is only one among many that work cooperatively to control the actual transcriptional machinery, RNA polymerase II (Goodrich, *et al*., 1994; Hernandez, 1993; Horikoshi, *et al*., 1992; Pugh, *et al.*, 1992; Struhl, 1994; Greenblatt, 1991). TBP alone can support basal levels of transcription. However, TBP-associated factors (TAFs) included in TFIID are required for activated transcription (Burley, *et al*., 1996).

During the initiation of transcription, the binding of TBP to the TATA box sequence results in dramatic structural changes in the promoter DNA. TBP has several unusual properties that distinguish it from most other DNA-binding proteins. X-ray crystallography reveals that TBP binds to the minor groove rather than the major groove of the TATA box. As TBP binds in the minor groove of the TATA sequence, it creates sharp kinks of about 80 º at either end of the sequence (Juo, *et al*., 1996). Between the kinks, the right handed double helix is smoothly curved and partially unwound, presenting a widened minor groove to TBP's concave, antiparallel β sheet (Kim, *et al*., 1993). Upon binding, TBP also induces a severe bend in the DNA that is directed away from the protein, which is in contrast to most other DNA-binding proteins (Figure 2) (Kim, *et al*., 1993; Kim, *et al*., 1994). This bending is due to DNA deformation throughout the center of the TATA box as well as to two pairs of phenylalanine residues on TBP that intercalate at each end of the TATA box (Figure 3b) (Kim, *et al*., 1993). Other changes include the widening of the minor groove

(Figure 3a), compression of the major groove, and untwisting of the DNA helix by approximately 120° (Parkhurst, *et al*., 1999).

Due to the unusual and dramatic structural changes upon TBP binding to DNA, other researchers have been interested in studying the dynamics of a TBP-DNA complex. (Hoopes, *et al.*, 1992; Petri, *et al*., 1995; Parkhurst *et al.*, 1996; Parkhurst *et al*, 1999).

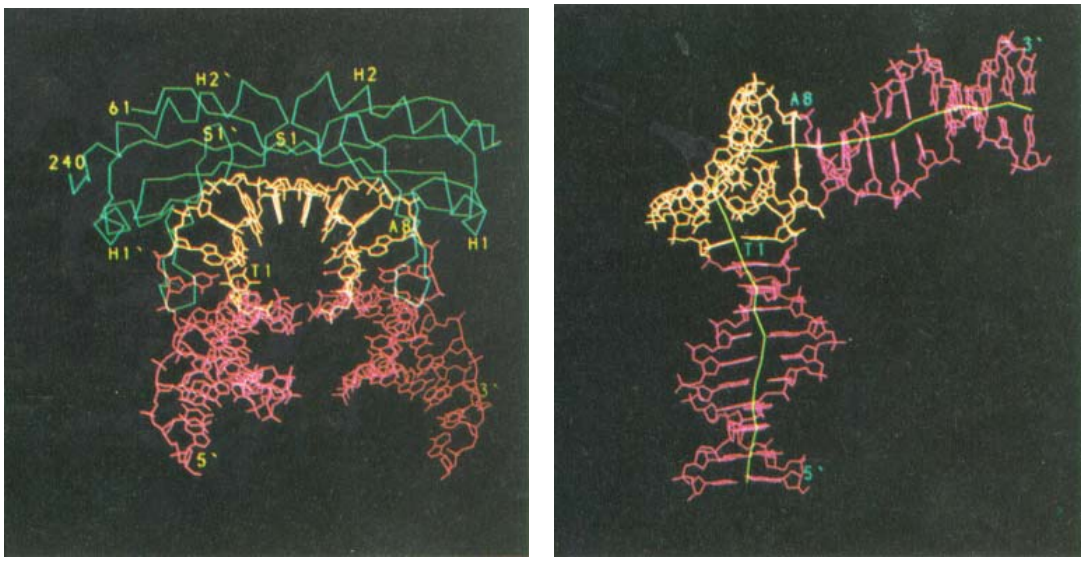

Figure 2. Crystal structure of a Yeast TBP/DNA complex. The left figure shows that Yeast TBP (green) binds to the TATA box (yellow) of the minor groove of the DNA (red). Deformation of the trajectory of the DNA with yTBP omitted is shown at the right. The internal angle is approximately 100 degrees. The DNA axis (bright green line) is the trace of the center of each base pair. (Kim, *et. al.*1993)

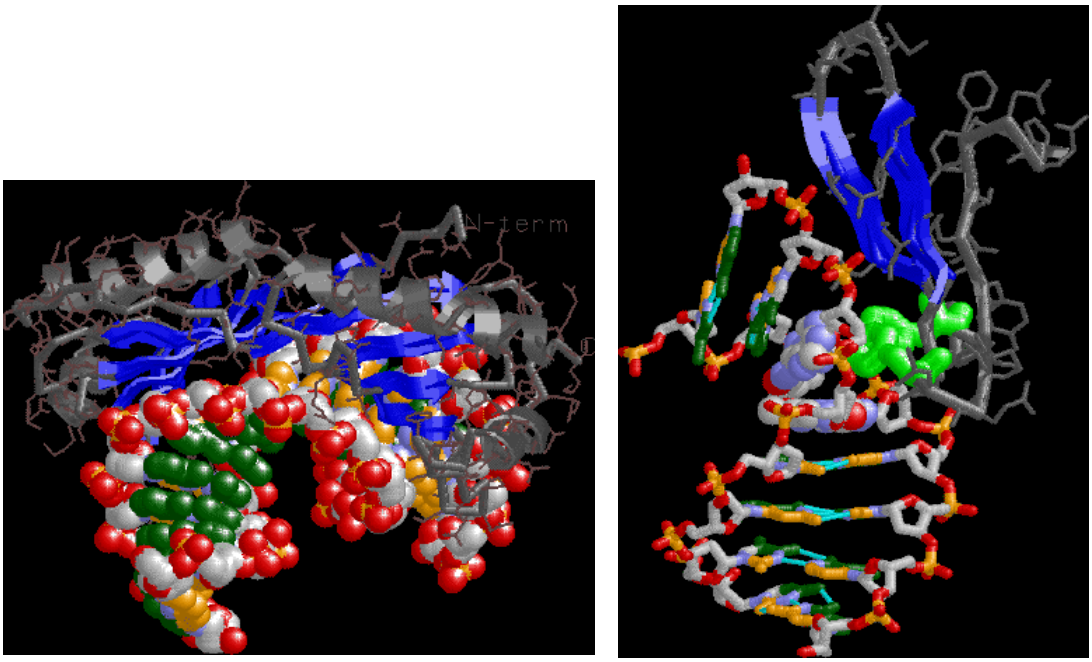

(a) **(b)**

Figure 3. Unusual features of TBP/DNA interaction from human TBP complex. (a) A view emphasizing the minor groove interaction surface. (b) A detail of one end of the TATA box view illustrates that one of the phenylalanine intercalation sites on the "stirrups" bends the DNA into the major groove. -Burley *et. al.* (1996)

Hawley et al. determined that the association rate constant for TFIID binding to the adenovirus Major Late promoter is too slow ($2 \sim 3 \times 10^5\ M^{-1}s^{-1}$) to be consistent with simple diffusion-limited association ($10^8\ M^{-1}s^{-1}$) (Hawley *et al.*, 1985). Likewise, the dissociation of TBP is slow, with a half-life of one hour, under comparable to physiological conditions (Schmidt, *et al.*, 1989). These studies along with the understanding of the profound macromolecular structural changes that occur upon

binding of TBP to a TATA sequence, suggest that the binding mechanism proceeds by more than a one-step pathway (Hoopes *et al*., 1992). In order to explore this multi-step hypothesis, Parkhurst et al. utilized stopped-flow fluorescence resonance energy transfer (FRET) to show that TBP binding and DNA bending occur simultaneously (Parkhurst *et al*., 1996). This observation ruled out a previously postulated mechanism in which the initial binding of DNA is followed by a slow bending.

The most recent time-dependent FRET studies from the Parkhurst group suggests that there are two intermediates along the pathway to a final stable TBP/DNA complex, and that both of the intermediates (I_1, I_2) contain bent DNA (Parkhurst *et al*., 1999).

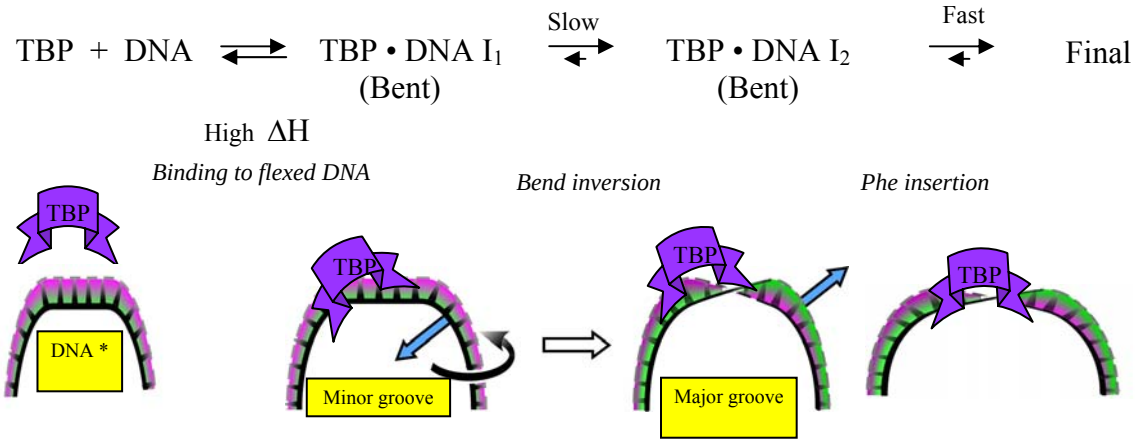

Figure 4. Mapping the TATA box bend inversion idea from cyclization onto FRET results

Figure 4 above is our interpretation about the role of TATA box bending based on the FRET and DNA cyclization results. A high enthalpy transition ($\Delta H^o = 16.9 \pm 2.2$

kcal/mol) from the initial reactants to the first intermediate state (TBP • DNA I) can be identified with recognition of a postulated rare flexed form of TATA box. The first kinetic intermediate identified in the FRET study converts relatively slowly to the second. This slow transition step, a possible rate limiting step, could be due to the inversion of the flexed TATA box since the intrinsic bend is directed opposite to the induced bend. The final step where TBP is locked down into a complex with the TATA box is most likely due to phenylalanine insertion or some other conformation change.

1-2 Connection of DNA supercoiling to transcription

DNA supercoiling is a change in the topological linking number (Lk), which is the number of times one strand of double helical DNA wraps around the other. The linking number remains the same as long as one strand is not broken and rejoined. The linking number is the sum of two components, Lk = Tw + Wr. The twist (Tw) refers to the local winding of the two strands about the helix axis, and writhe (Wr) is the coiling of the helix on itself. There have been many review studies for this linking number and its applications for geometric description (Bates and Maxwell, 1993; Cozzarelli and Wang, 1990; White, 1989; Bauer *et al*, 1980; Kahn, 2002). It has been known that these DNA topological parameters can be utilized as an experimental means to study DNA conformation and many biological processes including initiation of DNA replication, transcription, and site-specific recombination, which require changes in DNA topology (Kahn, 2002).

Most natural DNA is negatively supercoiled as isolated. Negative supercoiling is important in many biological events such as DNA replication, recombination, and transcription. Although there are some contrasting results, generally negative supercoiling enhances transcription, and negative superhelical tension is believed to facilitate to an early opening step of the DNA double helix in the reaction pathway (Parvin and Sharp, 1993; Leblanc and Benham, 2000). For example, it was reported that transcription of the E1b gene was stimulated three- to sevenfold when the template was supercoiled (Banerjee, 1992). Topoisomerase IIα has been found to be associated with the mammalian RNA polymerase II holoenzyme and to stimulate

transcription elongation on chromatin templates (Mondal and Parvin, 2001). The Far Upstream Element (FUSE) DNA sequence regulates the transcription of the c-Myc gene as single stranded DNA (Michelotti and Michelotti, 1996). In light of previous studies, dynamic supercoiling is important in the control of transcription initiation.

1-3. TBP Topology and its possible relationship to chromatin remodeling

Previously, our lab members demonstrated that TBP induces negative supercoiling ($\Delta Lk \sim -0.3$) upon cyclization when it is bound to a series of small (~160 bp) DNA fragments (Davis *et al*., 1999). The amount of negative supercoiling induced is consistent with the observed DNA untwisting in co-crystal structures. But, this was actually unexpected, as in most plasmid experiments, TBP had been shown not to affect DNA topology, and the x-ray crystal structures show that the bound DNA shape should contribute to positive writhe which cancels the negative twist from unwinding (Oelgeschläger *et al*, 1996; Lorch and Kornberg, 1993). According to our previous study of the topological changes of DNA at different lengths induced by TBP and TFIIA (S.S. Majee *et al.*, unpublished), the flattening effect is diminishing with increase in length. From this comparison of the minicircle results with previous plasmid studies, it was suggested that the observed TBP induced negative supercoiling or unwinding is specific to minicircles.

Minicircles are much more difficult to supercoil than larger DNAs (Horowitz and Wang, 1984). Circles larger than 1000 bp can supercoil readily because most of the

DNA in a plectonemic supercoil is not strongly bent. In a small minicircle, the bending free energy cost for making the sharp bends needed to cyclize or especially to writhe is much larger. Therefore, in a small circle any topological strain is partitioned into twist, and the free energy cost of supercoiling is higher at a given supercoil density than for a larger circle (Benham, 1989). In minicircle, the twist/writhe compensation observed in TBP-DNA complexes apparently no longer occurs. We suggest that since writhe for minicircles requires an energetically unfavorable amount of bending, a minicircle tends to flatten DNA in order to reduce the high energy of strain.

With these observations, a possible mechanism for minicircle writhe cancellation has been proposed (Kahn, 2000). Figure 5 shows a possible mechanism for minicircle writhe cancellation. In the TBP•DNA complex, the overall bending in the structure is due to two kinks at the edges of the TATA box introduced by two pairs of partially intercalated phenylalanines of the "stirrup" of TBP (Kim et al., 1993). The proposed flattening of the minicircle is due to progressive retraction of the phenylalanine residues which removes the large roll kinks at the edges of the TATA box. The structure of hTBP-DNA (Nikolov, *et a*l., 1996) is superimposed on low resolution models generated from DNA roll, tilt, and twist angles (Kahn and Crothers, 1993). The purple DNA represents the stirrup form of TBP-DNA complex (Kim and Burley, 1994).

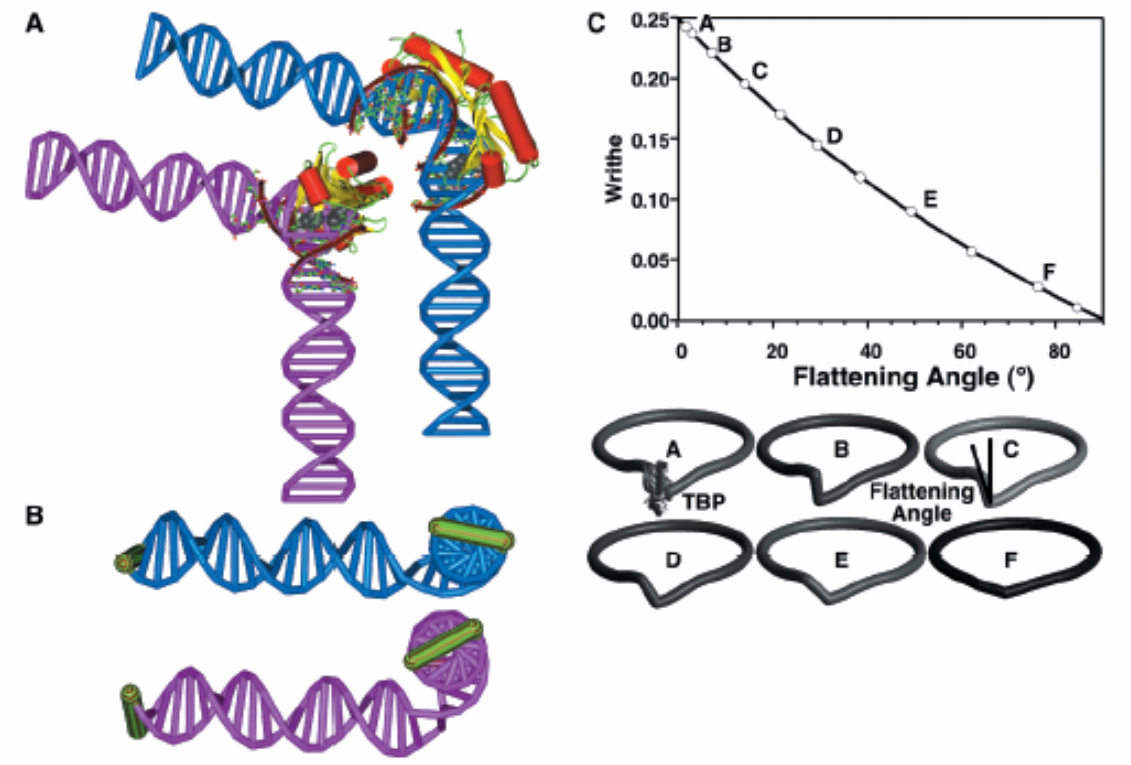

Figure 5. Speculative TBP stirrup retraction mechanism for writhe cancellation through minicircle flattening. (Kahn, 2000)

The blue DNA shows the consequences of stirrup retraction. Panel A shows that the overall bend angle is amazingly unaffected by retraction. Panel B represents flattening. The thick green bar shows the DNA torsional phase, indicating that flattened DNA embedded in a planar circle needs increased twist outside the fragment shown. Thus, loss of writhe upon flattening leads to a compensating positive ΔTw to maintain an integral linking number (Lk = Tw + Wr). This cancels negative superhelical tension in the DNA outside the bound region. Panel C illustrates varying extents of writhe

cancellation, calculated as a function of flattening angle by numerical integration in Matlab (The Mathworks, Inc.).

This model illustrates that the overall bend angle is essentially unchanged. This is because the original structure of TBP-DNA has about 180 ° of local bending, with the kinks oriented perpendicular to bending induced throughout the open minor groove of the TATA box. Thus, the kink removal leaves no change of the minor groove bending. At the molecular level, this proposed flattening model can be assigned to progressive retraction of the partially intercalating two pairs of phenylalanine stirrups of the DNA-TBP structure by removing the large kinks observed at the edges of the TATA box (Kim *et al*., 1993; Kim and Burley, 1994; Nikolov *et al.*, 1996). This "stirrup retraction model" could be tested by mutation of the intercalating phenylalanine residues in TBP. We therefore created two mutant TBPs: the C-stirrup TBP mutant (F99A-F116A) and the Quadruple TBP mutant (F99A-F116A-F190A-F207A) to test how these topological changes affect the binding interaction of TBP-DNA. According to the theory, mutants should bind much better to supercoiled minicircle DNA than to linear DNA, relative to wild type TBP.

It is very possible that supercoiled minicircle can provide an excellent model for studying topological effects in small chromatin domains. Because the minicircles used for these studies are similar in size to a nucleosomal repeat (~160 bp, typically one nucleosome contains 146 bp (Carey and Smale, 2000), the topological consequences of

a given ΔLk could be similar to nucleosome environment. Thus, nucleosome is the next possible candidate for connection of this model.

In eukaryotes, DNA packaging in the small chromatin domain generally represses transcription. Therefore, transcriptional activation requires chromatin remodeling machinery. This machinery has two classes: histone acetyltransferases (HATs) and ATPases. The general aspect is that each class releases the negative supercoiling from nucleosomes (Corona *et al*., 1999; Hamiche *et al*., 1999). Upon remodeling, the normal restrained ΔLk = -1 of the nucleosome becomes less negative and this can be detected because released negative supercoiling is removed by the topoisomerase. Previous studies in vitro show that the remodeling releases ΔLk = +0.7 per nucleosome on minichromosomal templates (Stafford and Morse, 1997) and acetylation of histone 3 and histone 4 in reconstituted minichromosomes gives ΔLk = + 0.2 (Norton *et al.*, 1990).

A possible model that relates chromatin remodeling to TBP binding has been proposed (Figure 6) (Kahn, 2000). Repressed nucleosomal chromatin (cyan DNA around a red histone core) is remodeled by an ATPase, and histones are released by unraveling DNA. By doing this, unrestrained negative supercoiling is released, shown as writhe (blue DNA). Then, TBP binds to the strained DNA and relaxes some of the writhe by absorbing superhelical strains as untwisting. The decreased negative writhe (to give the green DNA on right) provides a thermodynamic driving force enhancing TBP binding to the negatively supercoiled DNA. The dark blue termini represent fixed

attachment sites to neighboring chromatin. The model predicts that the binding of TBP to a small topologically closed domain like chromatin will be inhibited by a positioned nucleosome, because introducing substantial writhe and twist changes into the remaining short segment of unbound DNA is energetically too expensive. Remodeling the nucleosome, and the accompanying release of negative supercoiling, should then enhance TBP binding. Thus, it suggests a possible connection of mechanism between the remodeling machinery and TBP.

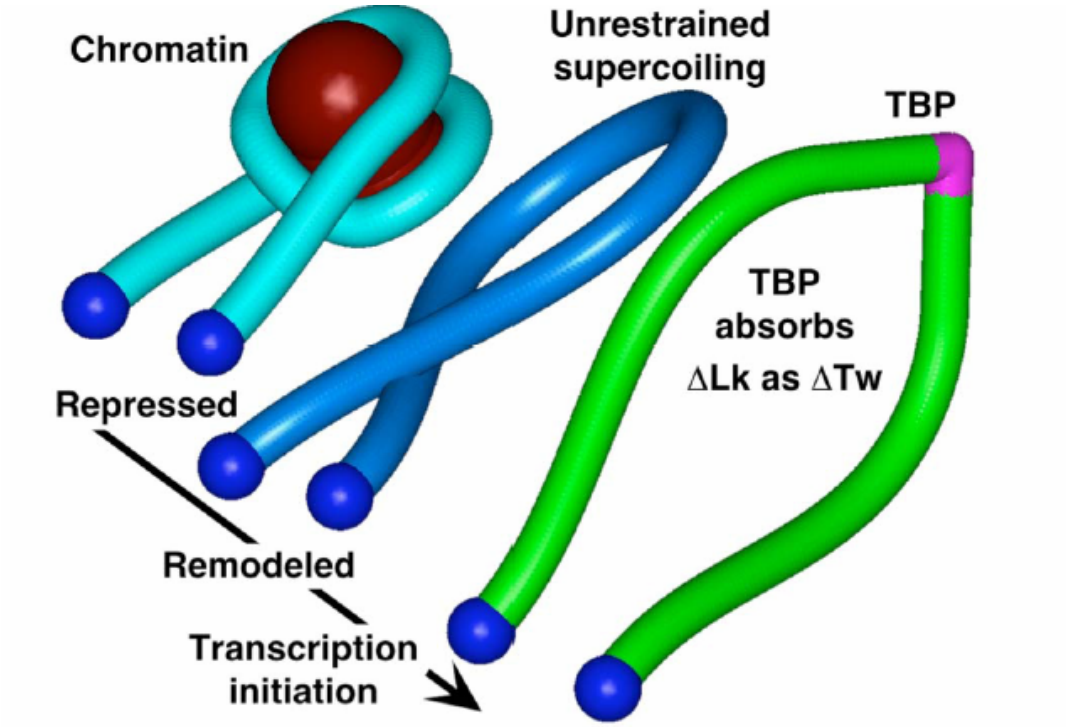

Figure 6. Proposed thermodynamic coupling of chromatin remodeling and TBP binding.

1-4. Characterization of DNA - protein system

Proteins regulate a target gene by binding to defined DNA sequence elements (Carey, 2000). Many molecular biological and chemical techniques have been developed to identify and characterize these DNA control sequences. Common assays for characterizing these binding sites and the effect of bound protein molecule are the electrophoretic mobility shift assay (Fried and Crothers, 1981; Garner and Revzin, 1981), DNase I footprinting (Galas and Schmitz, 1978; Dynan and Tjian, 1983), hydroxyl radical footprinting (Revzin, 1993), synchrotron x-ray footprinting (Dhavan, *et al*., 2002), and methylation interference assays (Siebenlist and Gilbert, 1980). The Electrophoretic Mobility Shift Assay (EMSA) relies on the principle that a fragment of DNA to which a protein has bound will move more slowly in gel electrophoresis than the same DNA fragment without bound protein. Although the EMSA provides the means of obtaining information on DNA-protein interaction, it can't be used to localize the exact area along the DNA strand of the contact between DNA and protein. For this purpose, the footprinting assay is used. The general idea of all footprinting methods is to identify DNA sequences that are protected from attack by a chemical (such as hydroxyl radical) or enzyme (such as DNase I nuclease). Typically one end of a DNA strand or duplex is radiolabelled before the reaction. After cleavage, separation of the fragments in a gel gives a ladder of bands representing the products of cutting at varying distance from the labeled end. Where a particular sequence of the DNA has been bound by a protein, however, it will be protected from digestion and hence the bands corresponding to cleavage at these points will be

absent. This is visualized as a blank area on the gel where labeled fragments would have been referred to as the footprint of the protein.

The methylation interference method is based on assessing whether the methylation of specific G residues in the target DNA affects protein binding. Partially methylated DNA is used in a DNA mobility shift assay and both the DNA which has failed to bind protein and that which has bound protein and formed a retarded band are subsequently cleaved at methylated G residues with piperidine. If methylation at a specific G residue has no effect on protein binding, the bound and unbound DNA will contain equal amounts of methylated G at the protein. In contrast, if methylation at a particular G prevents binding of the protein, only the unbound DNA will contain methylated G at this position. Taken together these EMSA, footprinting, and methylation interference assays can provide considerable information on the nature of the interaction between a specific DNA sequence and protein. To characterize TATA box binding protein (TBP) interaction with DNA, EMSA and hydroxyl radical footprinting assays were utilized.

1-5. Creativity of this thesis

To be able to test ideas proposed above, we developed a footprinting method for the circular DNA for the first time and applied it to the interaction of wild type TBP and mutant variants to supercoiled minicircles. The detailed content of the method will be introduced in next section.

2. MATERIALS AND METHODS

2-1 DNA labeling and purification

We chose the template as one of our favorite in phase molecules, Ad15A9 (one of the DNA constructs containing a TATA box separated by a variable length phasing adaptor from an A-tract bend), which previous lab members have constructed (Davis *et al.*, 1999). *Bst N1* restricted the plasmids were used as PCR templates (~ 10^{8} molecules / 100 μL) in a reaction mixture (100 mL) containing 0.2 μM primer, 20 μM of each dNTP, 2.5 unit of cloned *Pfu* polymerase (Stratagene), 10.2 % glycerol, 50 μCi of [γ-^{32}P] ATP, and 1x *Pfu* polymerase buffer. The mixture reaction was subjected to 25 cycles of 30 sec at 94 °C, 30 sec at 55°C, 1 sec at 60 °C, 1 sec at 66 °C, 1 min at 72 °C, and 1 cycle of 10 min at 72 ° C.

The bottom primer used for 203 bp molecule was

5'-ATT CCA TGC AAC GCG TTC CTG AAG -3'

The bottom primer used for 206 bp molecule was

5'-AAT CCA TGG CGC AAC GCG TTC -3'

The bottom primer used for 210 bp molecule was

5'- ATT CCA TAT GAG GCG CAA CGC GTT CCT GAA -3'

The blunt end top primer for all three molecules was

5'- CTG TAC GGA TCC GGA AA AAC GGG C -3'

PCR products were extracted with phenol and chloroform and the DNA was precipitated with using 150 mM NaOAc and 2.5 volumes of 100 % ethanol and

purified on a 6 % native polyacrylamide gel [40:1 acryl amide: N,N'-methylene bisacrylamide, 50 mM Tris-boric acid, 1mM EDTA]. (Figure 7). The DNA was eluted form the gel slice by soak and crush method in 50 mM NaOAc and 1mM EDTA for over night and concentrated by ethanol precipitation. The concentration was measured by scintillation counting considering the specific activity of the γ-^{32} P ATP.

2.2 Preparation of minicircles

In order to conduct this research with circular DNA, we utilized a minicircle DNA model, which offers topological domains that closely mimic the natural state of DNA in chromatin. Our minicircle systems (203 – 210 bp) are also essentially the similar size as the DNA in one nucleosome. (Figure 8).

The minicircle DNAs were prepared by blunt end ligation of the three linear blunt PCR product DNA molecules (203 bp, 206 bp, and 210 bp). We varied the DNA length in order to observe the effects of pre-bent and pre-twisted DNA upon TBP binding. The ΔLk = 0 topoisomer is pre-bent but not untwisted. The ΔLk = -1 topoisomer is pre-bent as well as unwound.

To maximize the blunt end ligation yields, 80,000 U/mL T4 ligase was used in 625 μL reaction volume containing 50 mM Hepes (pH 7.9), 90 mM K-Glutamate, 5mM EGTA, 2.5 mM DTT, 10.2 % glycerol, 10 mM $Mg(OAc)_2$, 100 mg/mL gelatin, 0.1 % Nonidet P-40, 0.4 mM ATP.

To generate ΔLk = -1 circular DNA, 0.25 μg/mL of the intercalating chemical ethidium bromide was added to the reaction mixture and incubated at 25 °C overnight. For the ΔLk = 0 circular DNA, the reaction mixture was incubated at much lower temperature, 4 °C overnight. After the reaction, mixture was inactivated at 65 °C for 10 min and ethanol precipitated to concentrate the sample. The concentrated sample was loaded onto a 6 % native gel containing 0.01 mg/mL chloroquine to resolve topoisomers [75:1 acrylamide: bis, 90 mM Tris borate, 1 mM EDTA, pH = 7.9] for ligation purification (Figure 9, 10). Each topoisomer was isolated from the gel and the gel slice was eluted by the soak and crush method in 50 mM NaOAc and 1 mM EDTA overnight. The circular DNA was extracted with phenol and chloroform to remove ethidium bromide and chloroquine and concentrated by ethanol precipitation. Exonuclease analysis was performed on the isolated topoisomers to verify that they are closed circular DNA (data not shown).

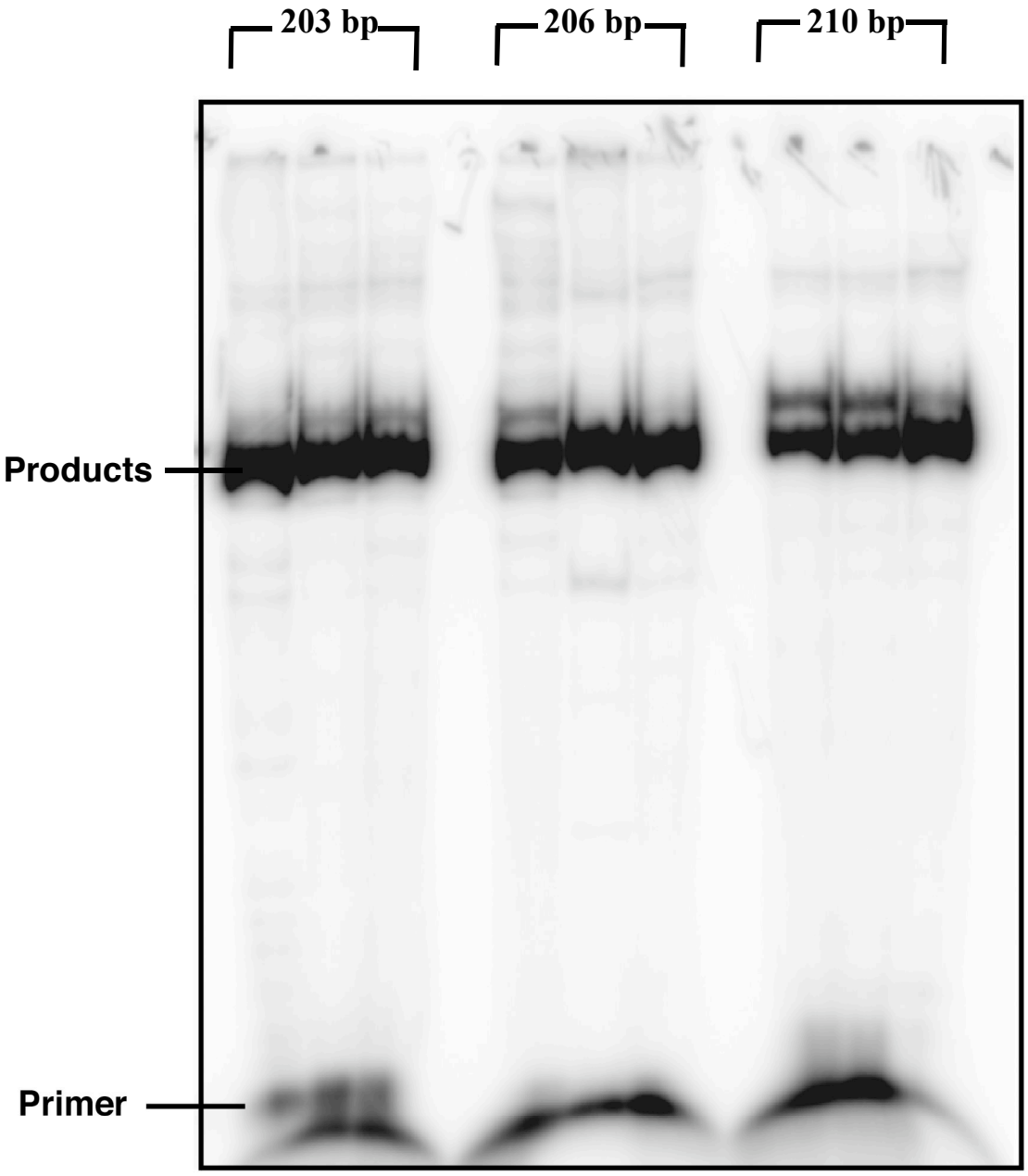

Figure 7 : PCR Products for 203 bp, 206 bp and 210 bp DNA Molecules

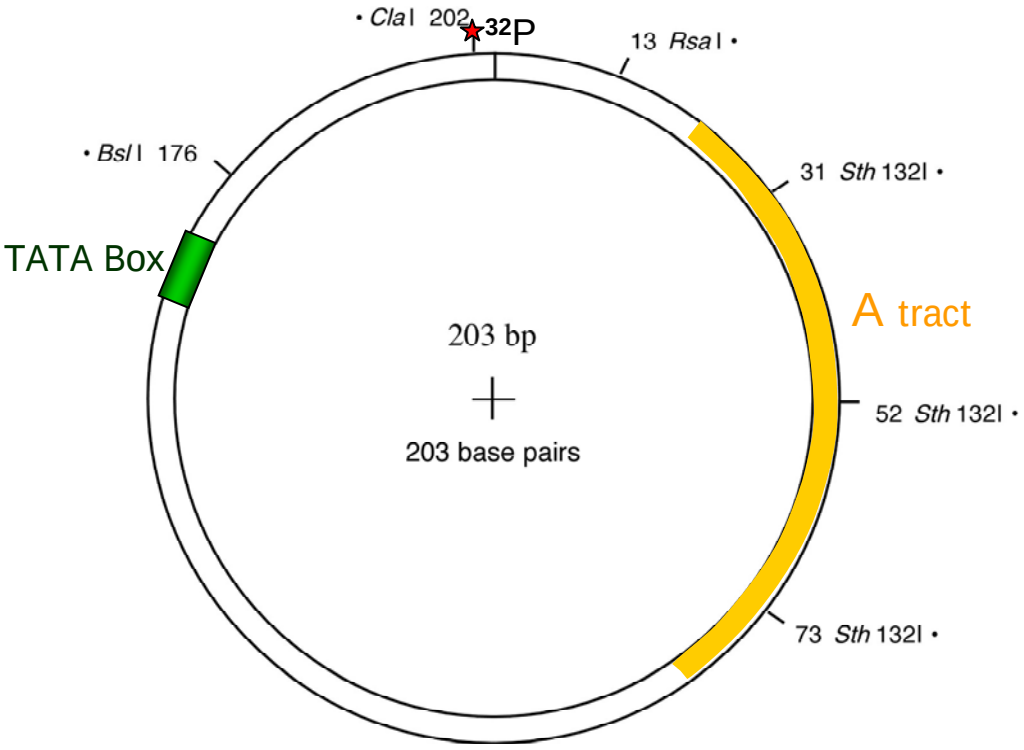

Figure 8. Schematic pre-bent minicircle DNA (203 bp). TATA box is located from positions –26 to 33 derived from Adenovirus Major Late promoter.

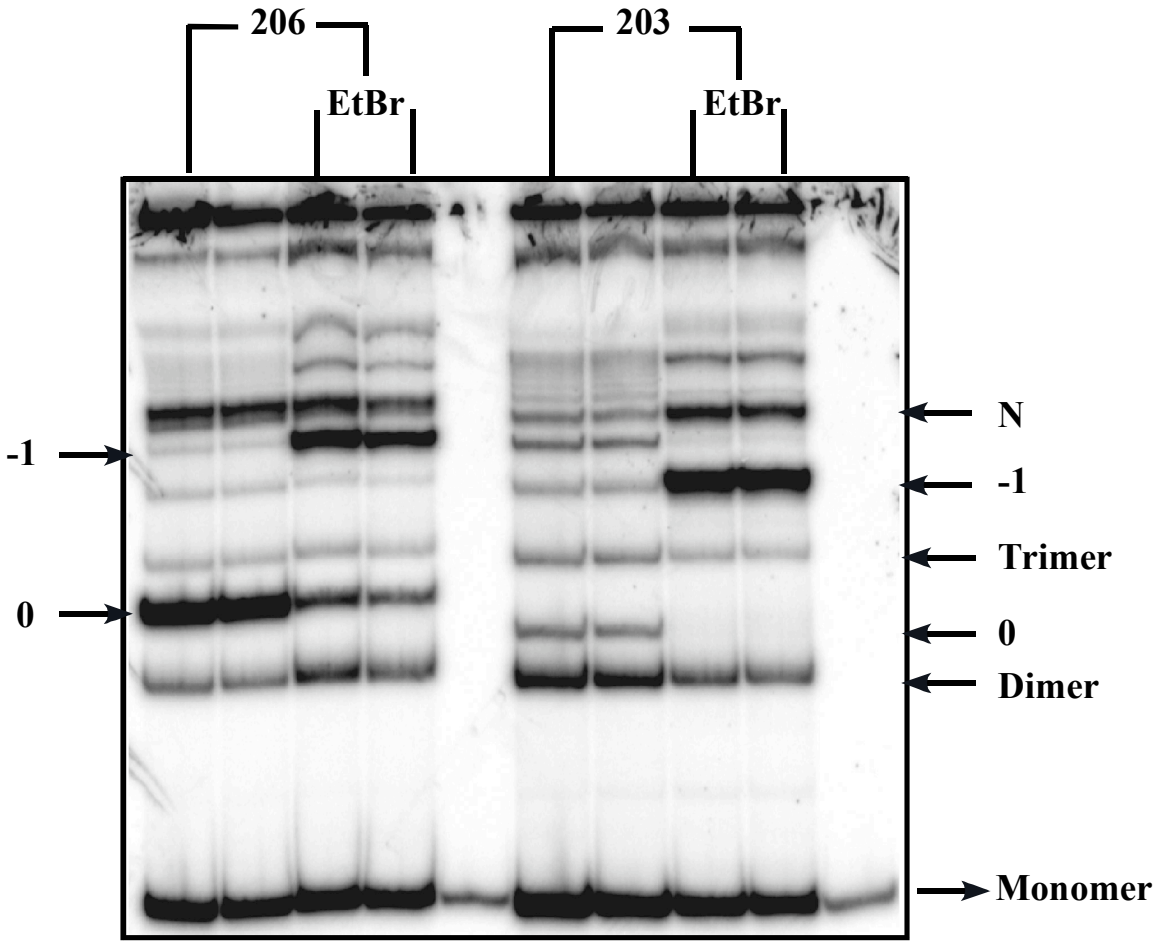

Figure 9 : Blunt End Ligation of 203 bp and 206 bp DNA minicircles analyzed on a 6 % PAGE with Chloroquine. N = nicked

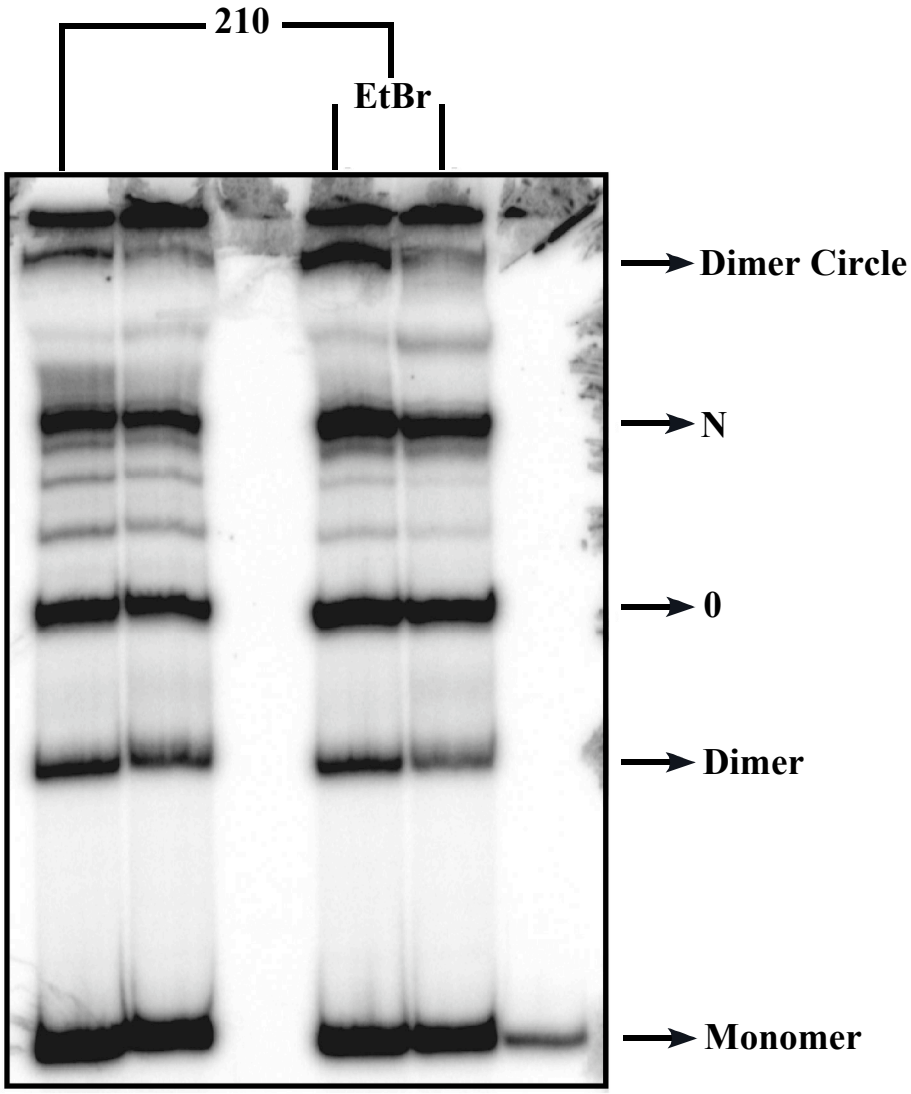

Figure 10 : Blunt End Ligation of 210 bp DNA analyzed on a 6 % PAGE with Chloroquine. N = nicked

2.3 Engineering plasmids containing mutated *SPT15* genes by site directed mutagenesis

TBP Expression vector

The *SPT15* (Arndt *et al*., 1992) gene that encodes the yeast (*Saccharomyces cerevisiae*) TBP was located in the plasmid pKA9, which was generously given to our lab by Dr. Michael Brenowitz (Albert Einstein College of Medicine). The pKA9 vector expresses TBP under the control of a T7 promoter and also contains the gene for resistance to ampicillin. The plasmid was isolated from the *E. coli* strain BL21(DE3) using a commercially available midi prep kit (Qiagen). 1-3 μL of the plasmid (5 pg to 0.5 μg) was mixed with 50 μL of electrocompetent cells for electroporation. An electric field of 17 kV/cm was applied to the mixture. 1 mL of SOC media was placed into the reaction mixture after the pulse to allow cells to recover. The cells were then plated out on LB plates with 50 μg/mL of ampicillin to isolate single colonies.

Engineering F99A and F116A

The PAGE purified top (5'-CATGATGACAGCAGCCGCACGCTTGGGGTTA TA-3') and bottom primers (5'- TATAACCCCAAGCG TGCGGCTGCTGTCATC ATG-3') for mutagenesis were purchased from Integrated DNA technologies (IDT). The mutagenic primers contained the mutation codon GCG (Ala) at the site of 99 codon of TTT (Phe) on the *SPT15* gene This single mutation was carried out by Quikchange Site-Directed Mutagenesis kit (Stratagene). The processed cycle was 1

cycle at 95 ° C for 30 seconds, 16 cycles of (95 ° C for 30 seconds, 55 ° C for 1 minute, and 68 ° C for 11 minutes). The mutated plasmid was transformed into XL-1 BLUE competent cells by electroporation. The transformed XL-1 BLUE was cultured. The mutated plasmids were sequenced at our DNA sequencing facility center and the successful plasmid was used for the second mutation of F116A using the same single mutation method described above.

Engineering F190A and F207A

Simultaneous mutations F190A and F207A on the C terminal side chain were conducted by Quikchange multi site-directed mutagenesis kit (Stratagene). The processed thermal cycle was 1 cycle at 95 ° C for 1 minute, 30 cycles of (95 ° C for 1 minute, 55 ° C for 1 minute, and 65 ° C for 12 minutes). The plasmid had mutations of F99A and F116A was used for the template. Top strand primer (5'-CCTCCTATG AGCCAGAATTGGCGCCTGGTTTGATCTATAGAATGG-3') for F190A has 45 bases with the mutation codon of GCG for TTT and top strand primer (5'-GAAGCC GAAAATTGTGTTGTTAATTGCGGTTTCAGGAAAGATTGTTCTTACTG -3') for F207A has 53 bases with the mutation codon GCG for TTT. These purified primers were also purchase by IDT. The resulted mutated plasmid was sequenced at the same DNA sequencing facility.

2.4 Purification of wild type TBP, C-stirrup TBP mutant, and quadruple TBP mutant

Plasmids containing either the wild type *SPT15* gene, the F99A, F116A mutant, or the F99A, F116A, F190A, F270A mutant were introduced into BL21(DE3) cells. The cells were grown in flasks in LB media containing ampicillin (50 μg/ml). Cells expressed wild type TBP were incubated at 37 °C. For the C-stirrup and quadruple mutants, the cells were grown at 30 °C to reduce the production of inclusion bodies and to promote better overexpression. When the optical density at 600 nm reached 0.4, IPTG was added to a final concentration of 1 mM and the cells were grown for 2 more hours. Cells were harvested by centrifugation at 6000 g for 15 min at 4 °C in a Beckman Avanti J-25I centrifuge and stored at – 80 °C.

Frozen cells were thawed on ice and resuspended (3 ml/gm of cells) in buffer A (25 mM Hepes-KOH, pH 7.9, 20% glycerol, 1mM EDTA, 1mM DTT) + 1 M KCl + 1 M ammonium acetate, supplemented with the following protease inhibitors added just prior to resuspension: aprotinin (1 μg/ml), chloromethylketone (20 μg/ml), leupeptin (1 μg/ml), PMSF (1 mM), and trypsin inhibitor (100μg/ml).
Cells were lysed by sonication and the suspension was centrifuged (Beckman Avanti J-25I centrifuge 18,000 rpm, 4 °C) for 20 minutes. The supernatant was ultracentrifuged (Beckman 45Ti at 45,000 rpm at 4 °C for 3 hours) to remove suspended particles. For the Quadruple stirrup mutant, this ultracentrifugation step was removed to avoid pelleting the protein. The supernatant was desalted by running HiPrep 26/10 column (GE Healthcare) with AKTA FPLC (GE Healthcare) and

precipitated the DNA by slowly adding a protamine sulfate solution (6 mg/ml) to a final concentration of 0.2 mg/ml. The suspension was centrifuged for 20 min (18,000 rpm, 4 °C).

The supernatant was eluted through SP XL 1 mL cation exchange column (GE Healthcare) by salt gradient method. Each fraction was analyzed by SDS-PAGE and the pure fraction region was combined, concentrated and loaded onto Sephacryl S-300 or S-100, gel filtration column (GE Healthcare). Purified protein samples were divided into small aliquots enough to be used one time only, and store at – 80 °C.

2.5 DNase I footprinting

Deoxyribonuclease I (DNase I, a random DNA cleaving enzyme) protection mapping, or footprinting, is a valuable technique for locating specific proteins binding sites on DNA (Galas and Schmitz, 1978; Weaver, 1999). (Figure 11)

TBP of various concentrations was allowed to bind the labeled DNA at 21°C for 30-45 minutes. Other experimental details are as discussed (Parkhurst, 1996). DNA and protein complexes were digested with 0.04 ~0.1 units of DNase I at room temperature for 1 minute in a buffer containing 50 mM HEPES (4-[2-Hydroxyethyl]-1-piperazineethanesulfonic acid, pH 8.0), 200 mM K+ Glutamate, 1 mM $CaCl_2$, 2.5 mM DDT, 10 % glycerol, 10 mM $Mg(OAc)_2$, 100 μg/ml gelatin, 5μg/ml poly(dI-dC), 50 μg/ml BSA (Bovine serum albumin), and 0.05 % Nonidet P-40 detergent (NP-40). Reactions were stopped by adding stop solution (100 % ethanol, saturated

(10M) ammonium acetate, 0.25 % linear polyacrylamide) .The DNA was precipitated with ethanol, resuspended into formamide loading dye (80 % formamide, 1 mM EDTA (Ethylenediamine tetraacetic acid), 10 mM NaOH, 0.1 % bromophenol blue), denatured by heating at 90 °C for 5 minutes and subjected to electrophoresis (8% denaturing gel: 50 ml 8M Urea with 8 % Acrylamide in 1× TBE, 250 µl of 10 % APS, 25 µl of TEMED [Tetramethylethylenediamine]). Chemical sequencing of the DNA with piperidine formate was performed as a marker (A+G), labeled DNA was incubated in 0.25M piperidine formate (pH 2.0) at 60°C for 15 minutes, lyophilized and resuspended into formamide loading dye.

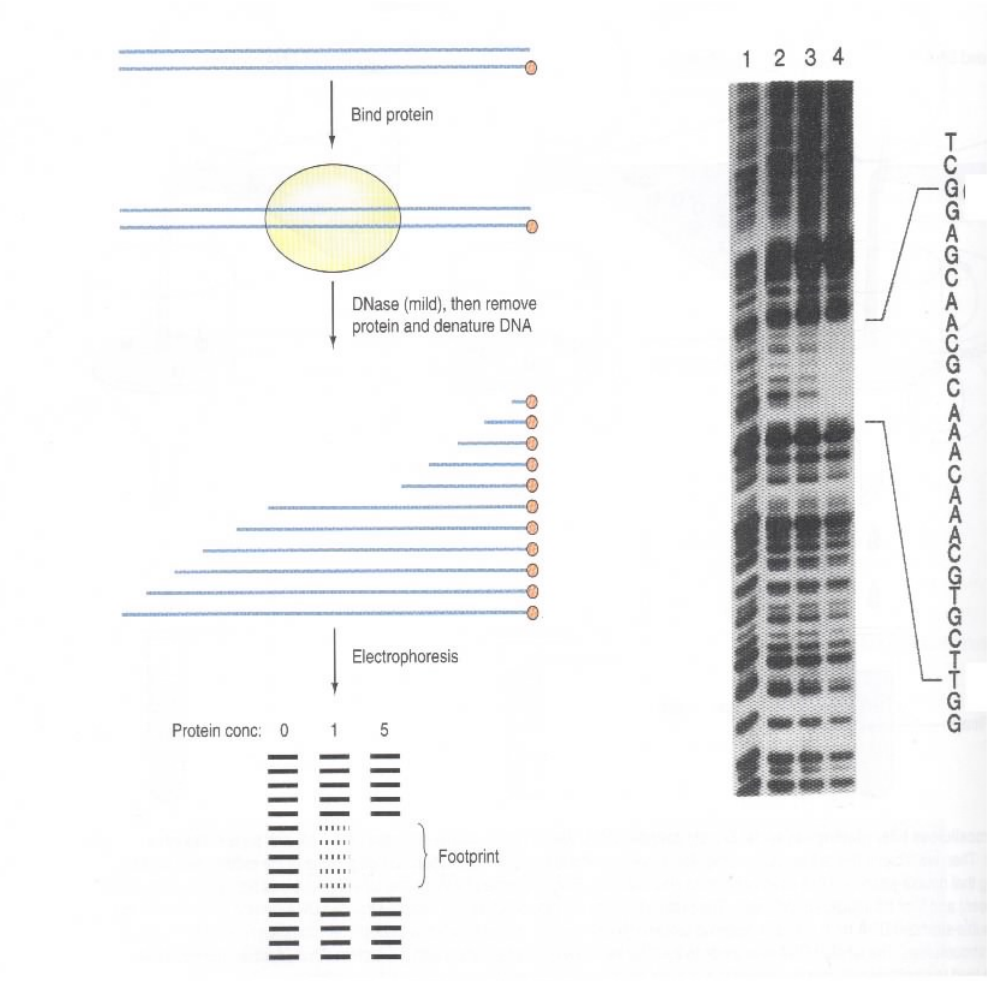

Figure 11. DNase footprinting. The outline of the method is on the left and actual experimental results are on the right (Weaver, 1999).

2.6 Quantitative hydroxyl radical footprinting

2000 cpm (~100 pM) of singly end labeled DNA was placed in 50 µL footprinting buffer containing 50 mM Hepes, 90 mM KCl, 1% glycerol, 1 mM EGTA, 2.5 mM DTT, 10 mM Mg(OAc)2, 0.01 % Nonidet P-40, 200 µg/mL gelatin, and 15 µg/mL poly dI-dC. 5 µL each of 10 mM sodium ascorbate, 10 mM $[Fe(EDTA)]^{2-}$, and 0.03 % H_2O_2 solution were added to a single spot on the wall of the Eppendorf tube, and then the drop was allowed to fall into the solution to initiate the Fenton reaction (Revzin, 1993). The solution was then gently vortexed and left for 30 seconds at room temperature. The reaction was quenched by adding 200 µL of stop solution from a stock composed of 6000 µL of 100 % ethanol, 520 µL of 8 M NH_4OAc, and 32 µL of 10 mg/mL of tRNA. Then, the eppendorf tubes were placed in a dry ice bath for 30 min and spun down for 20 min at 4 °C in a microcentrifuge. The supernatant was gently decanted. The pellet was resuspended with 80 % ethanol, and the eppendorf was gently inverted twice and placed in the dry ice bath for another 20 min to reprecipitate the DNA. The supernatant was removed and the pellet was washed one more time with 80 % ethanol followed by centrifugation at 4 °C for 10 min. The pellet was dried thoroughly in a SpeedVac concentrator (Savant). The sample was resuspended in 7 µL of sequencing loading dye (855 µL of deionized foramide, 25.6 µL of 2.5 % bromophenol blue, 25.6 µL of 2.5 % xylene cyanol).

For the analysis of circular DNA, the dried pellet was resuspended in water for *Rsa I* restriction reaction (Figure 12). 5 µL of 10 X *Rsa I* buffer, 1 µL of *Rsa I*

(Fermentas) was added in a total reaction volume of 50 µL and incubated for 2 hours at 37 ° C. The reaction was quenched at 65 °C for 20 min and DNA was precipitated, dried and resuspended in the sequencing loading dye as above and denatured by heating at 90 °C for 5 minutes and subjected to electrophoresis (8% denaturing gel: 50 ml 8M Urea with 8 % Acrylamide in 1× TBE, 250 µl of 10 % APS, 25 µl of TEMED [Tetramethylethylenediamine]).

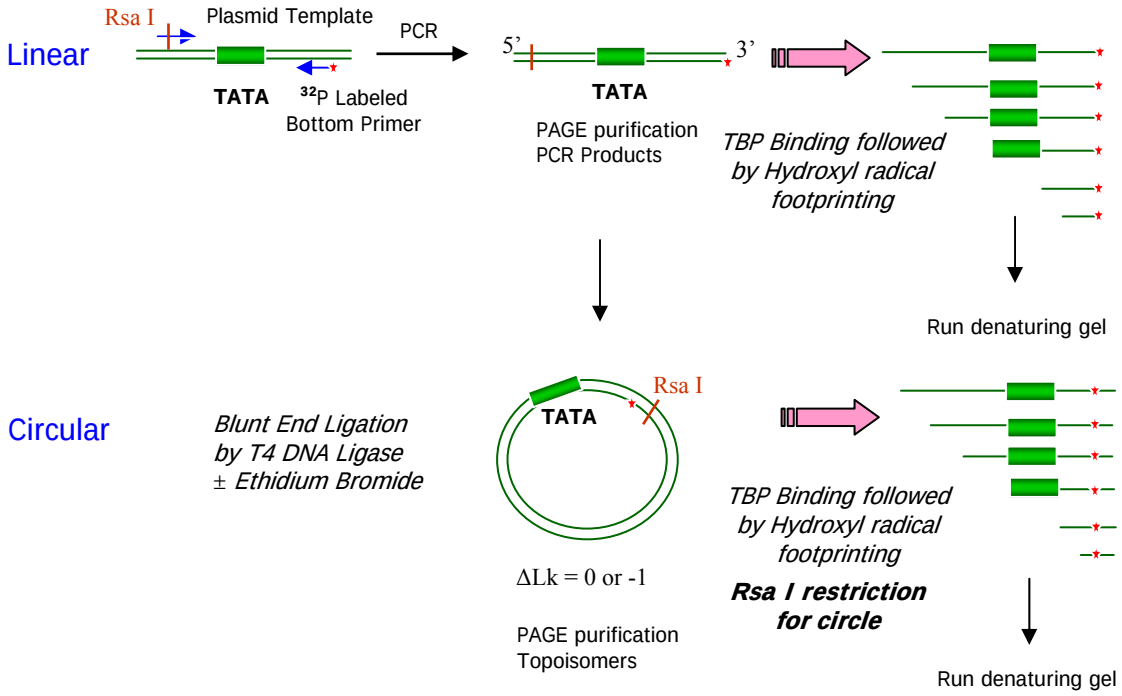

Figure 12. Hydroxyl radical footprinting method for linear and circular DNA.

2.7 Electrophoretic Mobility Shift Assay

Using various concentrations of wild type TBP and two mutants, the labeled DNAs were incubated for 30 ~ 45 min at 30 °C in the same buffer used for the footprinting experiment. The mixture of free DNA and bound TBP-DNA complex was analyzed on an 8 % native gel [75:1. acrylamide / N,N'-methylenebisacrylamide, 50 mM Tris-boric acid, 1 mM EDTA, 2 mM DTT, 3 mM $MgCl_2$, 1 % glycerol]. The gel was run for 2 hours at 24 V/cm at 21 °C in TBE running buffer containing 3 mM $MgCl_2$ and dried for analysis using Molecular Dynamics PhosporImager.

3. RESULTS

3-1. Site directed mutagenesis of TBP

3-1-1. Mutagenesis to produce F99A-F116A mutant

To test the proposed stirrup retraction model as previously described in the introduction section, the C-stirrup mutant TBP (F99A-F116A) and the Quadruple mutant TBP (F99A-F116A-F190A-F207A) have been produced by site directed mutagenesis.

Plasmid pKA9, containing the wild type TBP gene (*SPT15*) was generously provided by Michael Brenowitz (Albert Einstein). Its identity was verified by sequencing and restriction discussion as follows. The plasmid was restricted by two enzymes, *Ava I* and *Pst I,* which cleave at positions 2993 and 749 of pKA9 respectively. The resulting two DNA fragments after cleavage are 3499 bp and 2244 bp, and fragments matching this size were observed (data not shown). The pKA9 plasmid was also sequenced with two primers, the top primer (T7 primer : 5'- TAATACGACTCACTATAGGG- 3') and the bottom primer (5'-TGGTGG ATCGTCTCTATTAAGCGC-3') at the University of Maryland of College Park DNA Sequencing Center. We found the pKA9 was intact and no irregular mutations were present.

There are many phenylalanines in TBP but only four of them are responsible for causing the dramatic stirrups. These four phenylalanine sites 'N - 99 – 116 – 190 – 207- C' are colored green in Figure 13.

The first mutant TBP, F99A (Phe 99 → Ala 99) was constructed by QuikChange™ Site-Directed Mutagenesis (Stratagene) with mutated primers as indicated in the materials and methods section. With the resulting mutated plasmid as a template, the C-stirrup TBP double mutant, F99A-F116A, was engineered by the same thermal cycling method. Miniprepped plasmids were sequenced to verify the correct mutation.

3-1-2. Mutagenesis to produce F99A-F116A-F190A-F207A mutant

To generate the quadruple TBP mutant, F99A-F116A-F190A-F207A, the C-stirrup mutant plasmid was used as a template for QuikChange™ Multi Site-Directed Mutagenesis (Stratagene). We sequenced the mutant plasmid as above.

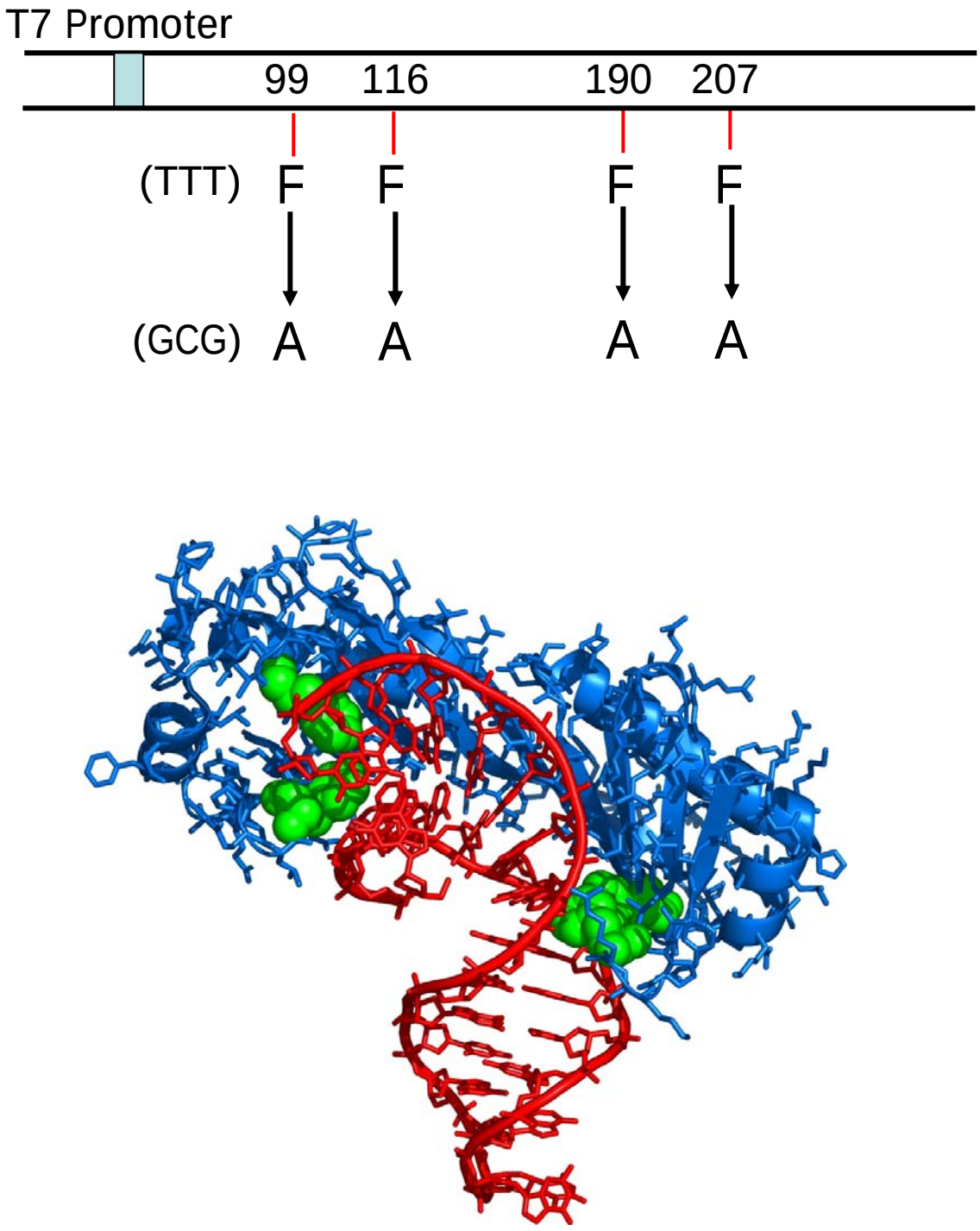

Figure13. yTBP-DNA structure (Kim *et al.*, 1993). Four phenylalanine residues are indicated in green, yTBP is shown in blue. The left side of protein is the C – terminal, half. DNA is indicated in red. This is generated by PyMOL. The top figure shows the scheme of the mutated sites in the yTBP gene.

3.2 Purification of TBP and mutant variants

The overexpression level of wild type and C-stirrup TBP in the BL21(DE3) and BL21(DE3)pLysS strains of *E. coli* was tested (Figure 14). These strains contain a λDE3 lysogen that encodes T7 RNA polymerase under control of a lac promoter. The pLysS plasmid encodes T7 lysozyme, which is natural inhibitor of T7 RNA polymerase, and will stop the leaky expression. Both BL21(DE3) and BL21(DE3)pLysS showed good induction levels for the wild type TBP and C-stirrup TBP mutant. We also checked for a good level of induction for the Quadruple TBP mutant with BL21(DE3) (data not shown). The BL21(DE3) strain of *E. coli* was used for TBP purification.

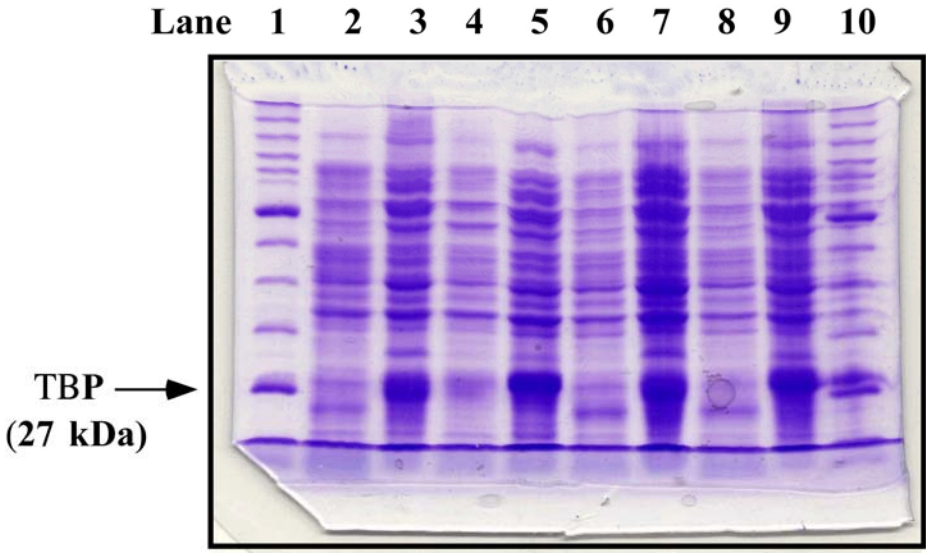

Figure 14. Wild type and C-stirrup TBP protein expressions in 15 % SDS-PAGE. 1 and 10: Protein Marker (MW for wild type yTBP: 27 kDa; 2, 3: wild type TBP expression in BL21(DE3) with and without IPTG; 4, 5: C-stirrup TBP mutant expression in BL21(DE3) with and without IPTG; 6, 7: wild type TBP expression in BL21(DE3)pLysS with and without IPTG; 8, 9: C-stirrup TBP mutant expression in BL21(DE3)pLysS with and without IPTG

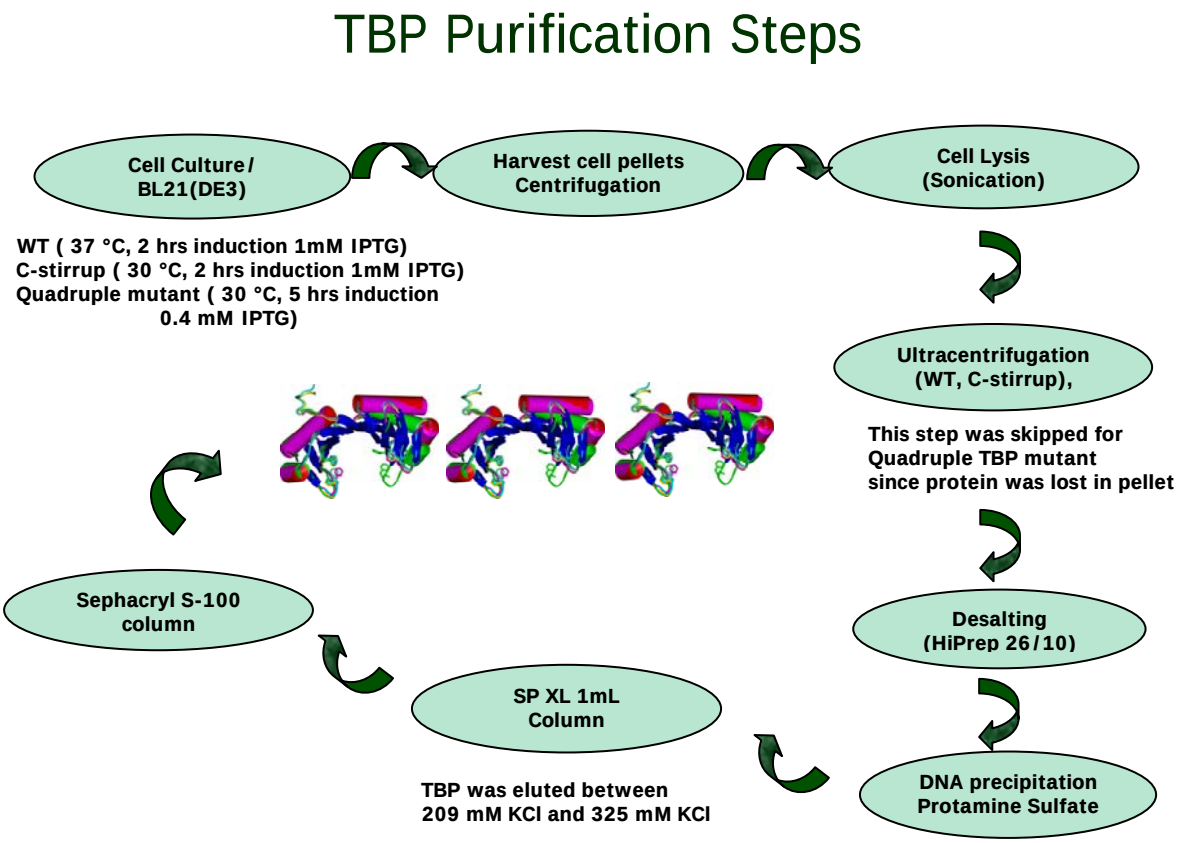

Figure 15. TBP purification process.

Protein purifications for wild type TBP and C-stirrup and quadruple TBP mutants were carried out as indicated in Figure 15. The detailed conditions for the process were described in the materials and methods section. Conditions for cell growth were optimized separately for wild type and each mutant. Wild type TBP expressing cells were incubated at 37 º C and induced with 1 mM IPTG for 2 hours. C-stirrup TBP mutant cells were grown at 30 º C and induced with 1mM IPTG for 2 hours, Quadruple TBP mutant cells were incubated at 30 º C and induced with 0.4 mM IPTG for 5 hours to reduce the level of inclusion bodies and optimize the stability. The Quadruple TBP mutant was pelleted at the ultracentrifugation stage. So, this step was

skipped for that particular purification. The solubility of the protein must have been changed upon changing four phenylalanine residues to alanine. All proteins were desalted by running HiPrep 26/10 desalting column, with a typical result shown in Figure A.1. The most important step for eliminating the majority of other proteins is cation exchange chromatography with elution by linear salt gradient. The isoelectric point for wild type yTBP is 9.39. When a protein is at a pH below its pI, it carries a net positive charge and binds to a cation exchange resin. The pH of buffers used to purify TBP throughout the prep is 7.9. While wild type TBP eluted between 209 and 300 mM KCl, the C-stirrup TBP mutant and Quadruple TBP mutant eluted in the ranges of 224.5 mM – 276.5 mM and 286 mM – 325 mM KCl respectively. (Figures A.2 ~ A.4) To polish each protein for improving purity, a gel filtration column (Sephacryl S-300, Sephacryl S-100) was used. (Figures A.5, A.6, A.7) All purified proteins were analyzed in 15 % Tris-glycine SDS-PAGE as shown in Figure 16. The protein concentration for wild type TBP and each mutant variant was measured by UV spectrometry using an extinction coefficient of 12700 $M^{-1}cm^{-1}$ (Petri *et al.*, 1995).

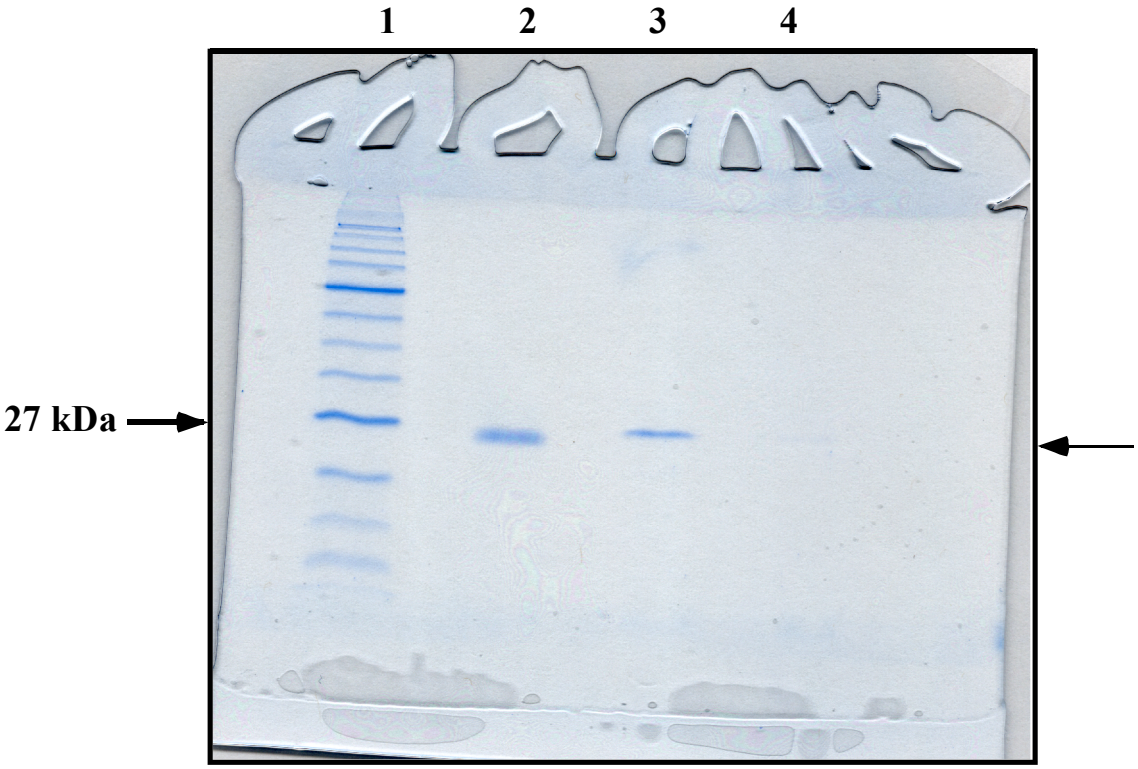

Figure 16. Purified TBP in 15 % Tris-glycine SDS PAGE

Ln 1: Protein marker
Ln 2: Wild type TBP (15 µL)
Ln 3: C-stirrup TBP mutant (15 µL)
Ln 4: Quadruple TBP mutant (5 µL)

3.3 Preliminary DNase I footprinting

We utilized minicircle DNA topoisomers of 203 bp DNA, described in materials and methods, to study TBP and minicircle DNA binding interactions, comparing them with linear DNA using DNase I footprinting. We observed slightly different footprinting patterns for circular versus linear DNA, with higher appearance of hypersensitivity not only around the TATA box but also elsewhere on the circular DNA (Figures 17 - 19). However, the control lanes (0 nM TBP) for all molecules appeared to have some degree of protection around the TATA box, and we found the cleavage by the enzyme DNase I was not uniformly distributed. We varied the concentrations (0.04 - 0.1 units per reaction) of DNase I to optimize the cleavage pattern, but the results all showed similarly irregular cleavage. Therefore, we decided to footprint using hydroxyl radicals, which are much smaller than DNase I, in order to obtain more uniform and clean cleavage around the TATA box.

3.4 Quantitative hydroxyl radical footprinting

We performed quantitative hydroxyl radical footprinting in order to observe TBP and minicircle DNA binding interactions, comparing them with linear DNA. We tested the nuclease activity of wild type TBP and mutant TBP variants by running control lanes (100 nM TBP and 100 pM DNA only) for each TBP. While the Quadruple TBP mutant showed some degree of nuclease activity (data not shown), the wild type TBP was essentially free of nuclease activity and C-stirrup TBP mutant

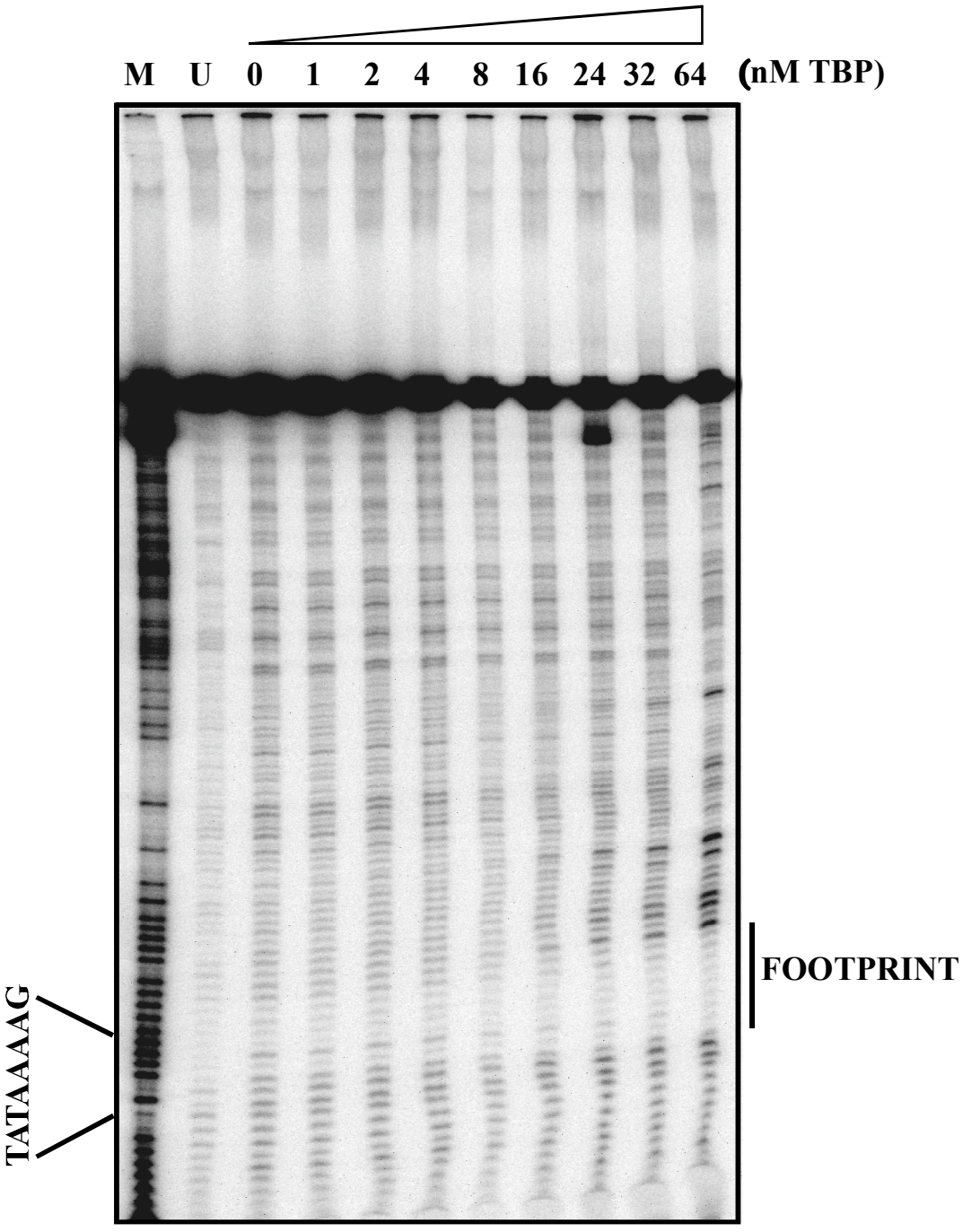

Figure 17. DNase I Footprinting of Wild Type TBP on 203 bp Linear DNA. M: 203 Linear MG (A+G); U: uncut

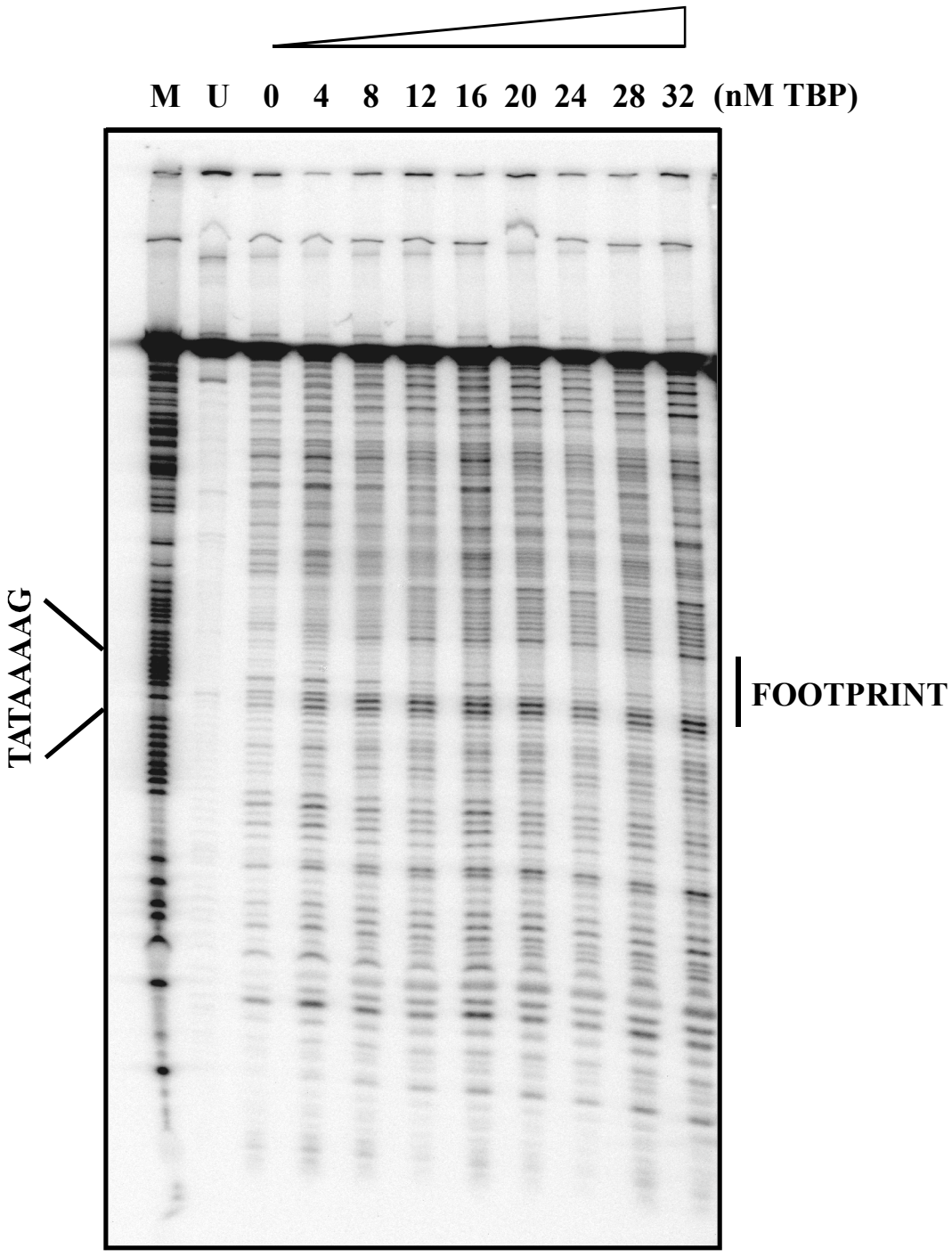

Figure 18. DNase I Footprinting of Wild Type TBP on 203 bp ΔLk = -1 Topoisomer. M: 203 -1 MG (A+G); U: uncut

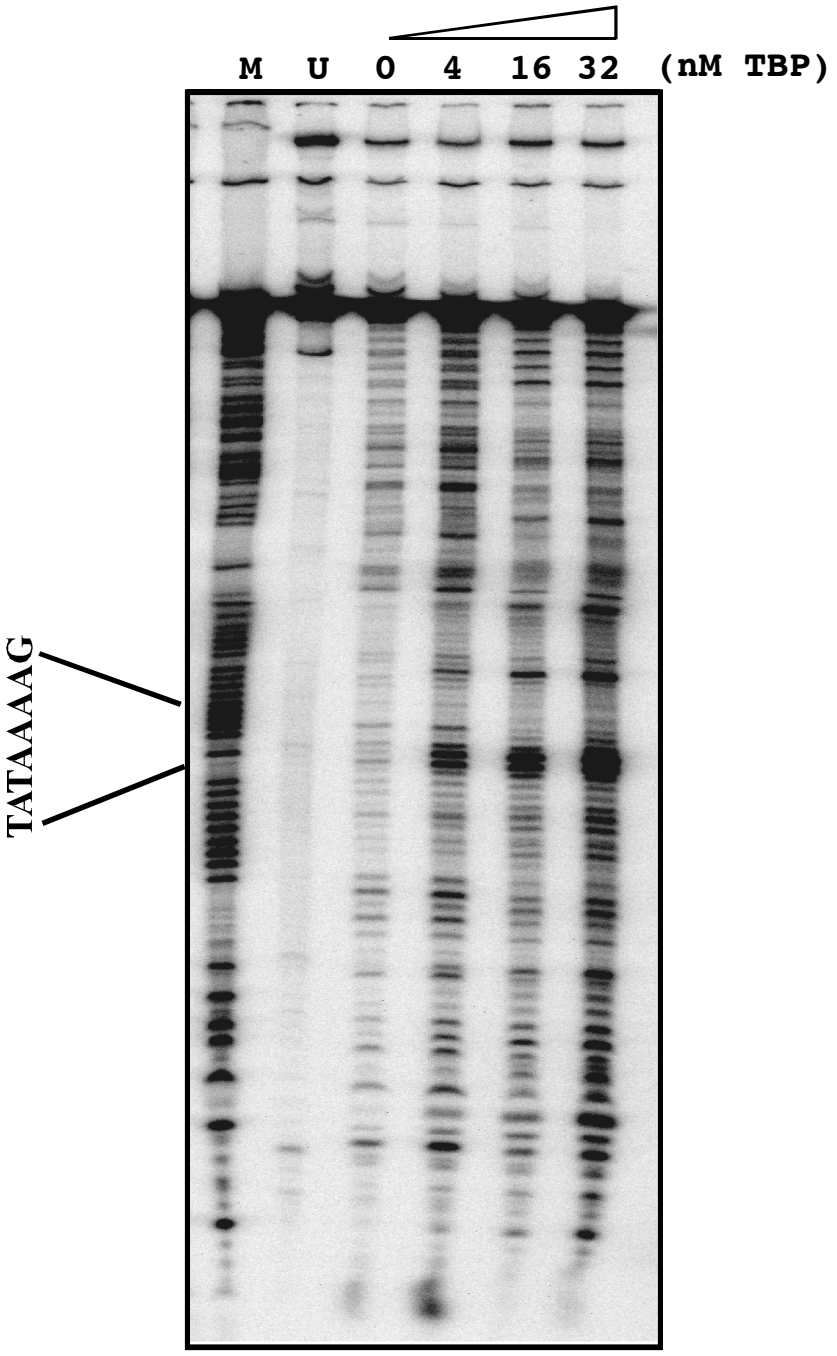

Figure 19. DNase I Footprinting of Wild Type TBP on 203 bp ΔLk = 0 Topoisomer. M: 203 Linear MG(A+G); U: uncut

has negligible nuclease activity (Figure 20, 21). Due to the slight contamination of nuclease activity in the quadruple TBP mutant preparation, which could cause misleading hydroxyl radical footprinting analysis, we analyzed only the data from the wild type TBP and C-stirrup TBP mutants.

The results of hydroxyl radical footprinting showed C-stirrup TBP mutant binds slightly better to the negatively supercoiled minicircle than to the linear DNA, in agreement with the predictions of the flattening model (Figures 21, 23). Wild type TBP also shows slightly enhanced binding to the negatively supercoiled DNA which was in agreement with our previous prediction; TBP induces negatively supercoiled DNA and it should bind better to the minicircle (Figure 20, 22).

We observed quite different footprinting patterns for negatively supercoiled minicircle versus linear DNA in hydroxyl radical footprinting. Protected areas are located at the TATA box, but for the minicircle additional protection is also seen in the region below the TATA box, for both wild type and C-stirrup TBP mutant (Figures 20, 21, 22, and 23). This suggests that the structure of TBP bound to minicircles may be different than the linear DNA. The $\Delta Lk = 0$ topoisomer, which is pre-bent but doesn't have the unwinding, shows no binding to both wild type and mutant TBP (Figures 20 and 21).

In order to measure the binding constant, the active concentration of wild type TBP needs to be determined. The fractional activity is obtained as follows

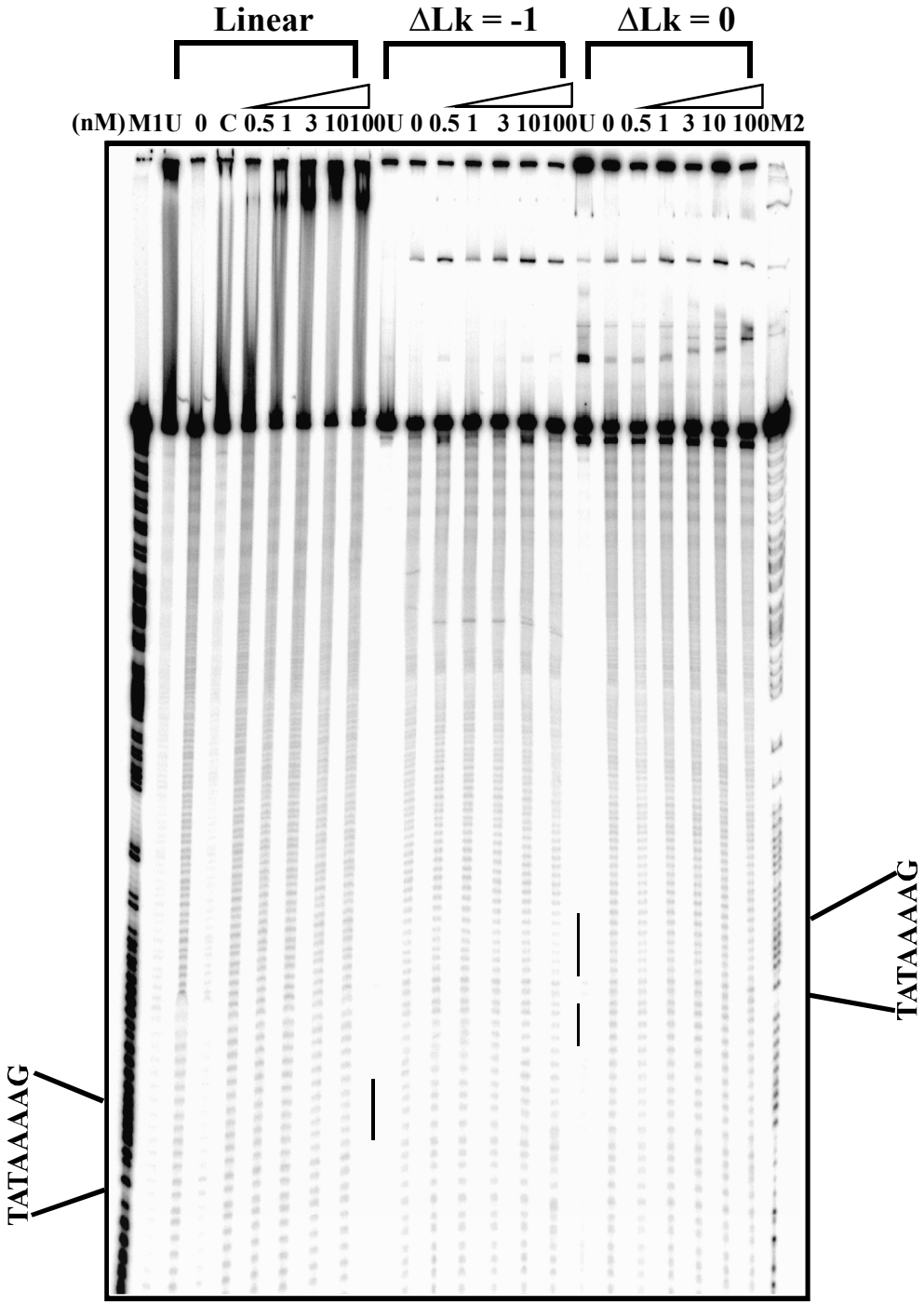

Figure 20 : Hydroxyl Radical Footprinting of Wild Type TBP on 203 bp DNA. M1: 203 Linear MG(A+G); M2: 203 -1 MG(A+G); U: uncut ; C: 100 nM TBP and DNA only; Bar: area of footprinting

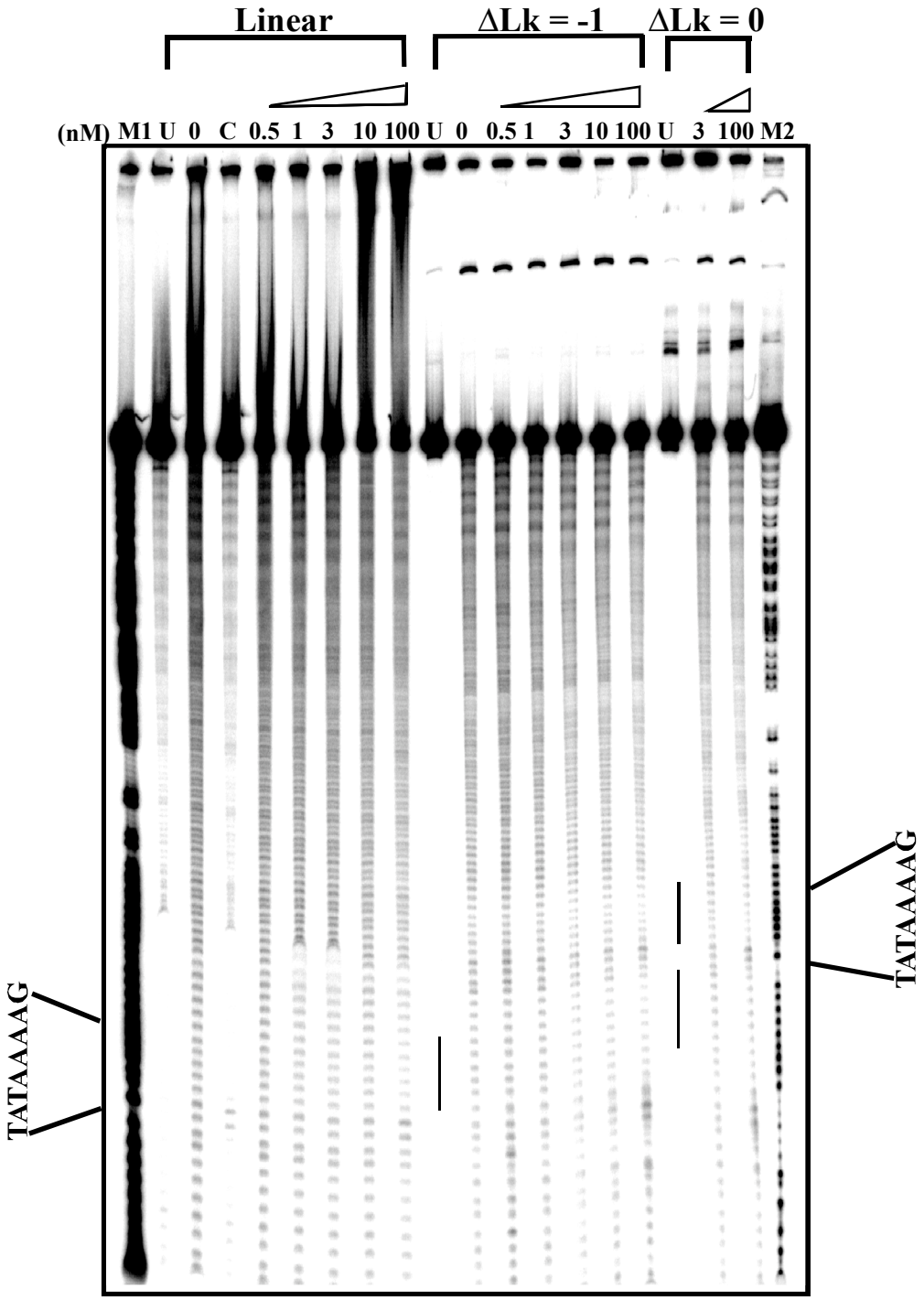

Figure 21 : Hydroxyl Radical Footprinting of C-stirrup TBP mutant on 203 bp DNA. M1: 203 Linear MG(A+G); M2: 203 -1 MG(A+G); U: Uncut, C: 100 nM TBP and DNA only; Bars: areas of footprinting

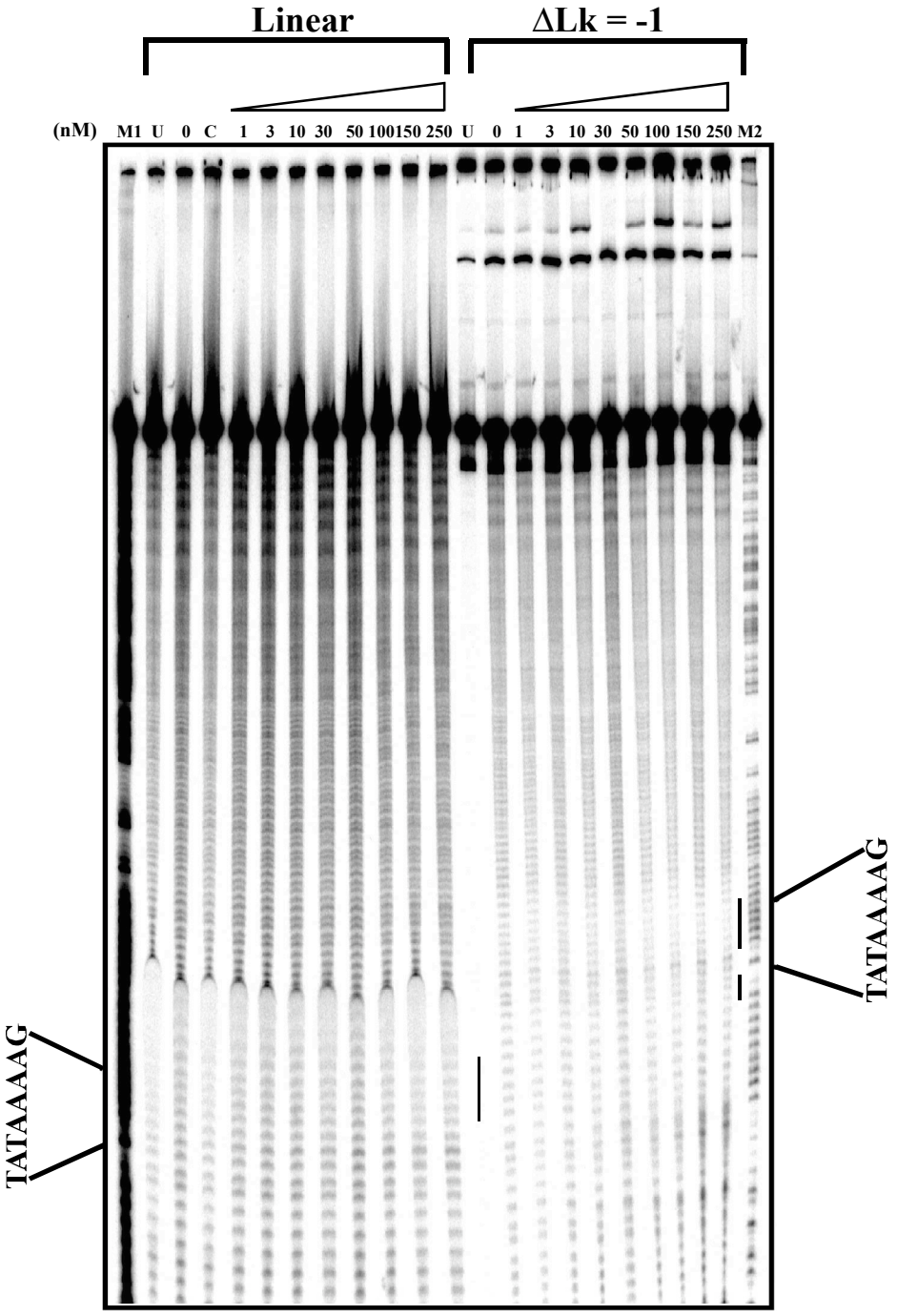

Figure 22 : Hydroxyl Radical Footprinting of Wild Type TBP on 203 bp DNA. M1: 203 Linear MG (A+G); M2: 203 -1 MG (A+G); U: uncut; C: 100 nM TBP and DNA only; Bar: area of footprinting

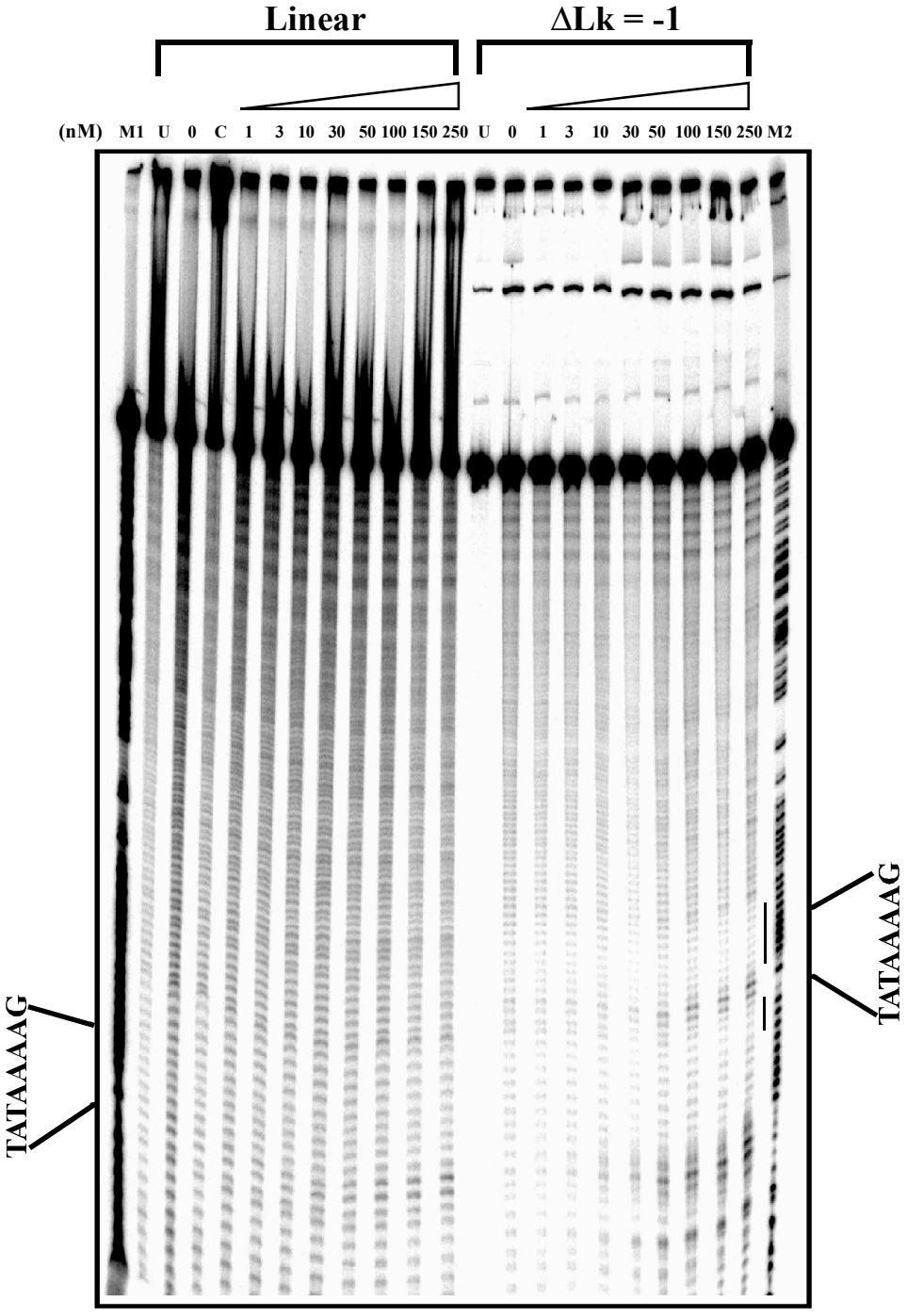

Figure 23 : Hydroxyl Radical Footprinting of C-stirrup TBP mutant on 203 bp DNA. M1: 203 Linear MG (A+G); M2: 203 -1 MG (A+G); U: uncut; C: 100 nM TBP and DNA only; Bars: areas of footprinting

$$\text{Fractional Activity} = \frac{[\text{DNA} \bullet \text{TBP}] \times 1/\alpha}{[\text{TBP}]}, \text{ if } [\text{DNA}] >> K_d \qquad \text{(Eqn. 1)}$$

where α is the fraction of the complex that survives in the gel. The concentration of the bound complex, [DNA • TBP] = Fraction bound × [Total DNA]. Thus,

$$\text{Fractional Activity} = \frac{\text{Fraction Bound}}{[\text{TBP}]} \times [\text{Total DNA}] \times 1/\alpha \qquad \text{(Eqn. 2)}$$

$$= \text{slope} \times [\text{Total DNA}] \times 1/\alpha \qquad \text{(Eqn. 3)}$$

where "slope" is the slope for the best-fit line to the first four titration points in figures 24 and 25, determined as follows:

The fraction bound for each concentration of TBP titration was determined from the intensity of the bound complex band and that of the total DNA using ImageQuant (Figures 24 and 25). These data were analyzed in KaleidaGraph to obtain the best fit slope. The dashed line is the mean value for % bound between 300 nM and 500 nM TBP (Figure 26, 27). For example, the mean value of % bound for wild type TBP with 203 bp linear DNA is 28.9 % and that with 203 bp ΔLk = -1 topoisomer is 54.6 %. This is assumed to represent the total amount of complex that survives the gel, allowing measurement of α.

From (Eqn 3), the fractional activity of wild type TBP determined from

$$\text{203 bp linear DNA is } \frac{0.1357}{\text{nM}} \times 28\,\text{nM} \times \frac{100\,(\%)}{28.9} = 0.13 \qquad \text{(Eqn. 4)}$$

$$\text{203 bp } \Delta\text{Lk} = -1 \text{ topoisomer is } \frac{0.2285}{\text{nM}} \times 29\,\text{nM} \times \frac{100\,(\%)}{54.6} = 0.12 \qquad \text{(Eqn. 5)}$$

The fractional activity of TBP mutants could not be determined because we could not reach a protein concentration at which the apparent binding was saturated. The concentration of DNA was calculated from the measured incorporation efficiency of the 5'- ^{32}P end-labeled PCR primer into products; the initial concentration of primer was 0.2 μM.

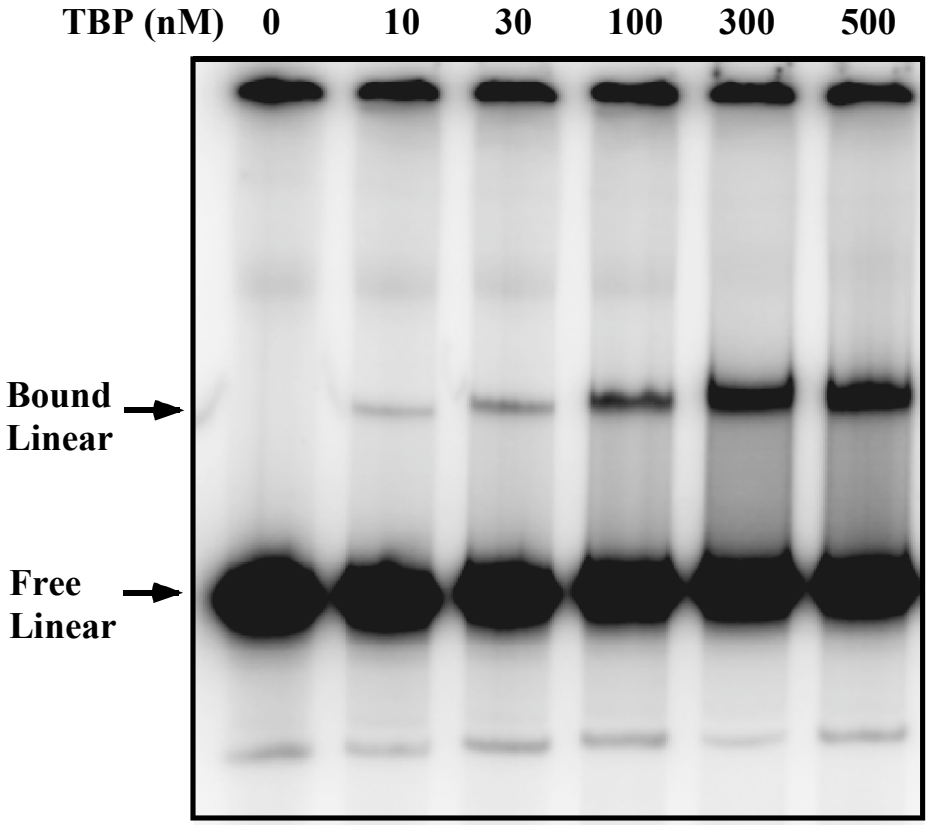

Figure 24 : Electrophoretic Mobility Shift Assay of Wild Type TBP on 203 bp Linear DNA. Total [DNA] in each lane is 28 nM. [DNA] >> K_d allows determination of the active [TBP].

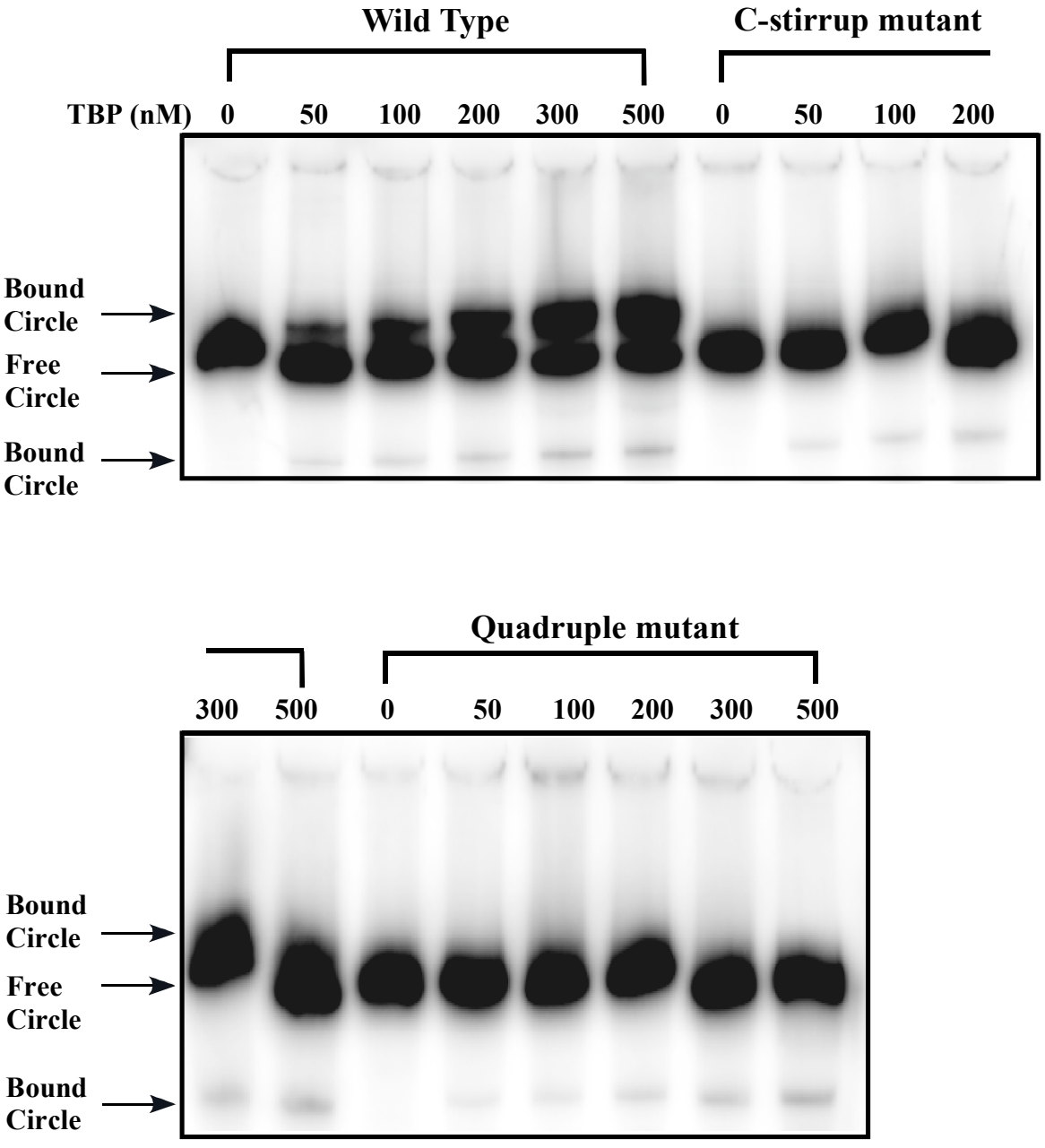

Figure 25 : Electrophoretic Mobility Shift Assay of Wild Type and Mutant TBPs on 203 bp ΔLk = -1 Topoisomer.
The total [DNA] in each lane is 29 nM.

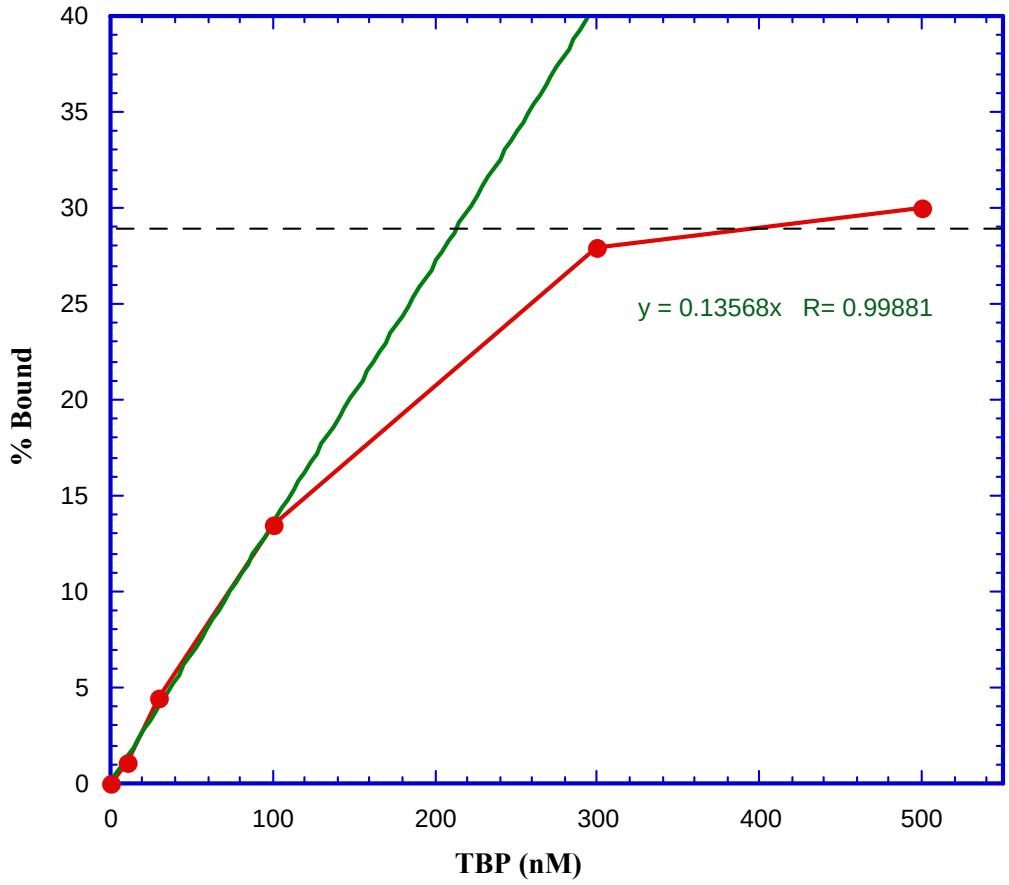

Figure 26. Determination of Active Wild Type [TBP] with 203 bp Linear DNA. The dashed line is the mean value of % bound between 300 nM and 500 nM TBP: 28.9 %. The fractional activity of the wild type TBP is calculated to be 0.13 using equations 4 to 5. The solid line is fit to the points between 0 and 100 nM TBP.

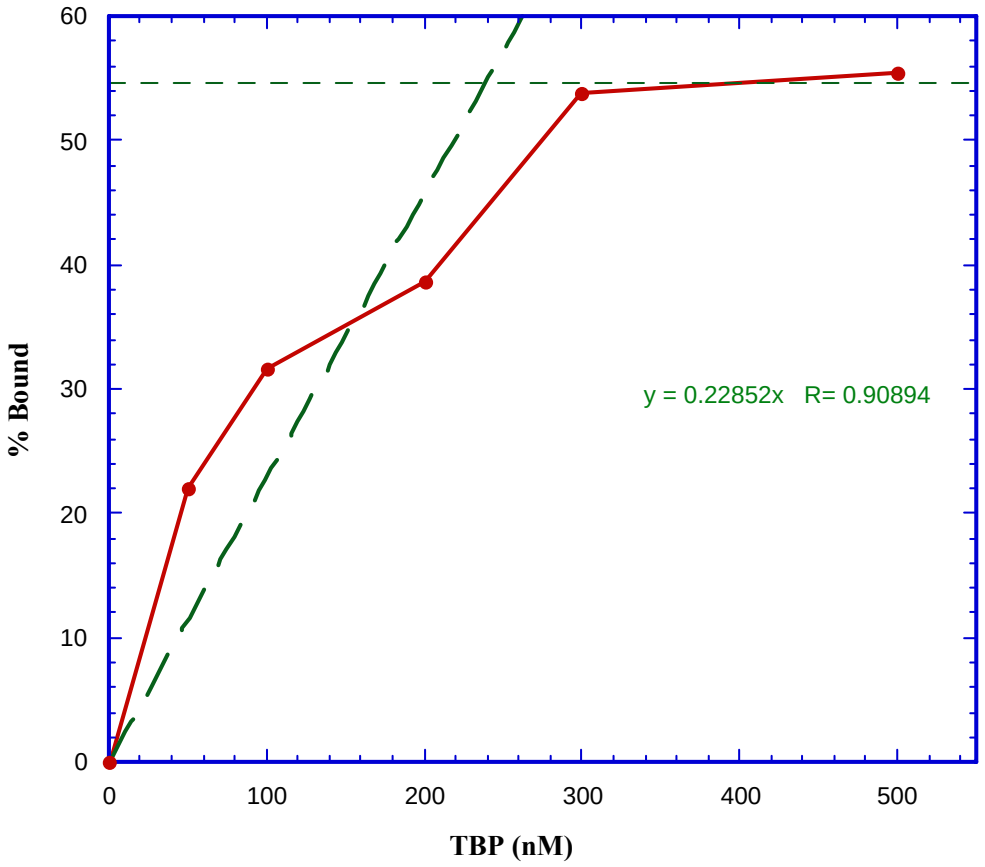

Figure 27. Determination of Active Wild Type TBP with 203 bp -1 Topoisomer. The thin dashed line is the mean value of % bound between 300 nM and 500 nM TBP; 54.6 %, which gives the surviving fraction α. The thick dashed line is fit to the points between 0 and 200 nM TBP. The fractional activity of the wild type TBP is calculated to be 0.13, from this graph and equations 4-5.

The dissociation equilibrium constant was determined from standard equations for protein –DNA binding reactions. The equilibrium for protein-DNA binding is

P + D = P•D. So K_d is given by $K_d = \frac{[P][D]}{[P \bullet D]} = \frac{(P_t - [P \bullet D])(D_t - [P \bullet D])}{[P \bullet D]}$ (Eqn. 6)

where P_t = total active protein concentration, D_t = total active DNA concentration, assumed to be equal to the actual DNA concentration.

We solve for $[P \bullet D]$ to give

$$[P \bullet D]^2 - (D_t + P_t + K_d)[P \bullet D] + D_t P_t = 0 \quad \text{(Eqn. 7)}$$

$$[P \bullet D] = \frac{D_t + P_t + K_d - \sqrt{(D_t + P_t + K_d)^2 - 4D_t P_t}}{2} \quad \text{(Eqn. 8)}$$

$$\theta = \frac{[P \bullet D]}{D_t} = \frac{1}{2D_t}\left[D_t + P_t + K_d - \sqrt{(D_t + P_t + K_d)^2 - 4D_t P_t}\right] \quad \text{(Eqn. 9)}$$

This is the rigorous equation for fractional saturation. If we include a parameter β , fractional activity of the protein, the above equation becomes:

$$\theta = \frac{[P \bullet D]}{D_t} = \frac{1}{2D_t}\left[D_t + \beta P_t + K_d - \sqrt{(D_t + \beta P_t + K_d)^2 - 4D_t \beta P_t}\right] \quad \text{(Eqn. 10)}$$

where now P_t is the measured protein concentration and βP_t is the active concentration. If $D_t << K_d$, under these conditions $D_t + \beta P_t + K_d >> 4\beta P_t D_t$.

Taylor expansion of the square root gives

$$\sqrt{b^2 - \varepsilon} \approx b - \tfrac{1}{2}\left(b^2\right)^{-1/2}\varepsilon = b - \frac{\varepsilon}{2b} = D_t + \beta P_t + K_d - \frac{4\beta P_t D_t}{2(D_t + \beta P_t + K_d)} \quad \text{(Eqn. 11)}$$

where $\varepsilon = 4\beta P_t D_t$. Therefore, we have

$$\theta = \frac{[P \bullet D]}{D_t} = \frac{1}{2D_t}\left[\frac{4\beta P_t D_t}{2(D_t + \beta P_t + K_d)}\right] = \frac{\beta P_t}{D_t + \beta P_t + K_d} \approx \frac{\beta P_t}{\beta P_t + K_d} \quad \text{(Eqn. 12)}$$

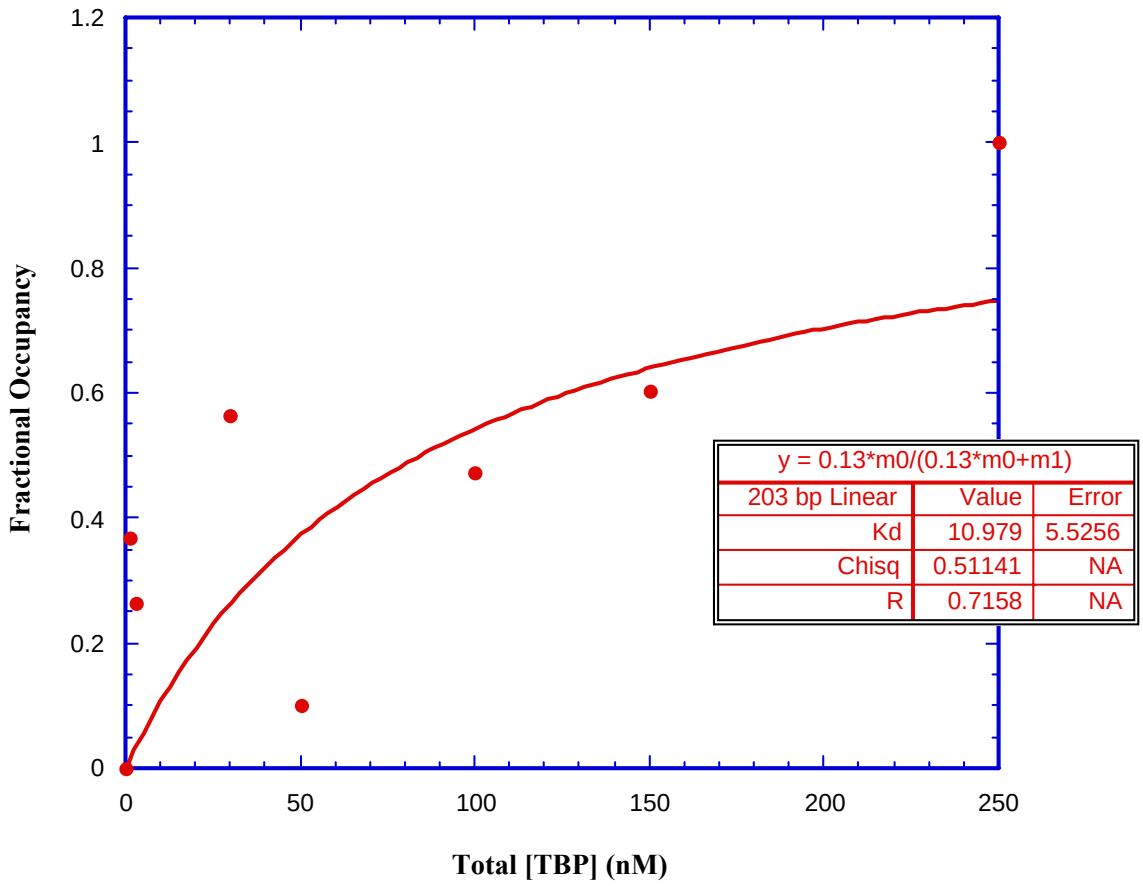

Figure 28. Binding Curve for Wild Type TBP on 203 bp Linear DNA. K_d = 11 nM ; the data are from Figure 22.

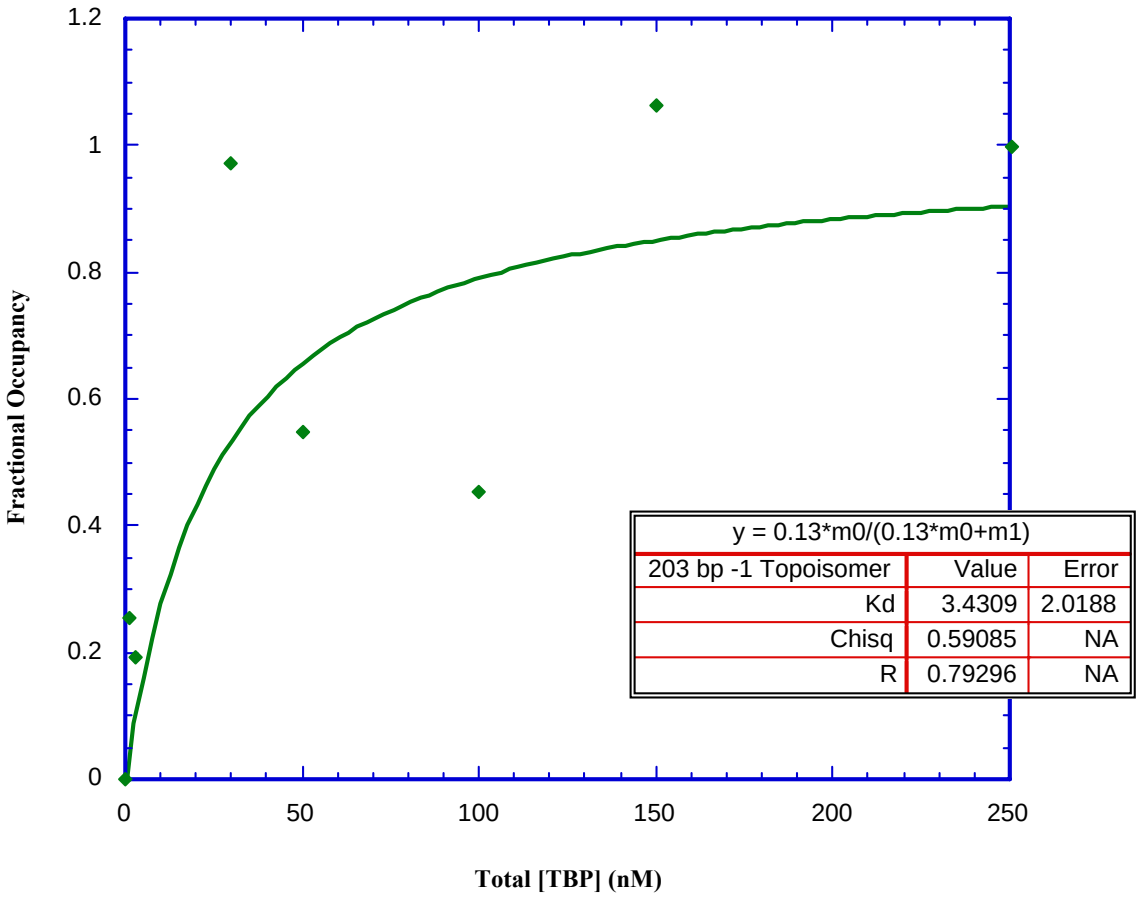

Figure 29. Binding Curve for Wild Type TBP on 203 bp -1 Topoisomer
K_d = 11 nM ; the data are from Figure 22.

Using the fractional activity of wild type TBP measured as above, the equilibrium dissociation constants (K_d's) of wild type TBP derived from hydroxyl radical footprinting titrations for the linear DNA and the -1 topoisomer of 203 bp DNA are 11 nM and 3 nM from Figures 28 and 29 using the equation

$$y = \frac{0.13 \times \mathrm{m0}}{0.13 \times \mathrm{m0} + Kd}$$, where m0 is the apparent TBP concentration (Eqn. 12)

The smaller K_d for the negatively supercoiled DNA suggests that pre-bending and unwinding of the TATA box enhanced DNA binding. The densitometric analysis from the hydroxyl radical gels shows that hypersensitivity below the binding site in circular DNA is much more marked than in the linear DNA (Figures 30, 31, 32 and 33). Also, the footprint area at and around the TATA box of circular DNA is also quite different from that of linear DNA.

3.5 Electrophoretic mobility shift assay (EMSA)

Gel mobility shift (EMSA) experiments for linear DNA and circular topoisomers for 203 bp, 206 bp, and 210 bp DNA were performed to further characterize the interaction between DNA and each wild type and mutant TBP. The results from the gels show much greater apparent binding for the negatively supercoiled DNA relative to either of the other two DNAs for 203 bp and 206 bp DNA (Figures 34, 35).

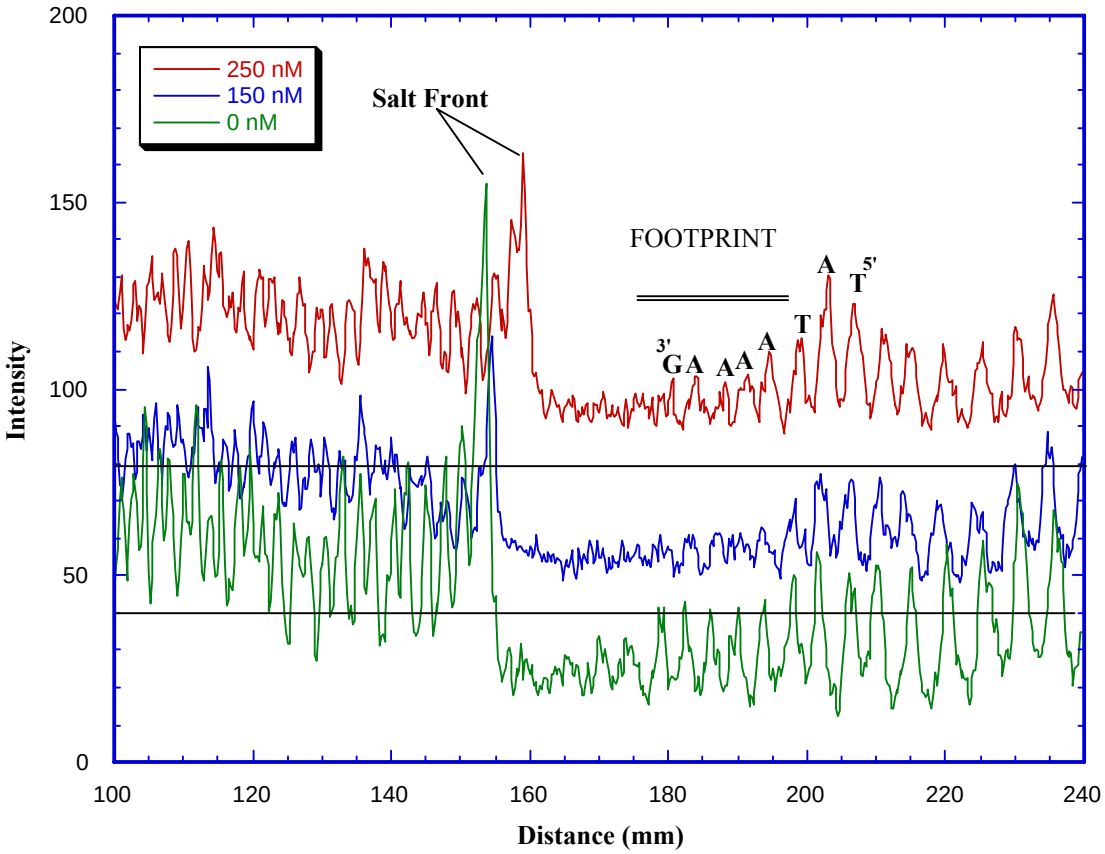

Figure 30. Densitometry of footprint of wild type TBP for 203 bp Linear DNA; data from Figure 22; horizontal line: base line, for each trace, arbitrarily offset for clarity.

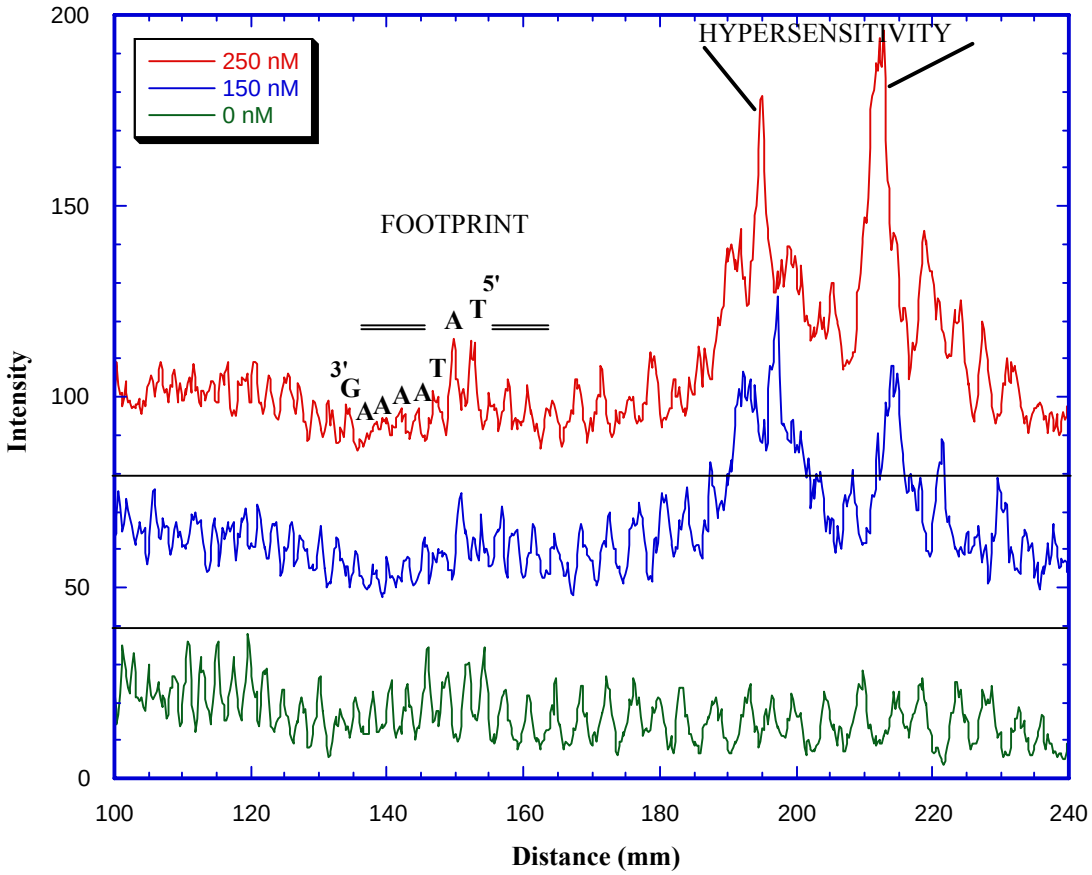

Figure 31. Densitometry of footprint of wild type TBP for 203 bp -1 Topoisomer; data from Figure 22; horizontal line: base line.

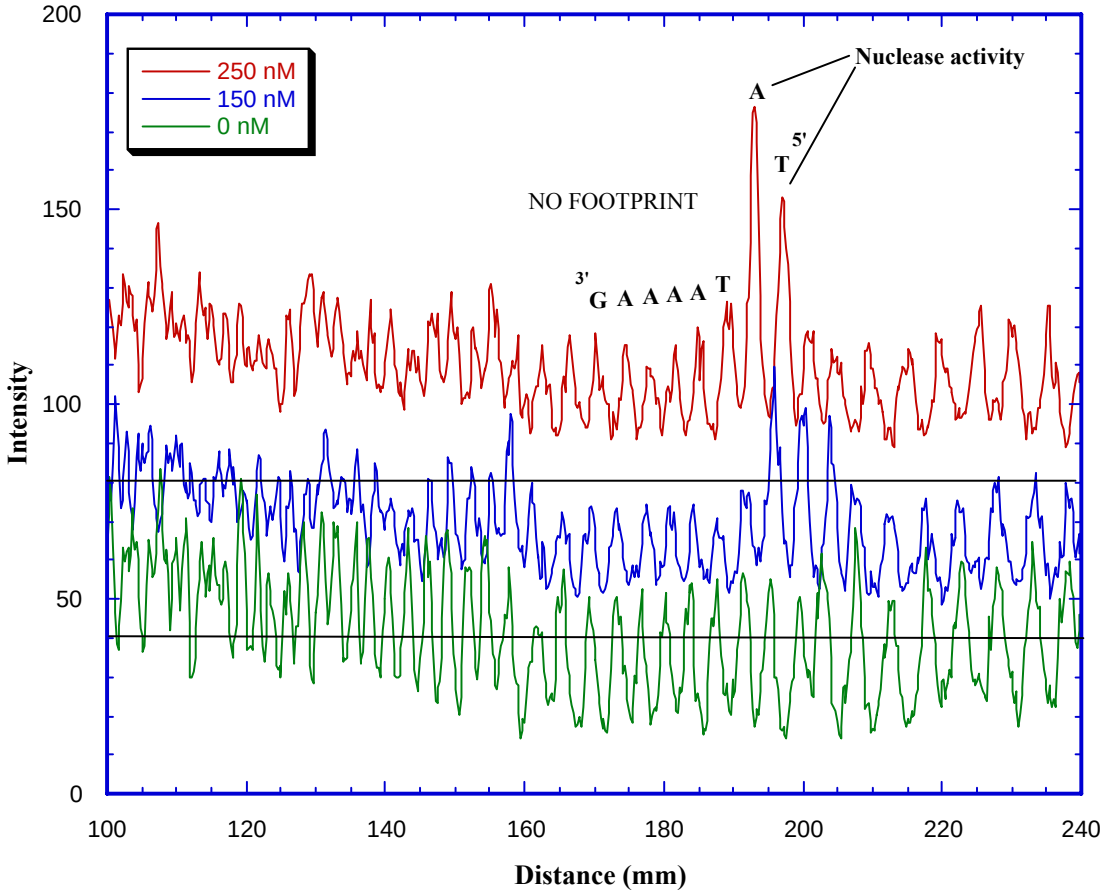

Figure 32. Densitometry of footprint of C-stirrup TBP mutant for 203 bp Linear DNA; data from Figure 23; horizontal line: base line.

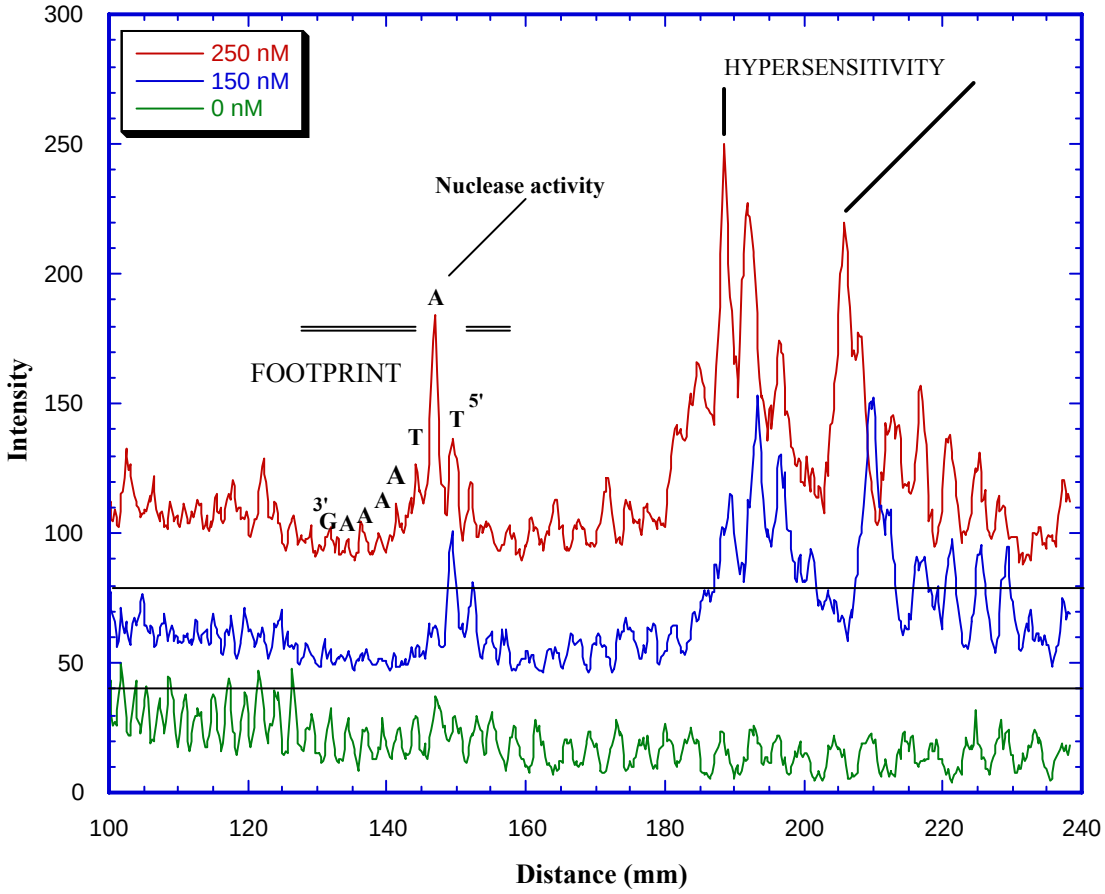

Figure 33. Densitometry of footprint of C-stirrup TBP mutant for 203 bp -1 Topoisomer; data from Figure 23; horizontal line: base line.

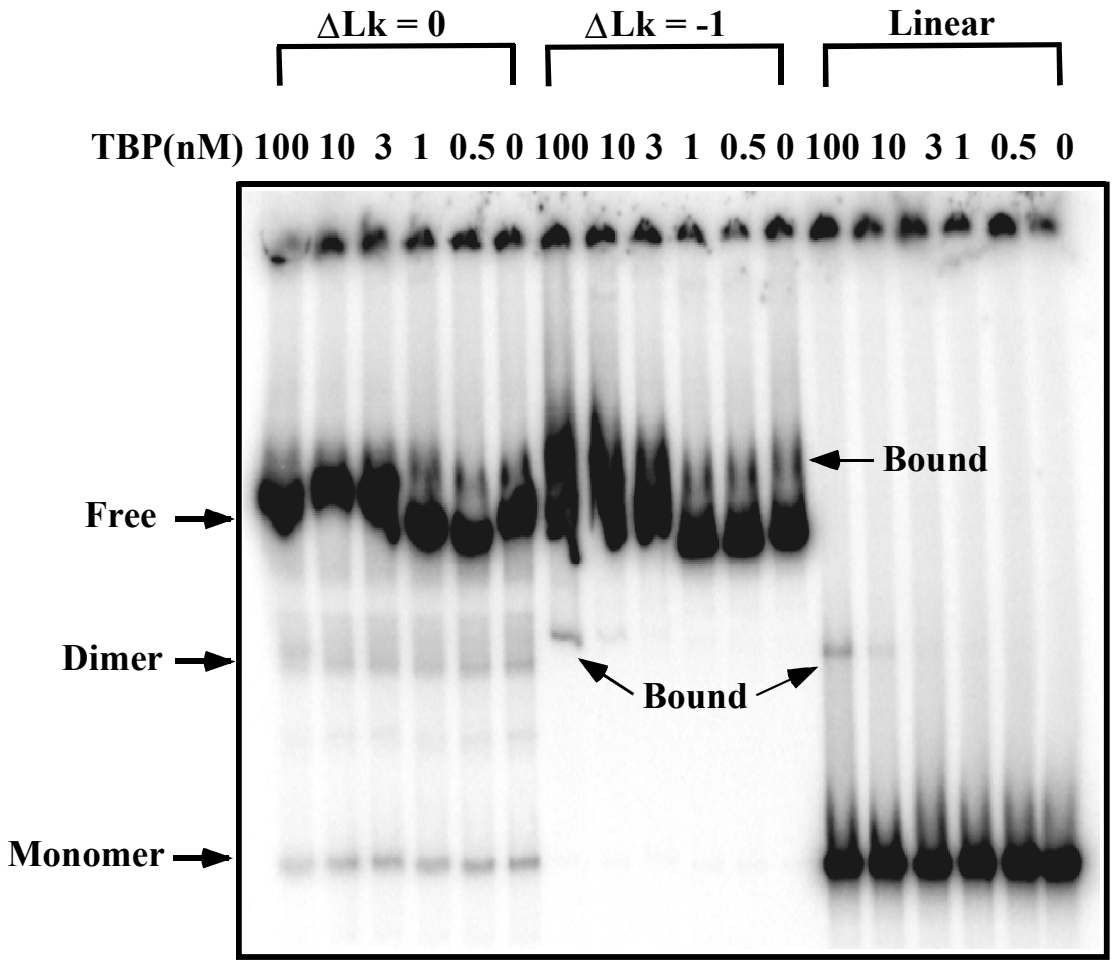

Figure 34 : Electrophoretic Mobility Shift Assay of Wild Type TBP on 203 bp DNA

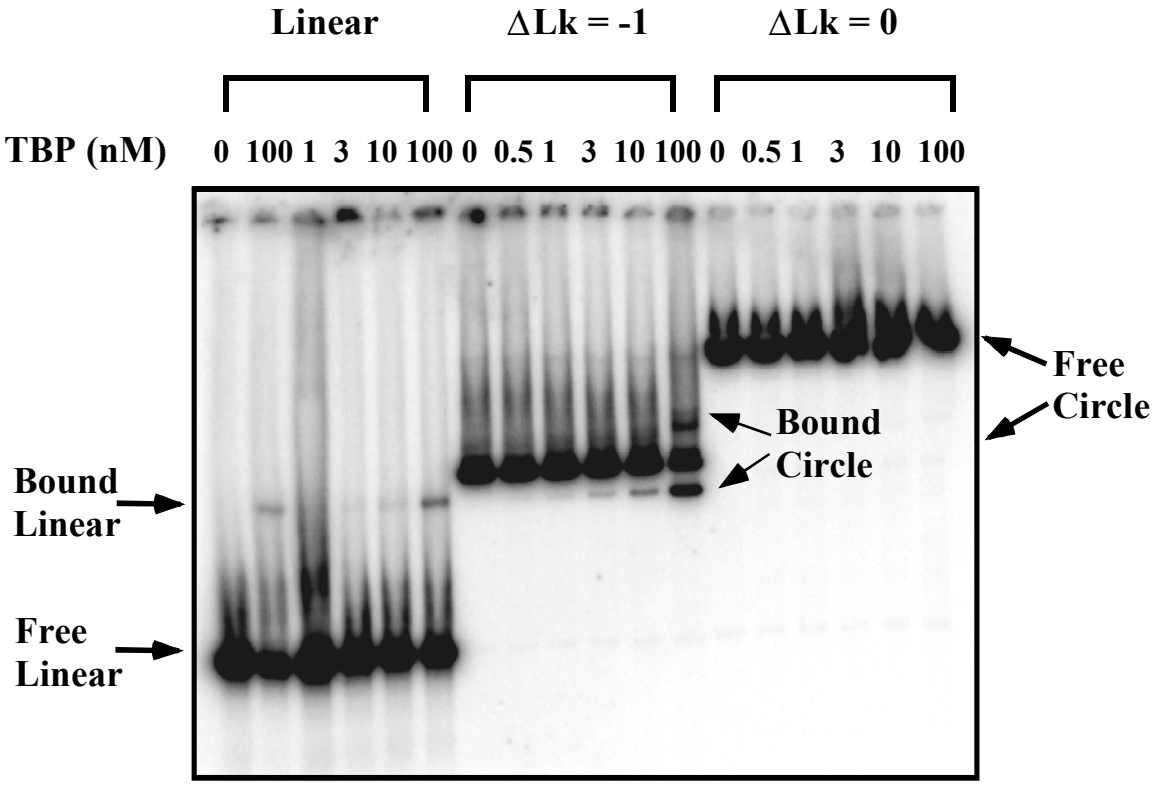

Figure 35 : Electrophoretic Mobility Shift Assay of Wild Type TBP on 206 bp DNA

Figures 34 – 42 show that the TBP • DNA complex is more kinetically stable on circular DNA than on linear DNA. TBP bound to linear DNA has previously been observed to dissociate during electrophoresis (Hoopes *et al*., 1992). Both the C-stirrup and Quadruple TBP mutants show binding to the negatively supercoiled DNA but not to the linear DNA, in strong agreement with the predictions of the flattening model (Figures 34 - 43).

In contrast to the hydroxyl radical footprinting results, the equilibrium dissociation constants (K_d) derived from EMSA titrations of wild type TBP to the linear DNA and the -1 topoisomers of 203 bp are similar. The data were analyzed with the assumptions that the fraction surviving the gel is 9 % for the linear DNA and 90 % for the circular DNA (Figure 44). The 210 bp DNA molecule, which didn't generate negatively supercoiled DNA, showed only binding to the linear DNA of wild type TBP (Figures 45 - 47).

There is also evidence from the gel mobility shift experiments for more than one conformation of the negatively supercoiled DNA bound by a single TBP; the faster moving band and slowly moving band (Figures 42, 43). The faster moving band probably represents a strongly distorted conformation with smaller hydrodynamic radius and is shown to be stable in both wild type and mutant TBP. We suspect that this could be a flattened form; it is shown both in wild type and in mutant TBP and the mutant should not be able to induce the kinks at the end of the TATA box.

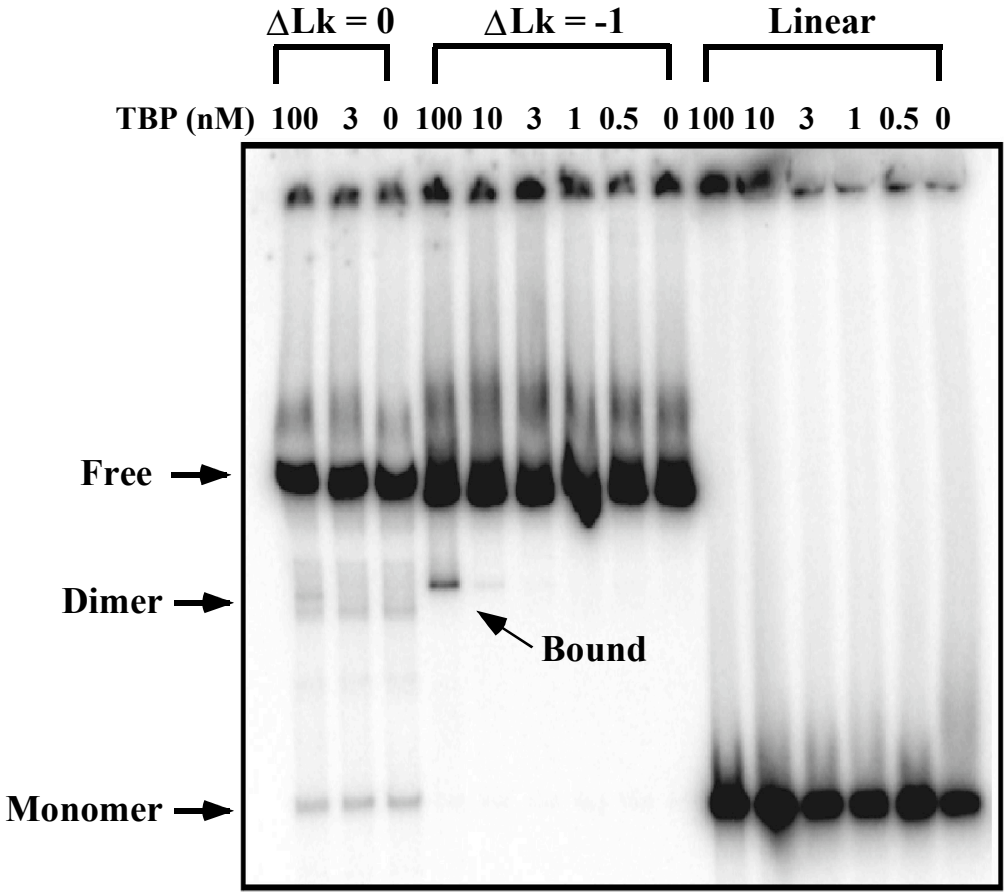

Figure 36 : Electrophoretic Mobility Shift Assay of C-stirrup TBP Mutant on 203 bp DNA

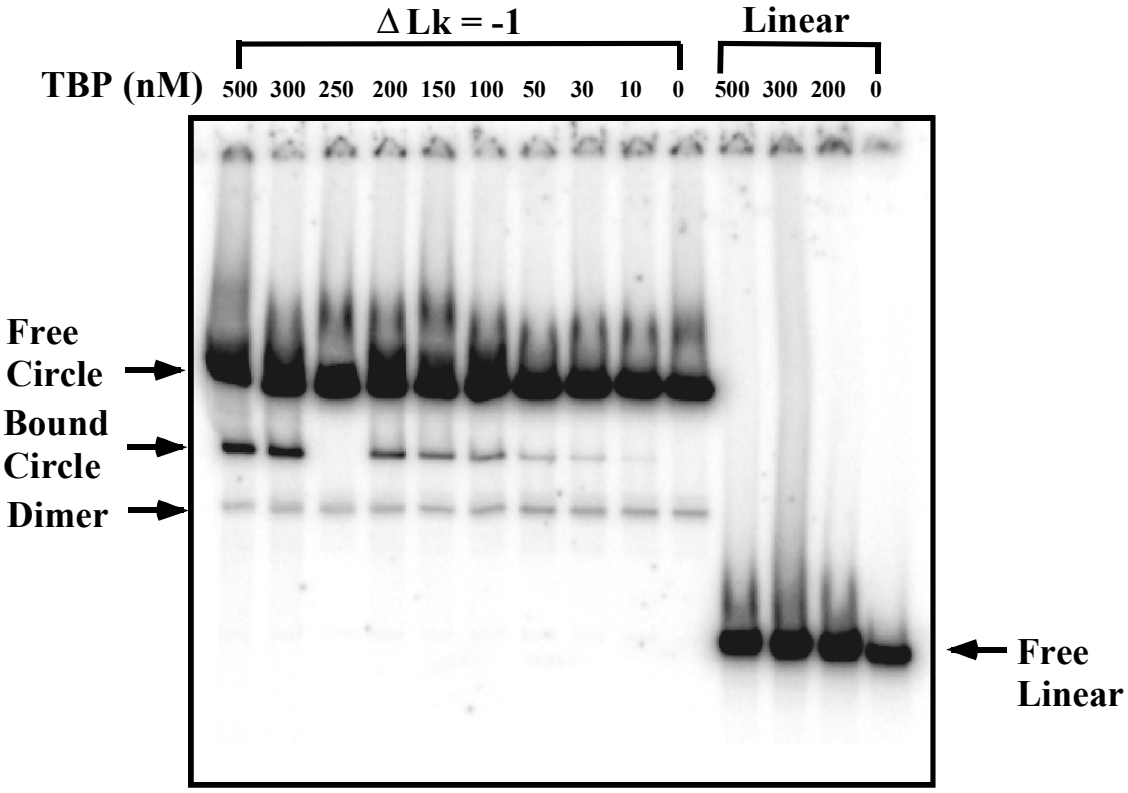

Figure 37 : Electrophoretic Mobility Shift Assay of C-stirrup TBP mutant on 203 bp DNA. This gel shows an example of using more closely spaced titration points of [TBP] for quantitative analysis.

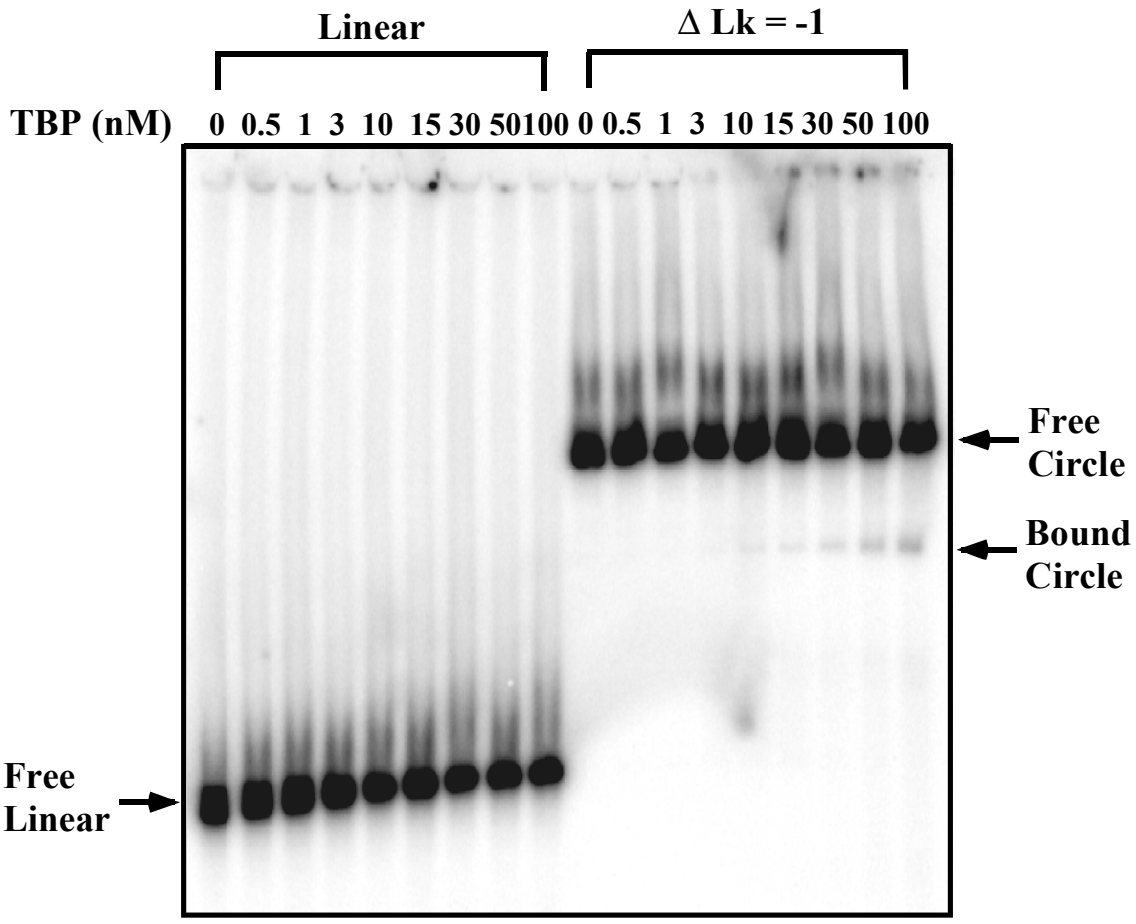

Figure 38 : Electrophoretic Mobility Shift Assay of Quadruple TBP mutant on 203 bp DNA

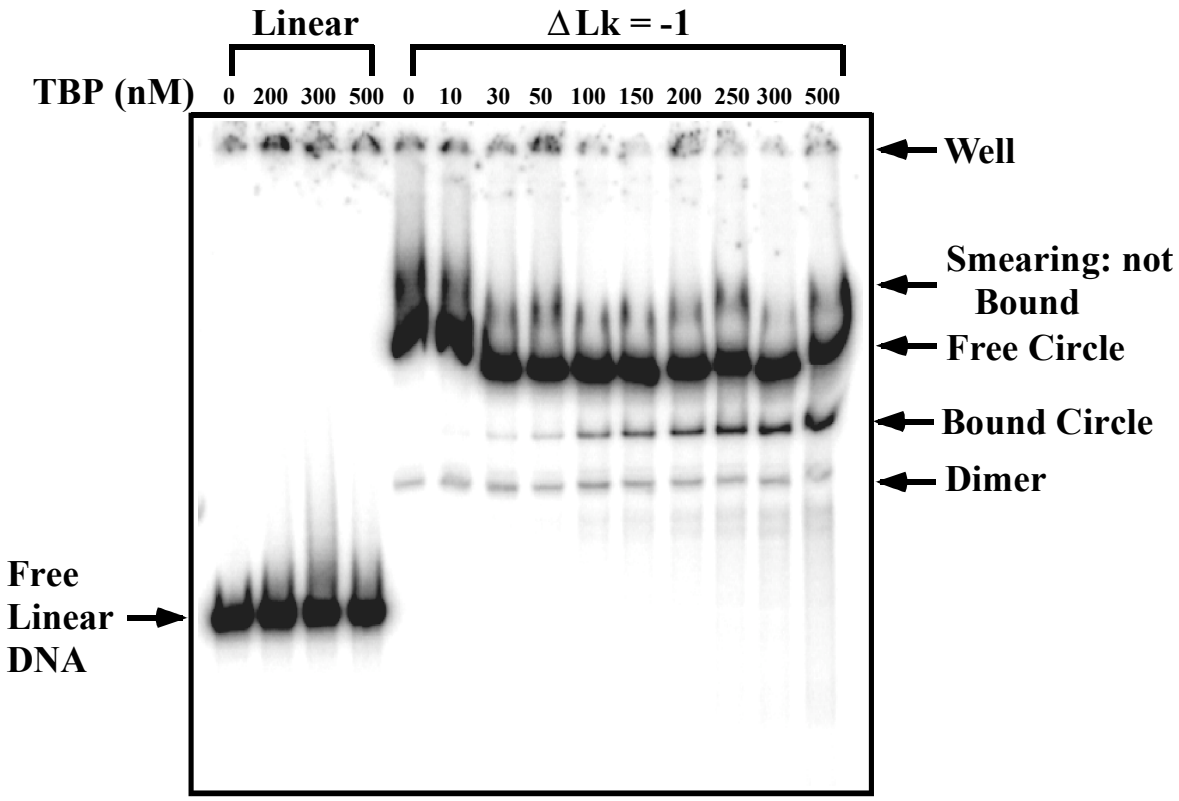

Figure 39 : Electrophoretic Mobility Shift Assay of Quadruple TBP mutant on 203 bp DNA. For further observation, more titration points of [TBP] were used.

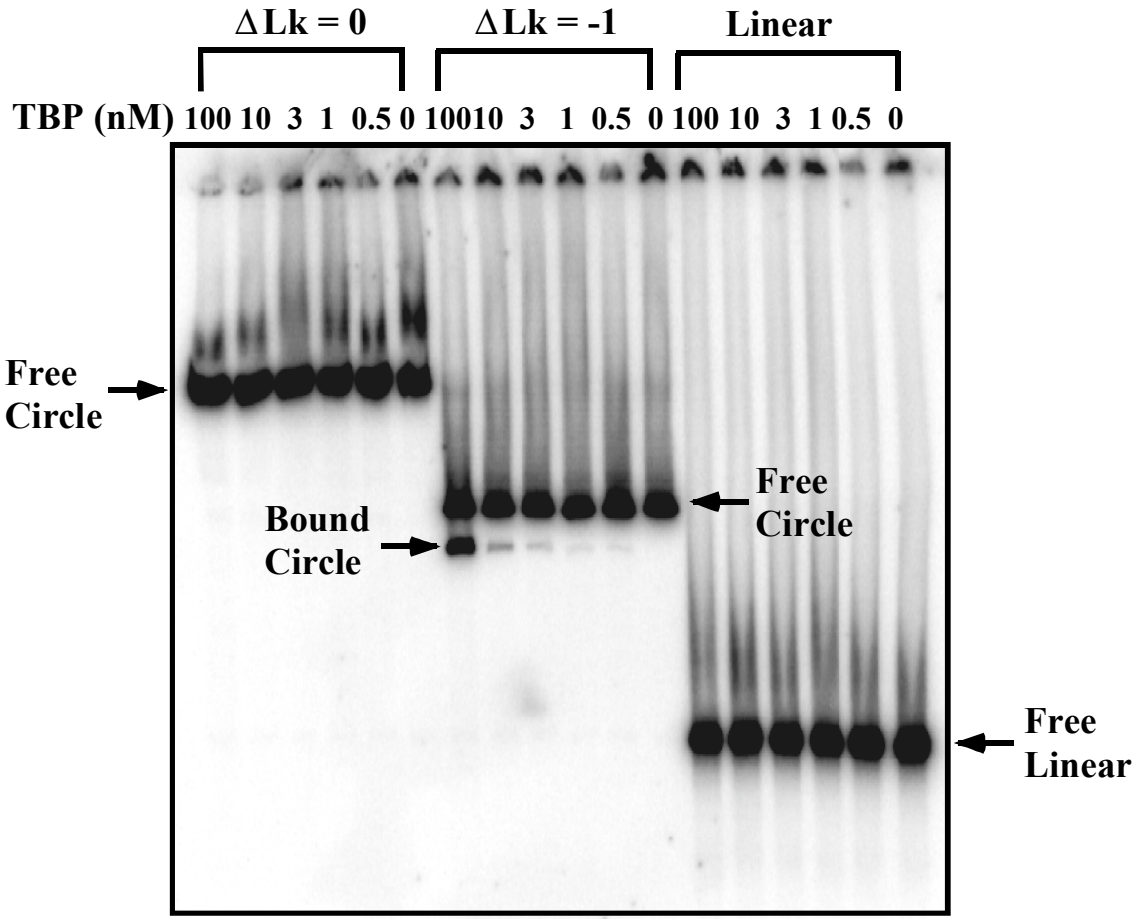

Figure 40 : Electrophoretic Mobility Shift Assay of C-stirrup TBP mutant on 206 bp DNA

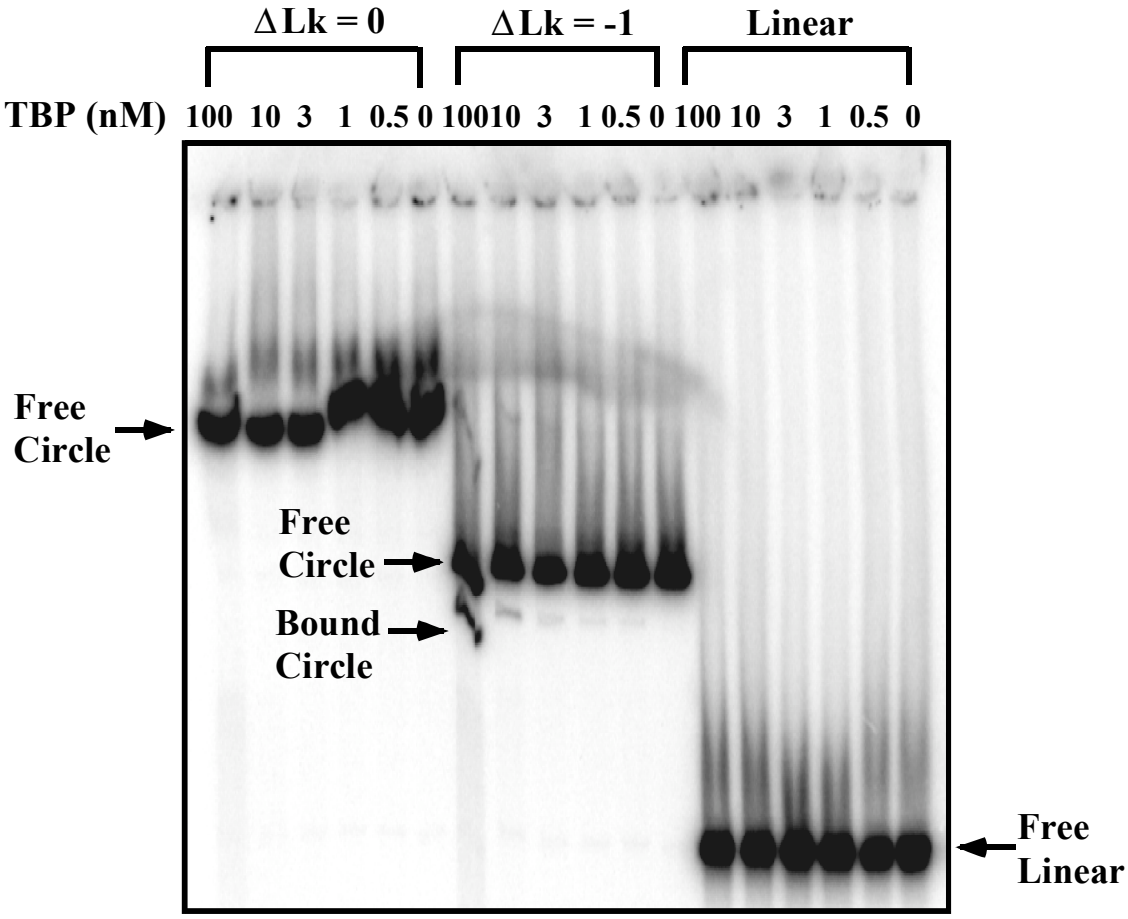

Figure 41 : Electrophoretic Mobility Shift Assay of Quadruple TBP mutant on 206 bp DNA

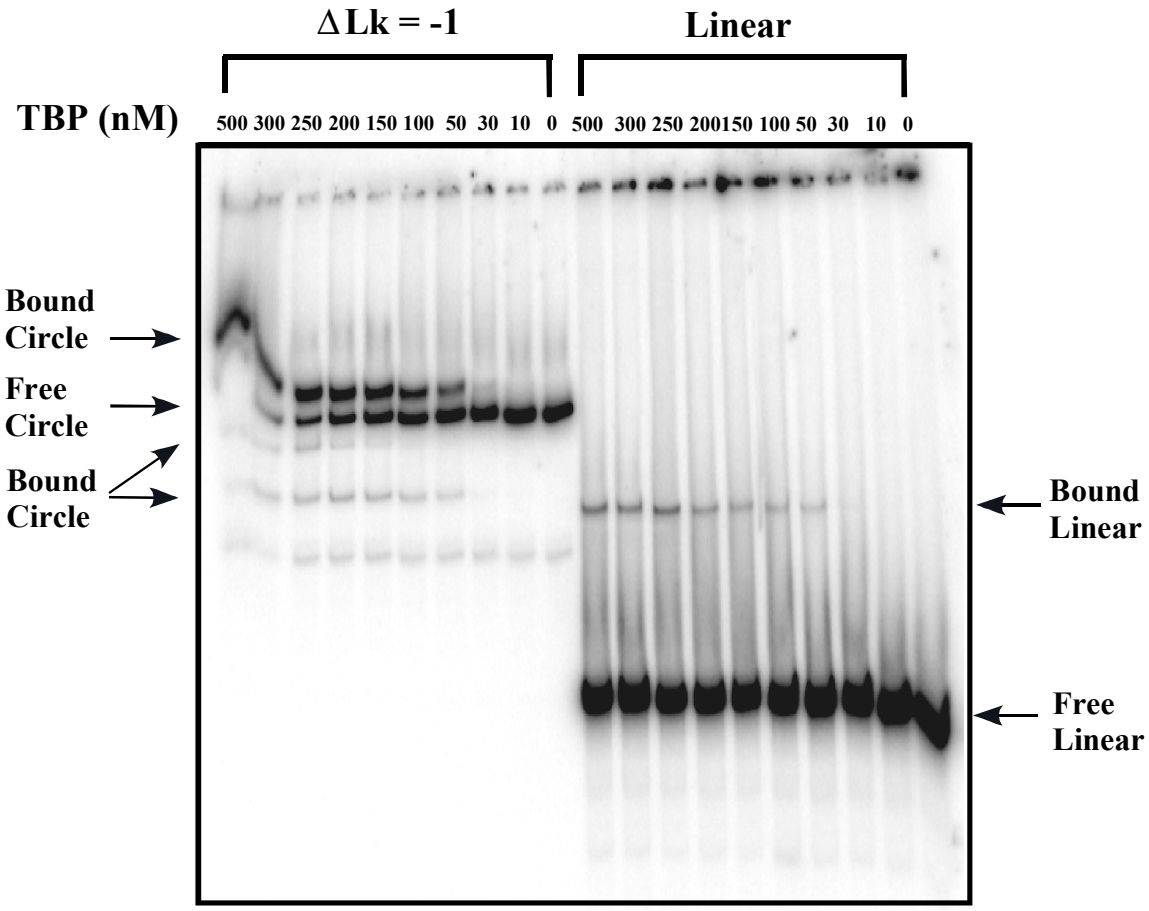

Figure 42 : Electrophoretic Mobility Shift Assay of Wild Type TBP on 203 bp DNA.

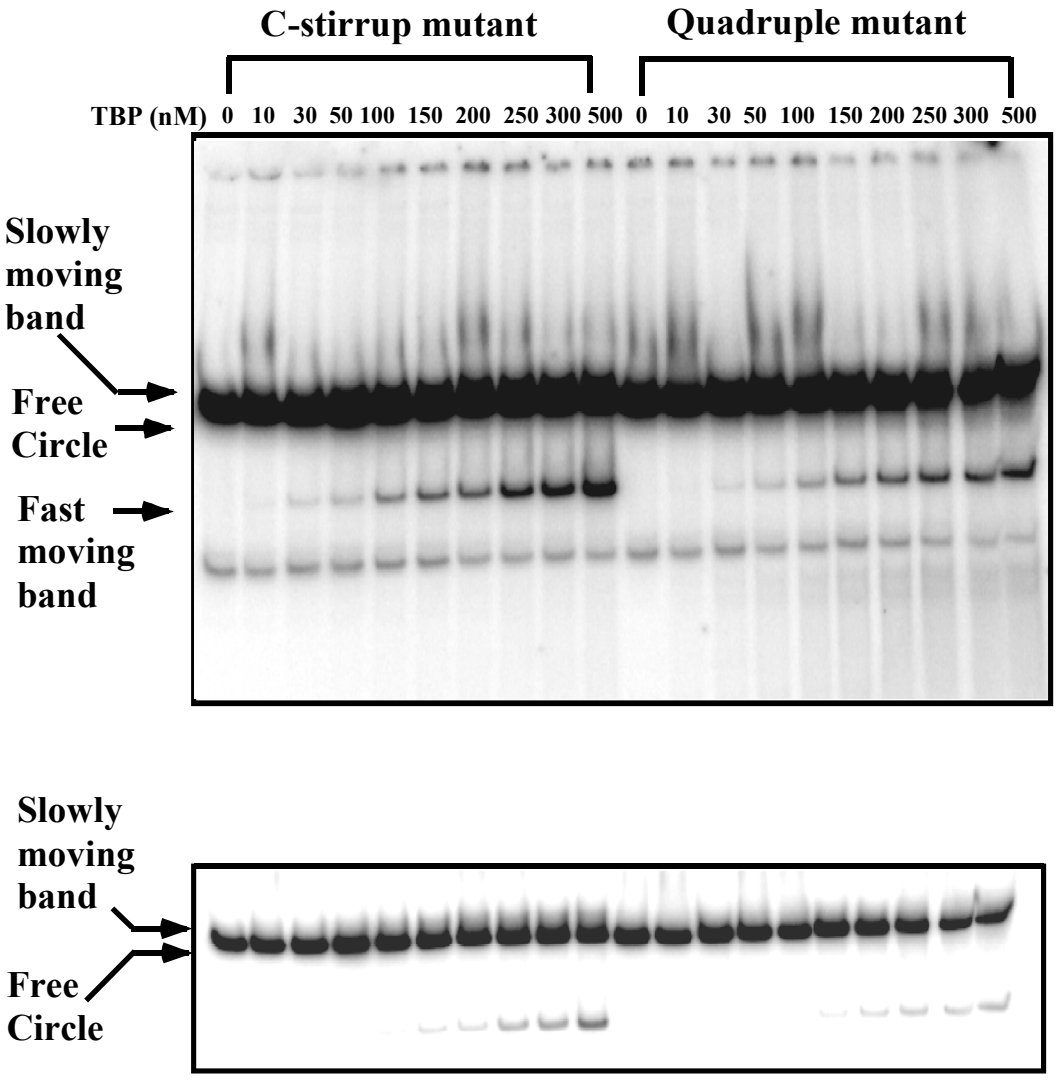

Figure 43 : Electrophoretic Mobility Shift Assay of C-stirrup and Quadruple TBP mutants on 203 bp -1 Topoisomer. Notice the slowly moving bound complex is tightly bound to the free DNA in the mutant. The bottom panel is a portion of the top gel varying the gray scale to detect the slowly moving band.

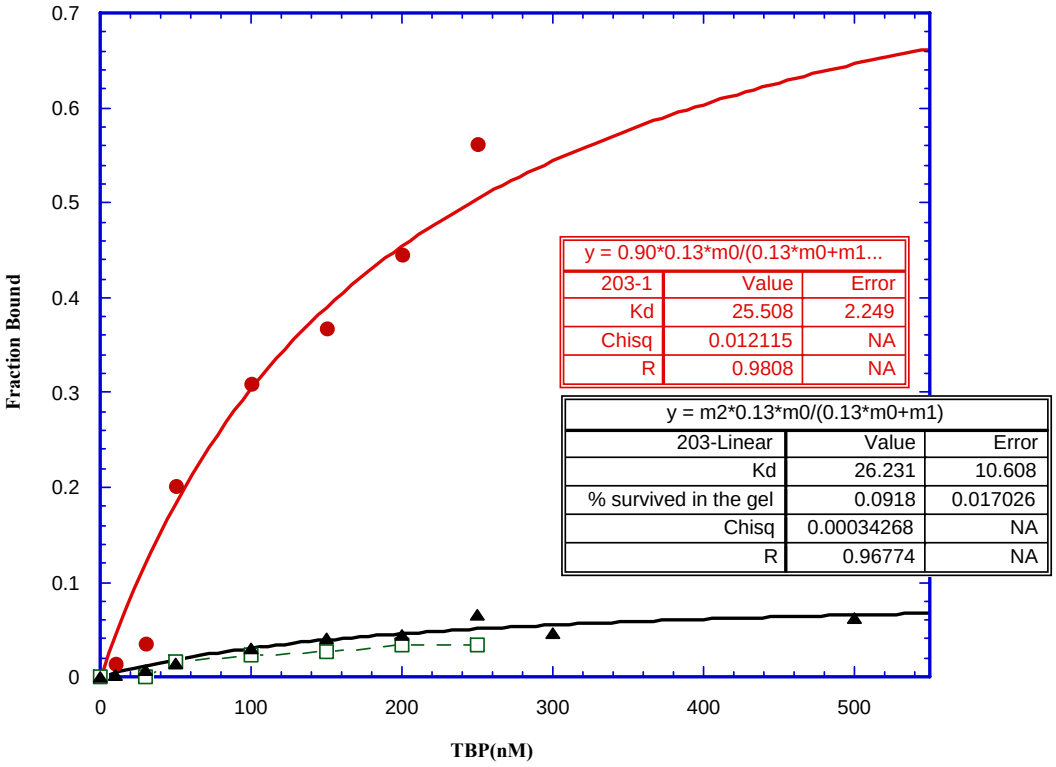

Figure 44. Fraction bound of wild type TBP on 203 bp DNA; data from Figure 42.

The bound fraction of bottom complex vs. total DNA from Figures 42 and 43 was plotted (Figure 45). The fraction of bottom complex from wild type was constant over the entire range of [TBP], whereas the fraction of bottom band from C-stirrup TBP mutant was not saturated and continuously increased as the TBP concentration is increased. This suggests that most of bound complex for the C-stirrup TBP mutant are the bottom band and it may be the flattened form.

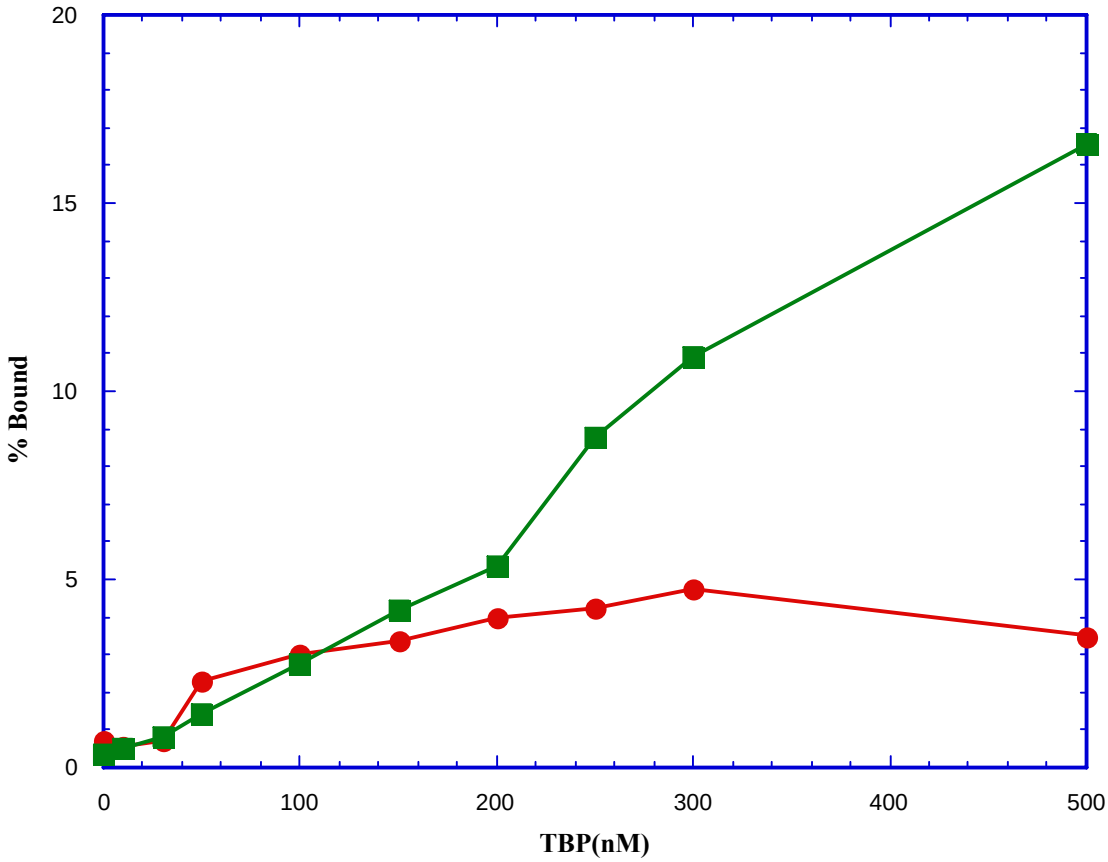

Figure 45. % Bound of bottom complex from wild type (●) and C-stirrup mutant TBP (■) on 203 bp ΔLk = -1 topoisomer. The % bound was calculated from $\frac{\text{bottom band intensity} \times 100\,\%}{\text{total lane intensity}}$. This data was analyzed from Figures 42 and 43.

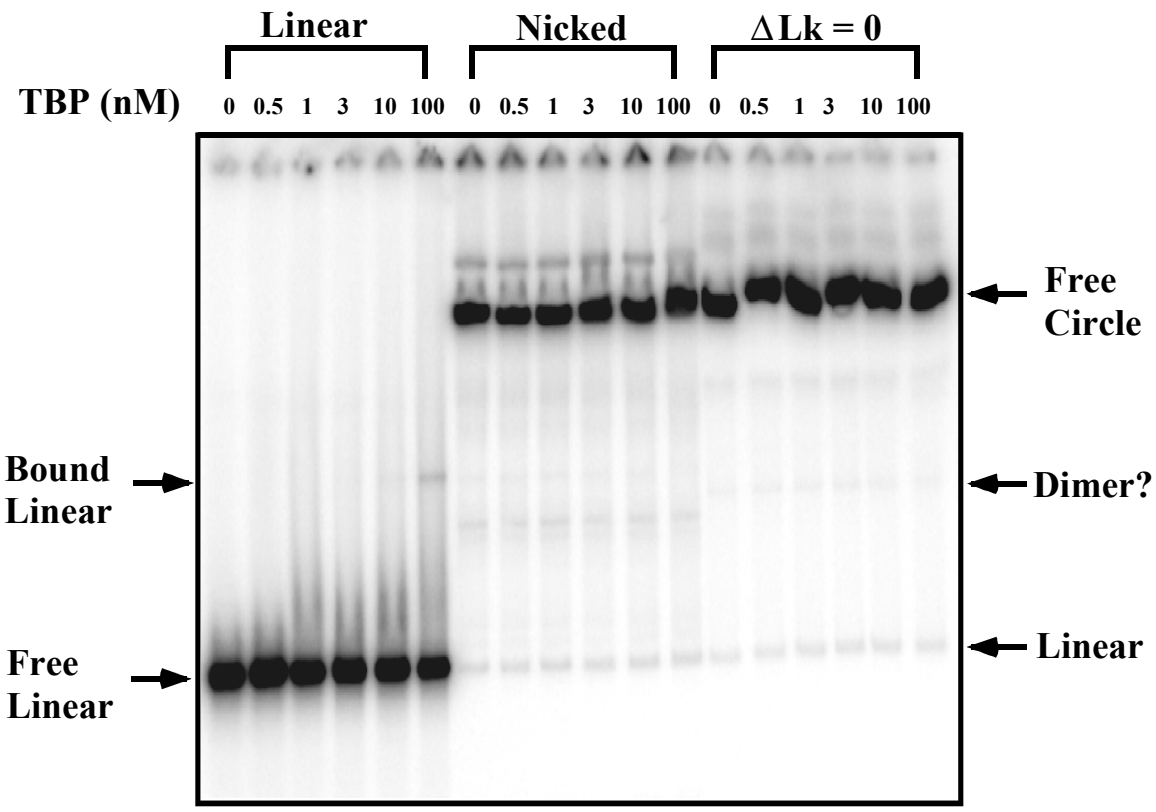

Figure 46 : Electrophoretic Mobility Shift Assay of Wild Type TBP on 210 bp DNA

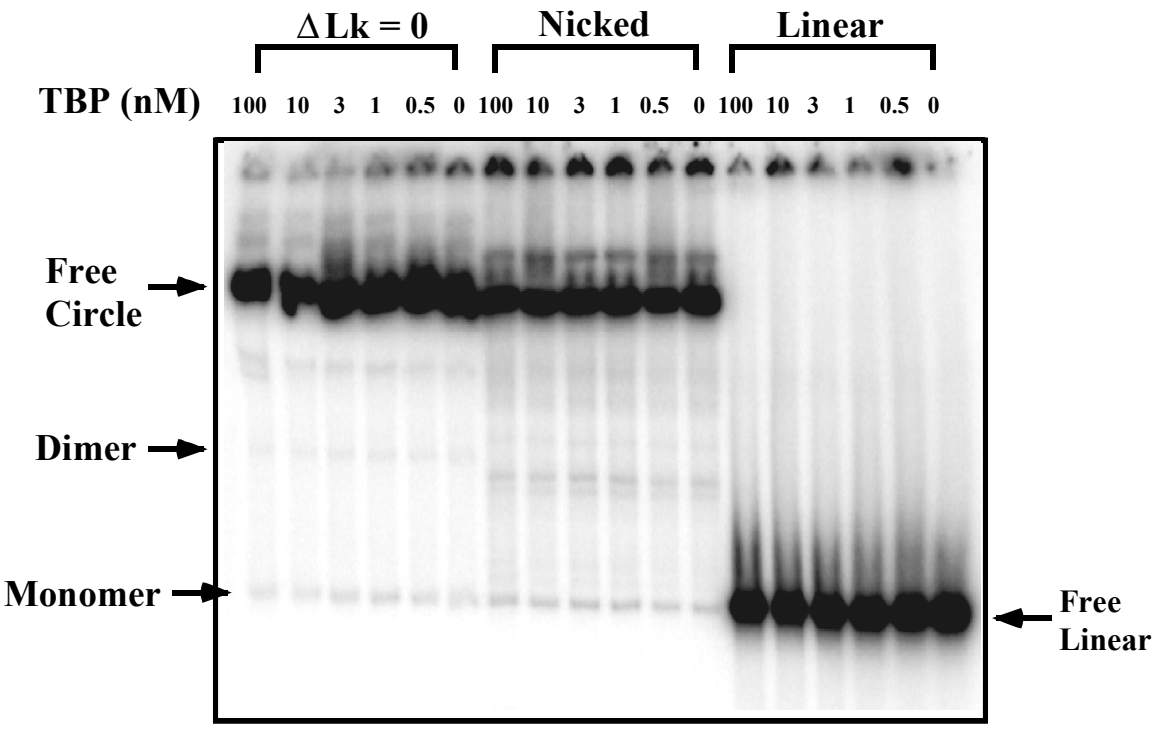

Figure 47 : Electrophoretic Mobility Shift Assay of C-stirrup TBP mutant on 210 bp DNA

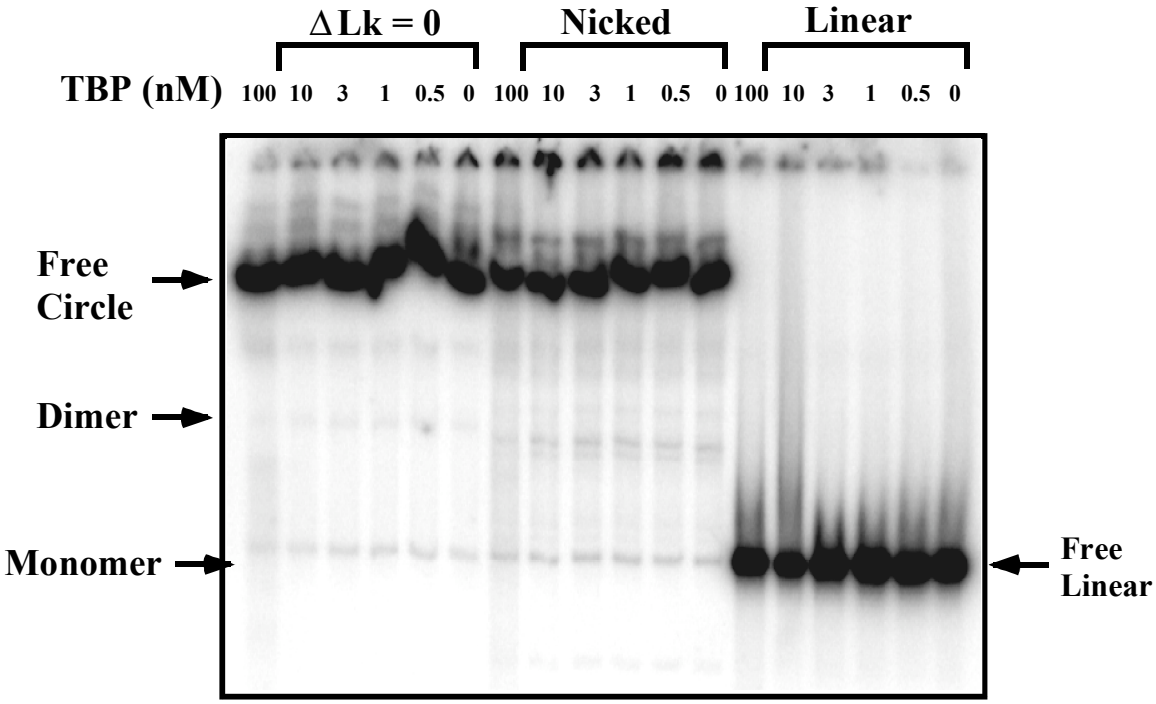

Figure 48 : Electrophoretic Mobility Shift Assay of Quadruple TBP mutant on 210 bp DNA

4.DISCUSSION

4.1 Demonstration of preferential minicircle binding and stability

The first objective of our study was to test the preferential binding of TBP to the negatively supercoiled minicircle DNA. We utilized minicircles as a model nucleosome system for testing the proposed chromatin remodeling theory (Kahn, 2000). The second objective was to measure the topological effects of phenylalanine stirrups on TBP binding by creating two forms of Phe-deletion mutants. The results were monitored by performing DNase I and hydroxyl radical footprinting as well as the EMSA assay.

Although the hydroxyl radical footprinting assay provided a detailed structure of cleaved DNA, it was difficult to optimize the resolution. This was especially true for circular DNA, where restriction enzyme digests were made immediately before running the denaturing gel. There have been many examples utilizing EMSA for studying DNA-protein binding interactions (Lahiri *et al*., 2005; Flick *et al*., 2002; Pruitt, 2004; Jungmann *et al.*, 2005), because it is relatively easy to execute, compared to the much more laborious footprinting assay, and can provide good qualitative data. However, the important aspect of locating the specific sequence to which the protein binds is not accessible using this assay. Thus, employing both assays to a DNA - protein complex may be ideal.

Both footprinting and EMSA results qualitatively agreed that TBP binds better to the negatively supercoiled minicircle DNA than to linear DNA. This suggests that the pre-bending and pre-twisting of the TATA box enhances DNA binding. The supercoiled minicircle is the same size as a nucleosomal repeat, with a similar constrained environment as the chromatin. Thus, we can connect the idea of the preferential binding of TBP to negatively supercoiled DNA with that of chromatin remodeling. There are three stages of initiating transcription in the chromatin, remodeling model: (1) Histones are loosely from repressed chromatin, producing a bound but negatively supercoiled DNA. (2) TBP, which has a higher affinity towards negatively supercoiled DNA, binds to the chromatin and relieves the supercoiling by reducing the writhe. (3) Once TBP is firmly bound, it initiates a cascade of binding event with other transcription factors and transcription begins.

4.2 Demonstration of binding of mutants only to the circular DNA

We have made two phenylalanine deletion mutants, the C-stirrup mutant (F99A-F116A) and the Quadruple mutant (F99A-F116A F190A-F207A), to test the stirrup retraction model. According to the model, which was described in the introduction, the mutants that lack phenylalanine stirrups should bind only to the negatively supercoiled DNA. Our EMSA results (Table 1) indicated that both C-stirrup and Quadruple mutants were indeed not bound to linear DNA, but only to negatively supercoiled minicircle DNA, in both 203 bp and 206 bp constructs.

Table 1. Summary from EMSA results of wild type, C-stirrup mutant, and quadruple mutant TBP binding to each topoisomer of DNA molecules

	Wild Type			C-stirrup			Quadruple		
	L	-1	0	L	-1	0	L	-1	0
203 bp	Y	Y (T)	N	N	Y (B)	N	N	Y (B)	N
206 bp	Y	Y (B)	N	N	Y (B)	N	N	Y (B)	N
210 bp	Y	n/a	N	N	n/a	N	N	n/a	N

T: dominant bound complex is Top band; B: dominant bound complex is Bottom band: Y: bind to the particular DNA; N: doesn't bind to the particular DNA; n/a: doesn't generate the topoisomer

The EMSA gels show that there is more than one conformation for monomeric TBP bound to negatively supercoiled DNA. It is observed that the faster moving band (bottom band) is stable in both wild type and mutant TBP. Only the wild type TBP produces a stable slower-moving form (upper band), whereas mutant TBP only produces the faster-moving form. These observations suggest that the faster moving band may be the flattened form and the slowly moving band may be the writhed form.

The significance of these studies is that they represent the first application of hydroxyl radical footprinting to minicircle DNA in order to study the binding interactions of TBP to nucleosome-like DNA. The EMSA and hydroxyl radical footprinting assays are in qualitative agreement. This system is a unique example of a

strain induced conformation of a protein-DNA complex and may be relevant to understanding the enhanced binding of TBP to remodeled chromatin.

Appendix

This appendix includes the chromatographs of strong cation exchange column (HiTrap SP XL) and gel filtration columns (Sephacryl S-100, S-300) for all proteins. The standard chromatograph of desalting column (HiPrep 26/10) for C-stirrup mutant TBP is illustrated as an example for the rest of wild type and Quadruple TBP mutant.

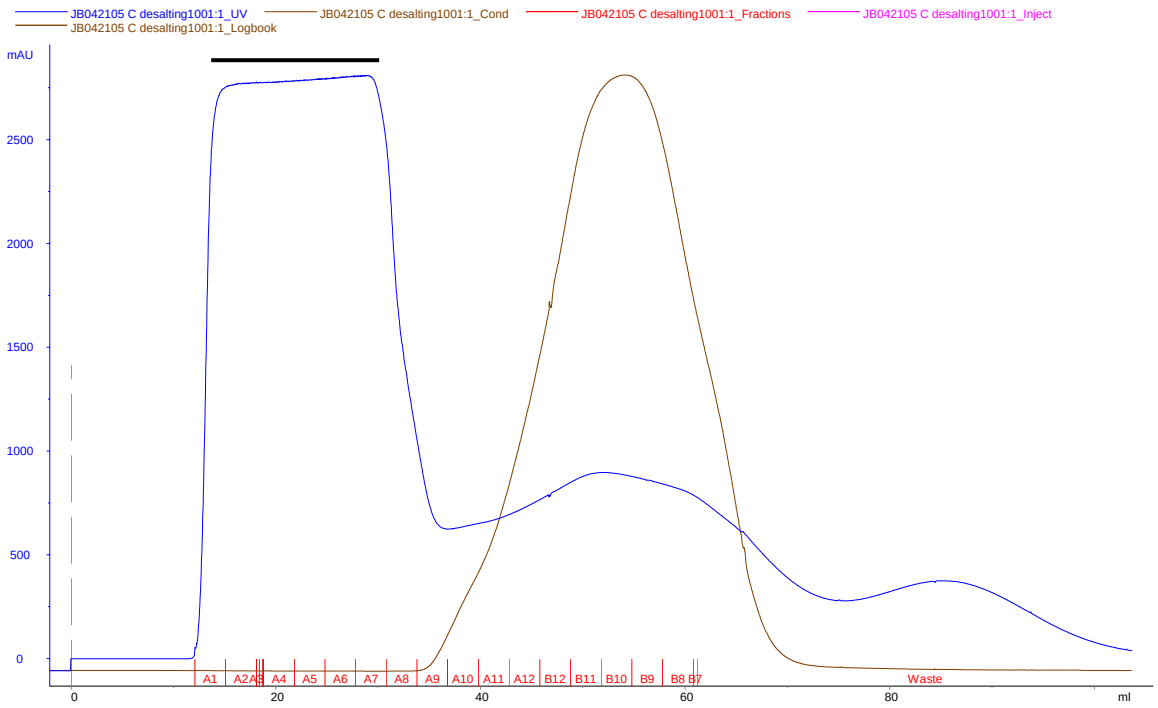

Figure A.1: C-stirrup TBP mutant chromatograph from HiPrep 26/10 desalting column. Retained protein fractions: (━)

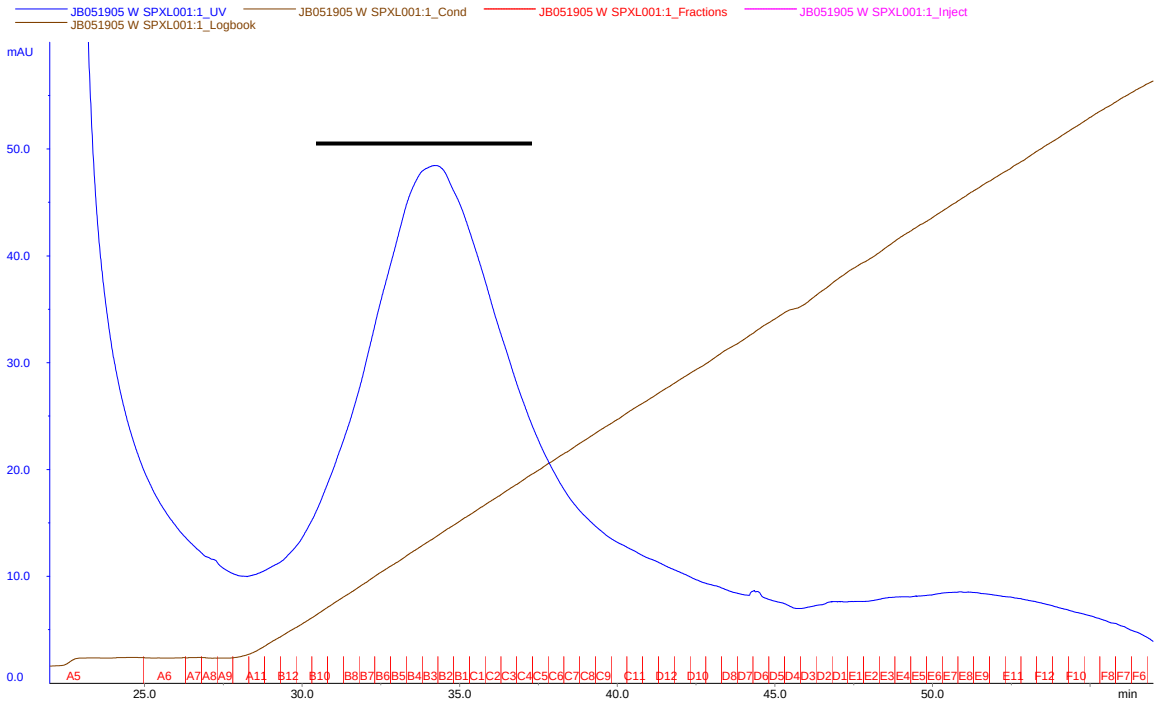

Figure A.2: Wild Type TBP chromatograph from HiTrap SP XL (1mL). Strong cation exchange column, retained peak: (━)

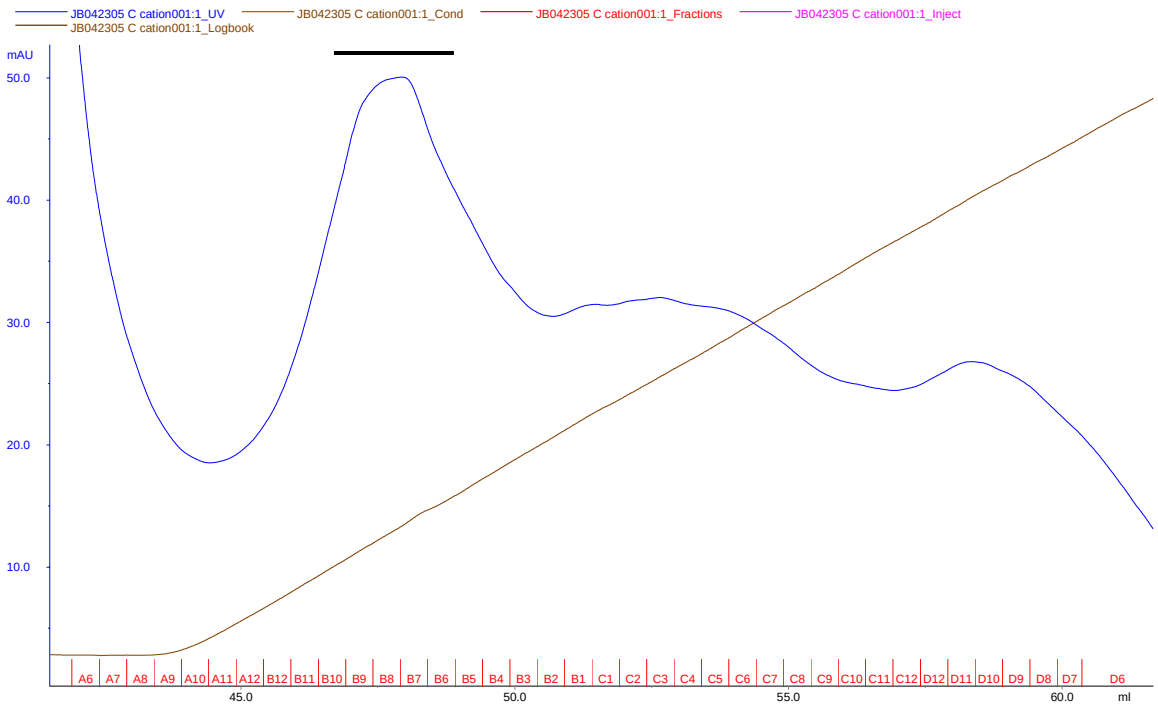

Figure A.3: C-stirrup TBP mutant chromatograph from HiTrap SP XL (1mL). Strong cation exchange column, peak retained: (—)

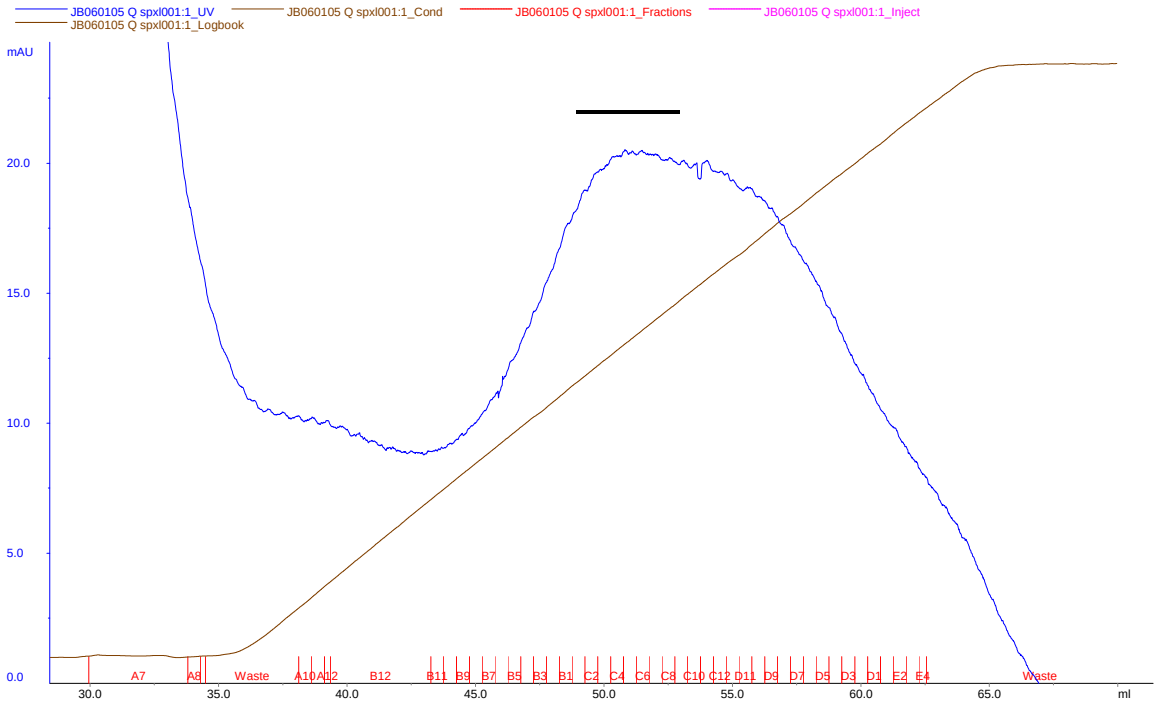

Figure A.4: Quadruple TBP mutant chromatograph from HiTrap SP XL (1mL). Strong cation exchange column, peak retained: (—)

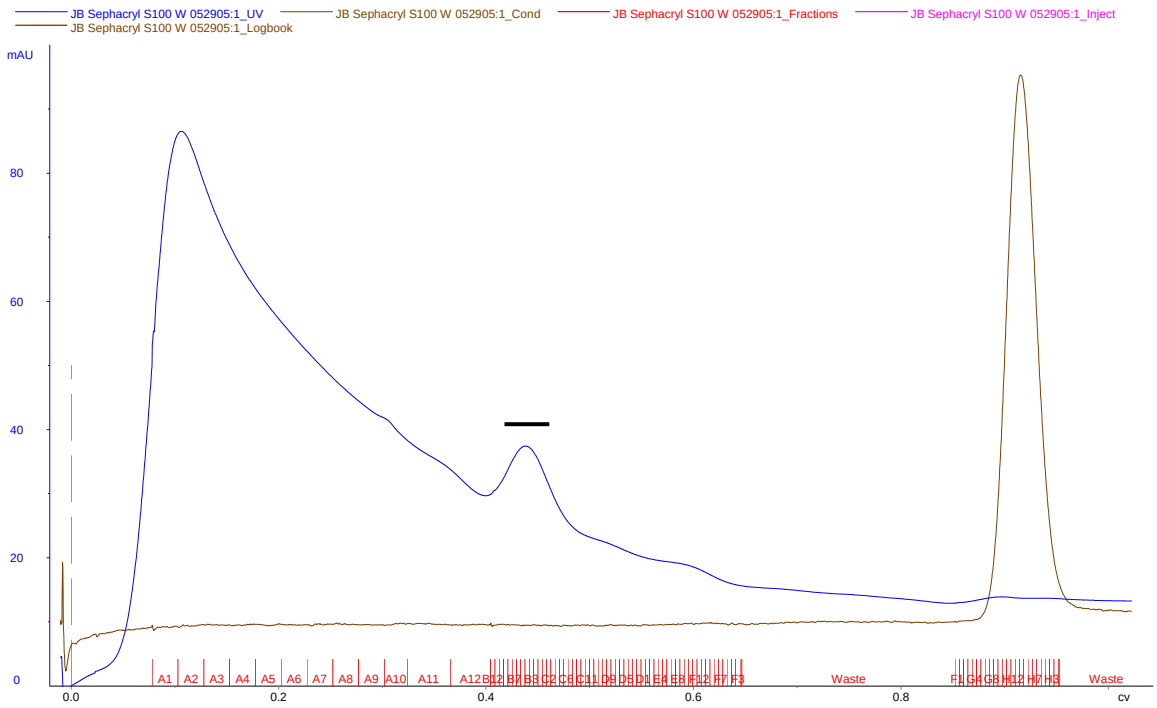

Figure A.5: Wild type TBP chromatograph from Sephacryl S-100. Retained protein Fractions: (━)

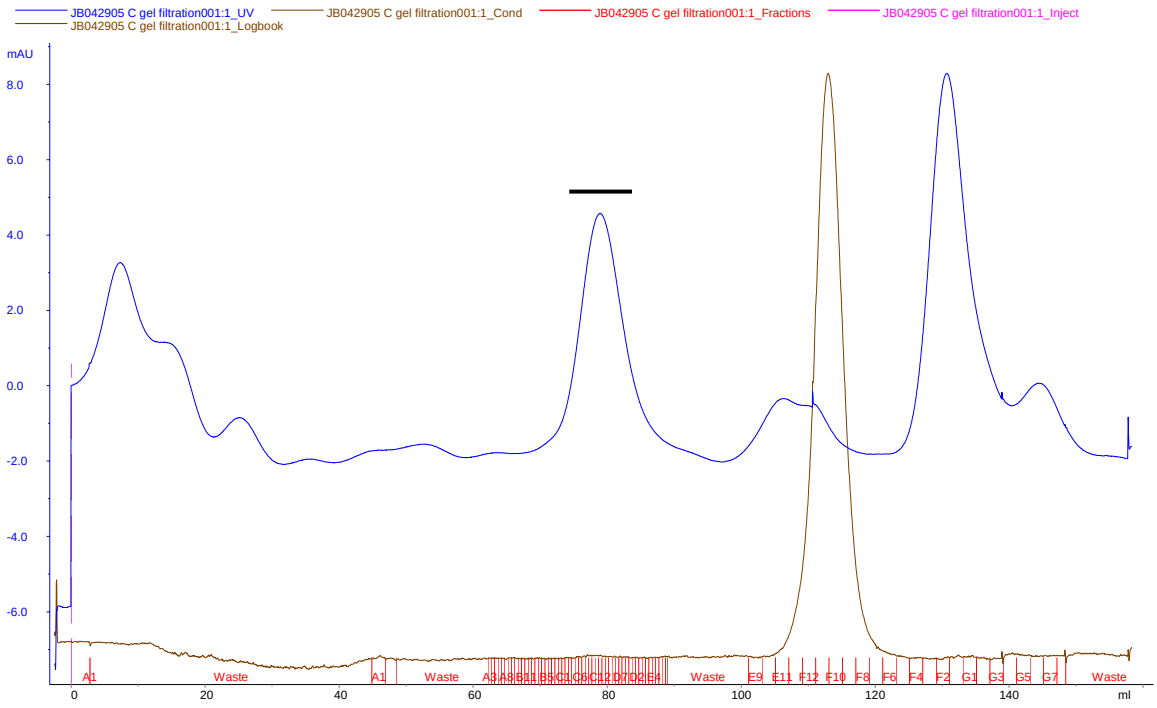

Figure A.6: C-stirrup TBP mutant chromatograph from Sephacryl S-300.Retained protein fractions: (━)

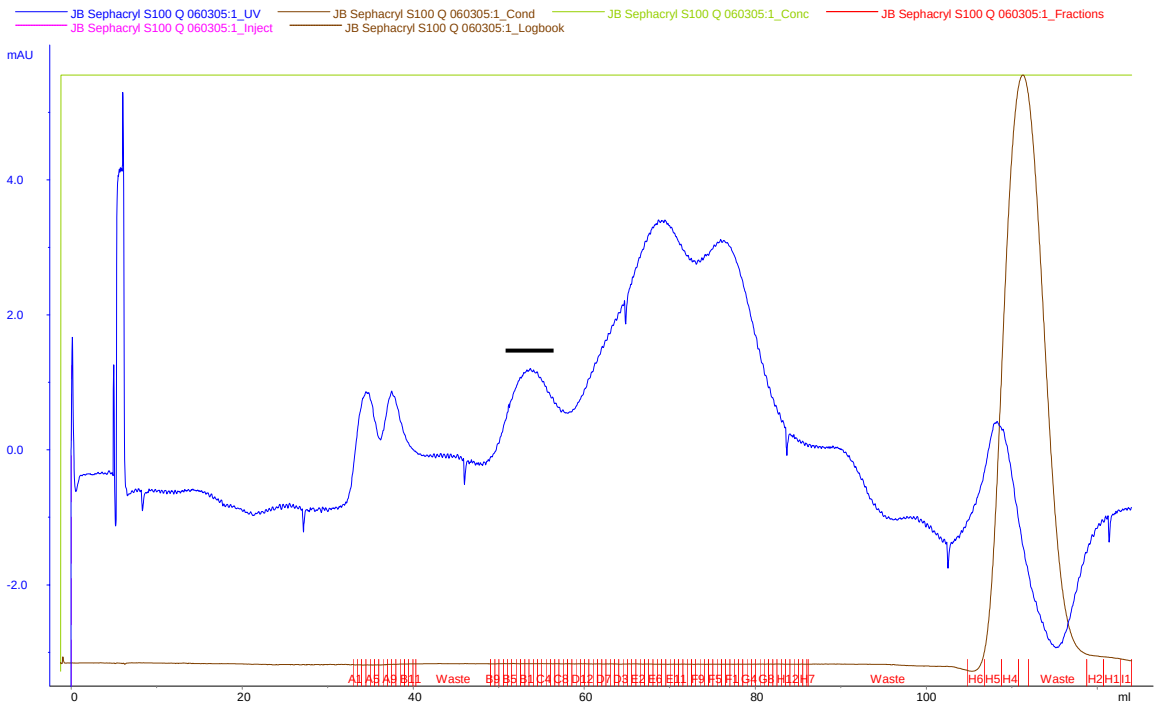

Figure A.7: Quadruple stirrup TBP mutant chromatograph from Sephacryl S-100.Retained protein fractions: (━)

REFERENCES

Alberts, B., Bray, D., Johnson, A., Lewis, J., Raff, M., Roberts, K., Walter, P. (1998). *Essential Cell Biology-An Introduction to the molecular biology of the cell*, Garland Publishing, Inc.

Arndt, K. M., Ricupero, S.L., Eisenmann, D.M., Winiston, F. (1992). Biochemical and genetic characterization of a yeast TFIID mutant that alters transcription in vivo and DNA binding in vitro. *Mol. Cell. Biol.* **12**, 2372-2382.

Banerjee, S. & Spector, D.J. (1992). Differential effect of DNA supercoiling on transcription of adenovirus genes in vitro. *J. Gen. Virol.* Oct; **73**, 2631-8.

Bates, A. D. & Maxwell, A. (1993). *DNA Topology*. In Focus (Rickwood, D. & Male, D., Eds.), IRL Press at Oxford University Press, Oxford.

Bauer, W. R., Crick, F. H. C. & White, J. H. (1980). Supercoiled DNA. *Scientific American* **243**, 118-133.

Benham, C. J. (1989). Onset of writhing in circular elastic polymers. *Phys. Rev. A: Gen. Phys*. **39**(5): 2582-2586.

Burley, S. K. & Roeder, R. G. (1996). Biochemistry and structural biology of transcription factor IID (TFIID). *Annu. Rev. Biochem.* **65**, 769-799.

Carey, M. & Smale, S. T. (2000). *Transcriptional Regulation in Eukaryotes: Concepts, Strategies, and Techniques*, Cold Spring Harbor Laboratory Press, Cold Spring Harbor, NY.

Corona, D. F., Längst, G., Clapier, C. R., Bonte, E. J., Ferrari, S., Tamkun, J. W. & Becker, P. B. (1999). ISWI is an ATP-dependent nucleosome remodeling factor. *Molecular Cell.* **3**, 239-45.

Cozzarelli, N. R. & Wang, J. C., Eds. (1990). *DNA Topology and Its Biological Effects.* Cold Spring Harbor, NY: Cold Spring Harbor Press.

Davis, N. A., Majee, S. S. & Kahn, J. D. (1999). TATA box DNA deformation with and without the TATA box-binding protein. *J. Mol. Biol.* **291**, 249-65.

Dhavan, G. M., Crothers, D.M., Chance, M.R. and Brenowitz, M. (2002). Concerted binding and bending during IHF-DNA complex formation by time-resolved X-ray hydroxyl radical footprinting. *J. Biol. Biol.* **315**, 1027-1047.

Dynan, W. S. & Tjian, R. (1983). The promoter specific transcription factor Sp1 binds to upstream sequences in the SV40 promoter. *Cell*, **35**, 79-87.

Flick, M. B., Sapi, E., Kacinski, B.M. (2002). Hormonal regulation of the c-fms proto-oncogene in breast cancer cells is mediated by a composite glucocorticoid response element. *J .Cell. Biochem.* **85**, 10-23.

Fried, M. & Crothers, D. M. (1981). Equilibria and kinetics of Lac repressor-operator interactions by polyacrylamide gel electrophoresis. *Nucl. Acids Res.* **9**, 6505-6525.

Galas, D. J. & Schmitz, A. (1978). DNAase footprinting: a simple method for the detection of protein-DNA binding specificity. *Nucl. Acids Res.* **5**, 3157.

Garner, M. M. & Revzin, A. (1981). A gel electrophoresis method for quantifying and binding of proteins to specific DNA regions; application to components of the Escherichia coli lactose operon regulatory system. *Nucl. Acids Res*, **9**, 3047-3060.

Goodrich, J. A. & Tjian, R. (1994). TBP-TAF complexes: selectivity factors for eukaryotic transcription. *Curr. Opin. Cell. Biol.* **6**, 403-409.

Greenblatt, J. (1991). Roles of TFIID in Transcriptional Initiation by RNA Polymerase II. *Cell,* **66**, 1067-1070.

Grove, A., Galeone, A., Yu, E., Mayol, L. & Geiduschek, E. P. (1998). Affinity, stability and polarity of binding of the TATA binding protein governed by flexure at the TATA Box. *J. Mol. Biol.* **282**, 731-739.

Hahn, S., Buratowski, S., Sharp, P. A. & Guarente, L. (1989). Yeast TATA-binding protein TFIID binds to TATA elements with both consensus and nonconsensus DNA sequences. *Proc. Natl. Acad. Sci. USA*, **86**, 5718-5722.

Hamiche, A., Sandaltzopoulos, R., Gdula, D.A., and Wu, C. (1999). ATP-dependent histone octamer sliding mediated by the chromatin remodeling complex NURF. *Cell*, **97**, 833-842.

Hernandez, N. (1993). TBP, a universal eukaryotic transcription factor? *Genes Dev.* **7**, 1291-1308.

Hoopes, B. C., LeBlanc, J. F. & Hawley, D. K. (1992). Kinetic Analysis of Yeast TFIID-TATA Box Complex Formation Suggests a Multi-Step Pathway. *J. Biol. Chem.* **267**, 11539-11547.

Horikoshi, M., Bertuccioli, C., Takada, R., Wang, J., Yamamoto, T. & Roeder, R. G. (1992). Transcription factor TFIID induces DNA bending upon binding to the TATA element. *Proc. Natl. Acad. Sci. USA.* **89**, 1060-1064.

Horikoshi, M., Hai, T., Lin, Y.-S., Green, M. R. & Roeder, R. G. (1988). Transcription Factor ATF Interacts with the TATA Factor to Facilitate Establishment of a Preinitiation Complex. *Cell,* **54**, 1033-1042.

Horowitz, D. S. & Wang, J.C. (1984). Torsional Rigidity of DNA and Length Dependence of the Free Energy of DNA Supercoiling. *J. Mol. Biol*. **173**: 75-91.

Jungmann, R. A., Kiryukhina, O. (2005). Cyclic AMP and AKAP-mediated targeting of protein kinase A regulates lactate dehydrogenase subunit A mRNA stability. *J. Biol. Chem.* **280**, 25170-25177.

Juo, Z. S., Chiu, T. K., Leiberman, P. M., Baikalov, I., Berk, A. J. & Dickerson, R. E. (1996). How proteins recognize the TATA box. *J. Mol. Biol.* **261**, 239-54.

Kahn, J. D. (2000). Topological effects of the TATA box binding protein on minicircle DNA and a possible thermodynamic linkage to chromatin remodeling. *Biochemistry,* **39**, 3520-3524.

Kahn, J. D. (2002). DNA Topology: Applications to Gene Expression. *Curr. Org. Chem.* **6**, 815-826.

Kahn, J. D. & Crothers, D. M. (1993). DNA Bending in Transcription Initiation. *Cold Spring Harbor Symp. Quant. Biol.* **58**, 115-122.

Kim, J. L., Nikolov, D. B. & Burley, S. K. (1993). Co-crystal structure of TBP recognizing the minor groove of a TATA element. *Nature,* **365**, 520-527.

Kim, J. L. & Burley, S.K. (1994). 1.9 Å resolution refined structure of TBP recognizing the minor groove of TATAAAAG. *Nat. Struct. Biol.* **1**, 638-653.

Kim, Y., Geiger, J. H., Hahn, S. & Sigler, P. B. (1993). Crystal structure of a yeast TBP/TATA-box complex. *Nature,* **365**, 512-520.

Lahiri, D. K., Ge, Y.W., Maloney, B. (2005). Characterization of the APP proximal promoter and 5'-untranslated regions: identification cell type-specific domains and implications in APP gene expression and Alzheimer's disease. *FASEB J.* **19**, 653-655.

Latchman, D. S. (1991). *Eukaryotic transcription factors*, Academic press, Harcourt Brace Jovanovich.

Leblanc, B. P., Benham, C. J. & Clark, D. J. (2000). An initiation element in the yeast CUP1 promoter is recognized by RNA polymerase II in the absence of TATA box-binding protein if the DNA is negatively supercoiled. *Proc. Natl. Acad. Sci. USA,* **97(20)**, 10745-10750.

Liu, L. F., Wang, J.C. (1978). DNA-DNA gyrase complex: the wrapping of the DNA duplex outside the enzyme. *Cell,* **15**, 979-984.

Liu, L. F. & Wang, J. C. (1987). Supercoiling of the DNA Template During Transcription. *Proc. Natl. Acad. Sci. USA,* **84**, 7024-7027.

Lorch, Y. & Kornberg, R. D. (1993). Near-Zero Linking Difference upon Transcription Factor IID Binding to Promoter DNA. *Mol. Cell. Biol.* **13**, 1872-1875.

Michelotti, G. A., Michelotti, E. F., Pullner, A., Duncan, R. C., Eick, D. & Levens, D. (1996). Multiple Single-Stranded *cis* Elements Are Associated with Activated Chromatin of the Human c-*myc* Gene In vivo. *Mol. Cell. Biol.* **16**, 2656-2669.

Mondal, N. & Parvin, J. D. (2001). DNA topoisomerase II alpha is required for RNA polymerase II transcription on chromatin templates. *Nature,* **413**, 435-438.

Morse, R. H. & Cantor, C. R. (1985). Nucleosome core particles suppress the thermal untwisting of core DNA and adjacent linker DNA. *Proc. Natl. Acad. Sci. USA,* **82**, 4653-4657.

Nelson, D. L., Cox, M.M. (2000). *Lehninger Principle of Biochemistry* (3rd, Ed.), Worth Publisher.

Nikolov, D. B., Chen, H., Halay, E. D., Hoffman, A., Roeder, R. G. & Burley, S. K. (1996). Crystal structure of a human TATA box-binding protein/TATA element complex. *Proc. Natl. Acad. Sci. USA,* **93**, 4862-4867.

Norton, V. G., Marvin, K. W., Yau, P. & Bradbury, E. M. (1990). Nucleosome Linking Number Change Controlled by Acetylation of Histones H3 and H4. *J. Biol. Chem.* **265**, 19848-19852.

Oelgeschläger, T., Chiang, C.-M. & Roeder, R. G. (1996). Topology and reorganization of a human TFIID–promoter complex. *Nature,* **382**, 735-738.

Parkhurst, K., Brenowitz, M. & Parkhurst, L. J. (1996). Simultaneous Binding and Bending of Promoter DNA by the TATA Binding Protein: Real Time Kinetic Measurements. *Biochemistry*, **35**, 7459-7465.

Parkhurst, K. M., Richards, R. M., Brenowitz, M. & Parkhurst, L. J. (1999). Intermediate Species Possessing Bent DNA are Present Along the Pathway to Formation of a Final TBP-TATA Complex. *J. Mol. Biol.* **289**, 1327-1341.

Parvin, J. D., McCormick, R. J., Sharp, P. A. & Fisher, D. E. (1995). Pre-bending of a promoter sequence enhances affinity for the TATA-binding factor. *Nature*, **373**, 724-727.

Parvin, J. D. & Sharp, P. A. (1993). DNA Topology and a Minimal Set of Basal Factors for Transcription by RNA Polymerase II. *Cell*, **73**, 533-540.

Petri, V., Hsieh, M. & Brenowitz, M. (1995). Thermodynamic and kinetic characterization of the binding of the TATA binding protein to the adenovirus E4 promoter. *Biochemistry*, **34**, 9977-84.

Pruitt, S. C., Bussman, A., Maslov, A.Y., Natoli, T.A., Heinaman, R. (2004). Hox/Pbx and Brn binding sites mediate Pax3 expression in the vitro and in vivo. *Gene. Expr. Patterns*. **4,** 671-685.

Pugh, B. F. & Tjian, R. (1992). Diverse Transcriptional Functions of the Multisubunit Eukaryotic TFIID Complex. *J. Biol. Chem.* **267**, 679-682.

Revzin, A. (1993). *Footprinting of nucleic acid-protein complexes*, Academic Press, San Diego.

Schmidt, M. C., Zhou, Q., and Berk, A.J. (1989). *Mol. Cell .Biol.* **9**, 3299-3307.

Schrödinger, E. (1944). *What is life?*, Cambridge University Press.

Siebenlist, U. & Gilbert, W. (1980). Contacts between *Escherichia coli* RNA polymerase and an early promoter of phage T7. *Proc. Natl. Acad. Sci. USA,* **77**, 122-126.

Smale, S. T. (1994). Core promoter architecture for eukaryotic protein-coding genes. In *Transcription: Mechanism and Regulation* (Conaway, R.C., and Conaway, J.W., Eds.), Raven Press, NY.

Stafford, G. A. & Morse, R. H. (1997). Chromatin Remodeling by Transcriptional Activation Domains in a Yeast Episome. *J. Biol. Chem.* **272**, 11526-11534.

Storl, J., Storl, J., Zimmer, Ch. and Lown, J.W. (1993). Minor groove binders are inhibitors of the catalytic activity of DNA gyrases. *FEBS Letters.* **317**, 157-162.

Storl, K., Burckhardt, G., Lown, J.W., Zimmer, Ch. (1993). Studies on the ability of minor groove binders to induce supercoiling in DNA. *FEBS Letters*. **334** (1), 49-54.

Struhl, K. (1994). Duality of TBP, the universal transcription factor. *Science,* **263**, 1103-1104.

Tobias, I. (1998). A Theory of Thermal Fluctuations in DNA Miniplasmids. *Biophys. J.* **74**, 2545-2553.

Waton, J. D. (2003). *DNA the Secret of Life*, Cold Spring Harbor, New York.

Weaver, R. F. (1999). *Molecular Biology*, (1st Ed.), WCB/McGraw-Hill, Boston.

White, J. H. (1989). An Introduction to the Geometry and Topology of DNA Structure. In *Mathematical Methods for DNA Sequences* (Waterman, M. S., ed.), CRC Press, Boca Raton, FL.